




Universitetet
i Stavanger

Faculty of Science and Technology

MASTER'S THESIS

Study program / Specialization Konstruksjoner og Materialer Fordypning Maskinkonstruksjoner	Spring semester, 2016 Open / Restricted Access
Writer: Anders Vikebø	 (Writer's signature)
Faculty supervisor: Torfinn Havn External supervisor: N/A	
Thesis title: <i>A comparison of cold strained and solution annealed bolts in super duplex stainless steel in regards to stress corrosion cracking and pitting resistance</i>	
Credits (ECTS): 30	
Key words: Key words: SCC, pitting, cold work, solution annealed, magnesium chloride, alternate immersion, Super Duplex, UNS S32760	Pages: 85 + enclosure: 69 Stavanger, 08.06.2016

Front page for master thesis
Faculty of Science and Technology
Decision made by the Dean October 30th 2009

(Page intentionally left blank)

Abstract

Corrosion place a high cost on the society and selecting the wrong materials in certain environments may have catastrophic consequences. When selecting materials there is also the different manufacturing methods to consider and there might be a difference in corrosion resistance depending on the way the material is manufactured. Also even high grade stainless steels like super duplex may suffer from corrosion in a specific environment.

The scope of the thesis compares the manufacturing methods solution annealing and cold straining on a super duplex stainless steel, and the potential effect on stress corrosion cracking and pitting resistance. Earlier research indicates that there might be some uncertainties regarding this, and the amount of research in this field was lacking compared to studies on austenitic stainless steels.

The objective of this thesis was to develop a test setup using modified versions of the ASTM G36 and G44 standards testing on as received super duplex stainless steel bolts (UNS S32760) of both solution annealed and cold strained quality.

Tensile testing was performed to determine the elongation at yield, and hence being able to determine the percentage of yield for the experiments. The results of the testing were surprising, as the Young's modulus was around 50 % less than what was expected, due to testing with a threaded bar instead of a smooth. All of the experiments were performed with the bolts stressed to 100 % of offset yield.

For the alternate immersion testing, a test jig was designed and used during the whole experiment which was executed over a time period of 936 hours. This setup used magnesium chloride instead of sodium chloride which was specified in the standard to examine if this would accelerate stress corrosion cracking or pitting corrosion. The results from this experiment showed that the solution annealed bolts seemed to exhibit a higher pitting resistance than the cold strained bolts. Also this experiment indicates that this type of experiment may take too long time to be effective. Four 316L bolts were also tested in the alternate immersion testing and exhibited obvious pitting as expected.

The results however must be considered with caution as only two solution annealed bolts and two cold strained bolts were tested. It is therefore not possible to conclude on this matter. In regards to stress corrosion cracking, no cracks were discovered at 10X magnification, but further metallographic testing should be performed to verify that no cracks are present.

The heated immersion testing in magnesium chloride was performed at 90°C instead of 155°C as specified in the standard. An initial test performed for 316 hours produced fracture in the two solution annealed and two cold strained bolts that were tested. No pitting was observed at 10X magnification.

A second heated immersion test was performed for 156 hours and this test may indicate that there is higher stress corrosion cracking resistance in the solution annealed bolts compared to the cold strained. There was however only two bolts of each type tested in this experiment as well, so it is not possible to conclude without further experiments. No pitting was observed with 10X magnification on any of the bolts.

The final results indicate that solution annealed bolts exhibits a higher resistance in regards to both stress corrosion cracking and pitting corrosion. Further testing needs to be performed however to verify this as there a low number of specimens tested.

Preface

This thesis has been very interesting in regards to both the theory aspect and the experimental. As corrosion has such an impact especially in the subsea industry, this thesis has helped me get a deeper understanding of the mechanisms as well as the practical aspect of experiments using what was available of equipment. I have had help from numerous people and companies which deserve acknowledgement.

My supervisor at the University of Stavanger, Torfinn Havn, guided me through this thesis with encouragement and suggestions for the experiments. His positive attitude and enthusiasm for corrosion combined with his support throughout the thesis has been invaluable.

Also my manager at DeepOcean where I work full time, Jostein Førland, has aided me through both the thesis and the rest of the master's degree. His problem solution-oriented approach to any issue combined with his patience, are values I highly regard and appreciate. The Structure and Design department at DeepOcean as well as the DeepOcean Base personnel deserves acknowledgment for their help on both the practical and theoretical aspects. I am also very grateful for the financial support from DeepOcean throughout the master's degree. For proof reading my colleague Geir Halleraker provided useful input as well as being a great discussion partner through the thesis.

In regards to materials and equipment there have been several contributors that helped at no cost and on short notice. Scandinavian Flanges and Fittings provided the flanges for the experiments and Tools Randaberg, together with Ome Metallurgica provided the superduplex bolts and nuts. The local workshop Mekan machined the flanges and Olufsen Skipsservice machined the holders for the tensile testing.

My earlier colleague and friend Edgar Valhammer helped with the programming and soldering required for the test jig, as well as being an extraordinary discussion partner on the practical aspects of the testing.

Hydro Aluminium Karmøy R & D provided all the tensile testing free of cost in their laboratory and also helped with general information in regards to tensile testing. Also the help from Ingunn Oddsen at the UIS laboratory for the initial testing of the setup is appreciated.

Least but not last, the aid from my family has been invaluable. My wife Charlotte and my two sons Vidar August and Odin have supported me in any way possible. Finishing this master's degree would not have been possible without their support and encouragement.

(Page intentionally left blank)

Contents

Abstract	I
Preface	III
List of figures	VII
Abbreviations	X
1 Introduction	1
1.1 Background.....	1
1.2 Scope of work.....	1
1.3 Limitations of the thesis	2
1.4 Method.....	2
2 Theory	3
2.1 Duplex Stainless Steels.....	3
2.2 The role of alloying elements in SDSS	5
2.3 Microstructure of SDSS.....	8
2.4 Mechanical properties of DSS and SDSS.....	11
2.5 Corrosion theory	13
2.6 Corrosion of SDSS	17
2.7 Manufacturing methods of the materials used for the experiments.....	22
2.8 Corrosion testing on SDSS in regards to SCC and pitting in chloride environments	24
2.9 Earlier studies on the manufacturing methods impact on corrosion resistance.....	25
3 Testing.....	31
3.1 Standards	31
3.2 Properties of bolted assemblies and necessary considerations	33
3.3 Tensile testing.....	36
3.4 Test materials.....	40
3.5 Summary of test materials	44
3.6 Test setup.....	45
3.7 Experimental.....	55

3.8	Results	60
4	Discussion	73
4.1	Tensile testing and torquing of bolts.....	73
4.2	Immersed test with heating.....	74
4.3	Alternate immersion testing.....	75
4.4	Further work	77
5	Conclusion.....	79
6	References	81
7	Appendices	85
	Appendix A: Torque calculations	86
	Appendix B: MSDS Gleitpaste	87
	Appendix C: MDS SDSS Flanges.....	91
	Appendix D: MDS SDSS bolts and nuts.....	93
	Appendix E: MDS 316L bolts and nuts	125
	Appendix F: Calculations on nut and holder.....	127
	Appendix G: MDS S165M holders	128
	Appendix H: Holder manufacturing drawing.....	130
	Appendix I: Calculations on theoretical strain	131
	Appendix J: Flange manufacturing drawing	132
	Appendix K: MSDS Magnesium chloride	133
	Appendix L: Magnesium chloride solutions	135
	Appendix M: Arduino code.....	137
	Appendix N: Stress-strain curves from tensile testing.....	138

List of figures

Figure 1: Stainless steel worldwide production compared to flat carbon steel [8]	4
Figure 2: Effect of alloying elements on the anodic polarization curve [7].....	5
Figure 3: Different microstructures of steel [3]	8
Figure 4: Thermocalc isopleth diagram showing the composition of a SDSS alloy at the dotted line [7]	9
Figure 5: TTT diagram showing three different duplex steel grades 2205 (DSS), 2304 (lean DSS) and 2507 (SDSS) [3]	9
Figure 6: Microstructure of a SDSS SAF 2507 (UNS S32750) aged for 10 min at 850 °C. σ phase is shown at ferrite / ferrite phase boundaries and secondary austenite is visible in bright contrast between the primary austenite and ferrite (SEM) [9]	10
Figure 7: Time-temperature-transformation (TTT) diagram for SAF 2507 (UNS S32750 SDSS) with a curve corresponding to 27J impact toughness indicating rate of embrittlement [9]	12
Figure 8: A polarization curve for a stainless steel in a sulfuric acid solution and also showing the pitting potential decreasing as the chloride concentration is increasing [2].....	16
Figure 9: The passive layer is repaired in a', while destroyed in b' [2].....	17
Figure 10: Illustration of the pitting mechanism [2]	18
Figure 11: The Fontana-Green mechanism of crevice corrosion [5]	19
Figure 12: Examples of crack propagation where a) is showing cracking through the ferrite (500X) and b) is showing cracking through both phases (400X) [7].....	22
Figure 13: Stress-strain diagram showing the elastic strain recovery and strain hardening. Initial yield (σ_{y0}) and yield (σ_{y1}) after releasing the load D is shown [11]	23
Figure 14: The effect of cold work in regards to UTS for several different SS [7]	23
Figure 15: Summary of several studies on a SDSS with varying temperature and chloride concentrations [29].....	29
Figure 16: Sketch of the holder setup with the bolt mounted	37
Figure 17: Linear part of the stress-strain curve	37
Figure 18: Offset yield stress and strain determined from the curve	38

Figure 19: ANSYS setup for verifying the tensile results.....	38
Figure 20: ANSYS result that shows the difference of deformation in the outer and inner parts of the threads	39
Figure 21: Sketch of tensile testing and assembly of bolt and flange	40
Figure 22: Before and after picture of flanges after cleaning and machining.....	41
Figure 23: Holders with a bolt mounted in the tensile testing machine	46
Figure 24: Setup for immersed testing with the left showing the solution at room temperature and the right one showing the temperature at 90 °C.....	50
Figure 25: Electrical linear actuator with specifications	51
Figure 26: Overview of Arduino setup	52
Figure 27: Close up of wiring	53
Figure 28: Framework with actuator and bolt assemblies.....	54
Figure 29: Inspection jig for visual inspection of bolts.....	55
Figure 30: Bolts after tensile testing	62
Figure 31: Details of SA bolts from test 1 of immersed testing at 90 °C.....	65
Figure 32: Details of CS bolts from test 1 of immersed testing at 90 °C.....	65
Figure 33: Details of the fractures. a) showing the surface of the fracture (10X), b) showing the crack in the nut for SA:1 (10X), c) the surface of the fracture for SA:2 and d) showing the surface of the fracture for CS:2	66
Figure 34: Details of CS bolts from the immersed testing at 90 °C.....	67
Figure 35: Progress pictures of the SA:6 bolt with hours in the test solution.....	67
Figure 36: Progress pictures of the 316L bolts alternate immersion experiment for 936 hours ...	68
Figure 37: 316L bolts from alternate immersion testing after cleaning	69
Figure 38: a), b), c) and d) showing pits at the root of the threads at approx. 10X. Picture e) shows a crack going from the top of the thread towards the root and f) shows the root before the experiment.....	69

Figure 39: Progress pictures of the SDSS CS:4 bolt in the alternate immersion experiment for 936 hours 70

Figure 40: The SDSS bolts after alternate immersion testing for 936 hours 70

Figure 41: Details of the pitting on the CS bolts. a) shows the pit on the top of the bolt (CS:3) on the side of the thread and b) shows the pit in the center of the bolt (CS:4) at the root of the thread 71

Figure 42: Supersaturated test solutions produced stalactites 76

Abbreviations

ASTM	-	American Society of Testing and Materials
BCC	-	Body Centered Cubic
CS	-	Cold Strained
DSS	-	Duplex Stainless Steels
FCC	-	Face Centered Cubic
HBW	-	Brinell Hardness measured with a spherical tungsten carbide ball
HISC	-	Hydrogen Induced Stress Cracking
IGC	-	Intergranular Corrosion
IMOA	-	International Molybdenum Association
MDS	-	Material Data Sheet
MSDS	-	Material Safety Data Sheet
PREN	-	Pitting Resistance Equivalent Number
ROA	-	Reduction of Area
SA	-	Solution Annealed
SCC	-	Stress Corrosion Cracking
SDSS	-	Super Duplex Stainless Steel
SEM	-	Scanning Electron Microscope
SS	-	Stainless Steel
TEM	-	Transmission Electron Microscope
TPI	-	Threads Per Inch
UIS	-	University of Stavanger
UNC	-	Unified Coarse Threads
UTS	-	Ultimate Tensile Strength

1 Introduction

1.1 Background

For new constructions today there is a lot of discussion on what materials to use on the bolts for example in subsea or topside environments where the materials are exposed to chlorides. Risk of corrosion makes the initial choice of materials crucial in order to avoid having to replace the bolts before the expected lifetime or failure. Regarding corrosion there is many different parameters that need to be evaluated as corrosion is very environment specific. A material may be ideal for one specific environment while in another one it may fail after a very short time. The potential cost of choosing the wrong material is huge and the decisions should therefore be evaluated with focus on results from research and experience.

As well as having different materials to select from, there is also the possible effect of different manufacturing methods affecting the stress corrosion and pitting resistance. The motivation for this thesis is to evaluate if there is a difference in stress corrosion resistance and pitting resistance between cold strained and solution annealed bolts in super duplex stainless steels based on the manufacturing method. Also testing the bolts in as received condition might give valuable information in regards to the standard test specimens that are usually used for testing.

1.2 Scope of work

The focus of this thesis is to compare the stress corrosion resistance and the pitting resistance of super duplex stainless steel (SDSS) bolts that have different manufacturing methods. One type of bolts have been solution annealed (SA) while the other are cold strained (CS). There has also been performed testing on an austenitic stainless steel to compare the results and to verify the test setup.

Also to be able to determine that the bolts are in yield when tested, tensile testing were performed.

The layout of this thesis is therefore the following.

- An overview of super duplex stainless steels (SDSS)
- A summary of the corrosion mechanism that are relevant
- Review earlier studies and theory on the subject
- Evaluate and choose parameters to perform experiments according to
 - Procure / design / construct equipment for the experiments
- Perform experiments
 - Tensile testing of the bolts

- Torqueing of bolts
- Create test jig
- Immersed testing with heating
- Alternate immersion testing

1.3 Limitations of the thesis

Some simplifications are done in this thesis including use of commercial grade chemicals as opposed to laboratory grade chemicals, and also the use of tap water instead of laboratory grade distilled water.

The experiments are performed according to modified standards as it was not easily available laboratory equipment to reach all the requirements defined in the standards with the given dimensions of the specimens used in the testing. Also the experiments are performed directly on the bolts in as received condition instead of producing test specimens according to the standards.

The time schedule was also limited as when all the parameters were determined and the test setup was ready, it was only around 2 months left available for testing.

It was evaluated to perform hydrogen induced stress corrosion (HISC) testing, but this was not possible in the short timeframe of the experiments.

1.4 Method

A standard outline of the project was created to obtain an outline to help during the pre-study. This highlighted the important aspects and defined the main chapters and subchapters.

To keep track of the progress a Gantt diagram was used, and this was updated regularly to identify the progress. Some tasks were also defined in a work breakdown structure (WBS) to further aid with the planning.

The experimental part of this thesis required a lot of planning. A pre-study was performed on what parameters and the amount of testing required.

Materials and other equipment needed to be purchased or procured for the test setup, and machining of the required components had to take place afterwards.

There was also the building and programming of the test jig for the alternate immersion tests which needed to be constructed.

2 Theory

2.1 Duplex Stainless Steels

Stainless steels is the name of a family of steels consisting of minimum 10,5 % chromium. There are several different grades of stainless steels and the five basic families are [1]:

- ferritic
- martensitic
- austenitic
- duplex
- precipitation hardened

Sorting into families by microstructure is due to the similarities of the mechanical and physical properties of each type of microstructure. The precipitation hardened family is based on the type of heat treatment performed [1].

The modern DSS can be divided into groups according to their corrosion resistance as shown in Table 1. The corrosion resistance is measured according to the empirical relationship between the additions of chromium, molybdenum and nitrogen. This number is defined as the pitting resistance equivalent number (PREN) and larger numbers indicate better corrosion resistance [2]. The equation for calculation the PREN is given in (1). The effect of the different alloy materials regarding the corrosion resistance is discussed in more detail in subchapter 2.2.

$$PREN = \%Cr + 3.3 \times \%Mo + 16 \times \%N \quad (1)$$

Table 1: Overview over the different duplex steels [3]

<i>Description</i>	<i>Weight % Cr</i>	<i>Weight % Mo</i>	<i>PREN</i>
Lean duplex	19 – 24,5	0,1 – 0,8	21 – 28
Molybdenum - containing lean duplex	19 – 25	0,3 – 2,0	27 – 34
Standard duplex	24 – 27	0,8 – 3,5	33 – 38
Super duplex	24 – 30	1,5 – 5,0	38 – 43
Hyper duplex	26 – 33	3,0 – 5,0	49 – 53

The first generation of stainless steel was developed almost hundred years ago [4]. While the first grades were ferritic and austenitic steels, it was discovered that introduction of ferrite into austenitic steels resulted in better castability, and also increased the mechanical properties. This combination of the ferritic and austenitic microstructure became known as duplex (double or

twofold) steels due to the steels consisting mainly of two phases. In effect they combine the toughness and weldability of the austenitic steels, with the strength and corrosion resistance of the ferritic steels [5].

DSS's were developed to increase the resistance to chloride stress corrosion cracking (SCC) that the austenitic stainless steels in the 300 series were susceptible for. Also by reducing the level of nickel as well as obtaining higher strength, the material costs were reduced [6]. One alloy that was specifically designed for increased chloride stress corrosion resistance was the 3RE60 (UNS S31500) developed by Sandvik in the 1950s [4]. The forerunner to the modern 25 Cr DSS, and later the super duplex stainless steels (SDSS) was Ferralium. This was deliberately added nitrogen, which reduced the problems with cracking during casting and welding by producing more ductile welds [4].

There has been a great interest in DSS due to the attractive service properties and the excellent cost versus properties ratios in the oil and gas, chemical industry, pulp and paper industry and other industries. In the early 1980s the DSS had established itself as a common engineering material [7]. Even if the production of DSS is only about 1 % compared to the carbon steel production as seen in Figure 1, these materials have been getting a lot of interest [8]. SDSS represents about 10 % of the total DSS production [8].

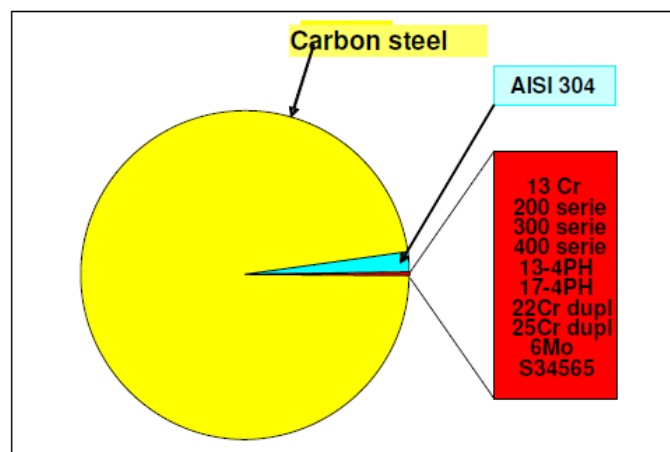


Figure 1: Stainless steel worldwide production compared to flat carbon steel [8]

The SDSS are usually defined as having a PREN above 40. They were developed for the Norwegian sector of the North Sea to meet alloy compositions [2]. As these materials contain a high amount of chromium, molybdenum and nitrogen, they offer high pitting and crevice corrosion resistance.

2.2 The role of alloying elements in SDSS

Understanding the effect of the different alloying elements is crucial when SDSS are manufactured. The role each element has in the total composition is important for the microstructure and again the corrosion resistance and the mechanical properties. Also the interactions between the major alloying elements are complex. Obtaining the correct levels of each alloying element is crucial to achieve a stable duplex structure that responds well to fabrication and processing [3]. The main alloying elements and their properties are discussed next.

2.2.1 Chromium

Stainless steels are dependent on a passive surface film of chromium oxide to resist corrosion. The minimum level of chromium required is 11 % and there also need to be oxygen present to form this layer [5]. This is due to the fact that the passive range is extended which further reduces the general corrosion as can be seen in Figure 2.

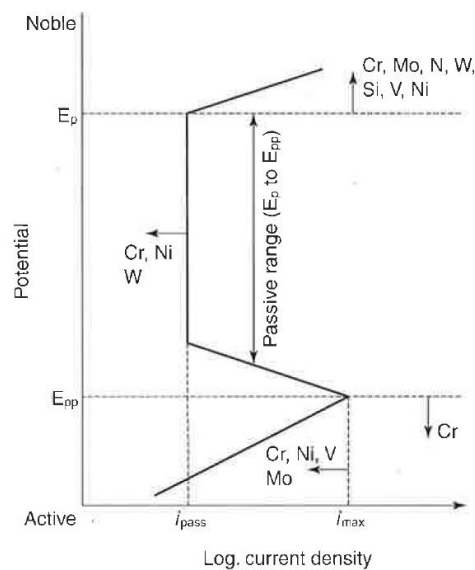


Figure 2: Effect of alloying elements on the anodic polarization curve [7]

This film is self-healing in air at room temperature and it is crucial that this passive film is maintained for the steel to maintain the corrosion resistance. Also the corrosion resistance increases with increasing chromium content. As chromium is a ferrite former, this means that adding chromium promotes the body-centered cubic (BCC) structure of iron. The higher the chromium contents are, the more nickel is necessary to form an austenitic or duplex structure [3]. There is however a limit to how much chromium that can be added, as the beneficial effects of very high levels is negated by the enhanced precipitation of intermetallic phases such as the

sigma phase [7]. As seen from equation (2) and (3), equations have been derived to quantify the elemental effects.

$$Cr_{eq} = \%Cr + \%Mo + 0,7 \times \%Nb \quad (2)$$

$$Ni_{eq} = \%Ni + 35 \times \%Cr + 20 \times \%N + 0,25 \times \%Cu \quad (3)$$

These equations need to be balanced to obtain the wanted percentage of ferrite / austenite balance [7].

2.2.2 Carbon

Carbon is an important alloy element to consider for stainless steels. DSS are limited to 0,02 – 0,03 % carbon content. If the carbon content is higher than 0,03 %, carbide precipitation in the form of chromium carbide may occur [5]. When chromium carbide is formed it depletes areas of chromium from the matrix below the critical amount, and in effect stops the chromium oxide forming. The depleted zones will then act as anodes and the rest of the oxide coated material as cathodes [5]. Quenching the material from 1000 °C will negate the carbide precipitation. However if the material is reheated by for example welding, carbide precipitation may occur on the grain boundaries. The material is then said to be sensitized which is dangerous in regards to corrosion as the chromium content is lowered. This makes the material susceptible to intergranular corrosion if not corrective measures as reheating is taken [5]. Several issues have occurred with austenitic stainless steels due to sensitization. Today however both AISI 316 and AISI 304 austenitic steels can be acquired with carbon content below 0,03 % and are assigned as AISI 316L and AISI 304L.

2.2.3 Molybdenum

Molybdenum is a ferrite former and increases the resistance against pitting corrosion. If there is 18 % or more chromium added, adding molybdenum becomes three times as efficient as chromium additions in regards to pitting and crevice corrosion. This also is evident in the PREN equation where molybdenum has a coefficient of 3.3 [3]. Also according to Trethewey and Chamberlain [5] it has been shown that highly alloyed steels containing molybdenum are more resistant to SCC. The reason molybdenum increases the pitting and crevice corrosion resistance is that it suppresses active sites via formation of an oxy-hydroxide or molybdate ion [7]. As with chromium, there is an upper limit where adding more molybdenum enhances the sigma formation. According to Gunn [7] this is around 4 %, while a minimum limit is set at 3 % to avoid crevice corrosion.

2.2.4 Nitrogen

Nitrogen increases the pitting and crevice corrosion resistance and also increases the strength of the material. As chromium and molybdenum, nitrogen increases the passive potential and it has also been suggested that molybdenum and nitrogen has a synergistic influence on pitting characteristics [7]. Nitrogen is a very cheap alloying material and a strong austenite former, and can be used to replace some of the nickel content in regards to austenite stabilization [3]. This results in improved toughness in nitrogen-bearing DSS due to the greater austenite content and less intermetallic content. The reason there are less intermetallic phases is due to the fact that nitrogen delays the formation of intermetallic phases such as sigma and chi [3]. Nitrogen also increases the resistance to crevice corrosion, which is due to nitrogen altering the crevice solution chemistry [7]. According to Gunn [7], both carbon and nitrogen strengthens the ferrite and austenite by dissolving at interstitial sites in the solid solution. However as carbon increases the risk of sensitization, nitrogen is preferred.

2.2.5 Nickel

The main role of nickel as an alloy element is to control the phase balance. Nickel is an austenite stabilizer that promotes a change in the crystal structure of stainless steel from BCC (ferritic) to face-centered cubic (FCC) (austenitic). It stabilizes austenite according to equation (3). The amount of nickel is therefore dependent on the chromium content, and in a DSS it is approximately 7 %. As nitrogen, the nickel delays the formation of detrimental intermetallic phases, but it is not as effective as nitrogen [3]. As with both chromium and molybdenum, too high nickel content may enhance the formation of intermetallic phases. It will accelerate the alpha prime formation, which is an intermetallic phase in ferrite that causes embrittling [7]. In regards to corrosion it extends the passive range as chromium and molybdenum.

2.2.6 Manganese

According to Gunn [7], the ability of manganese as an austenite stabilizer is debated, especially at the levels normally found in duplex alloys. Manganese additions increase the abrasion and wear resistance and also the tensile properties without loss of ductility. Too high content of manganese may also significantly decrease the critical pitting temperature. This is likely caused by the manganese sulphide inclusions that may act as initiation sites for pits. But for normal levels, adding both manganese and nitrogen will increase the pitting resistance [7].

2.2.7 Copper

Copper additions are beneficial in certain environments like boiling *HCl* by reducing the crevice corrosion rates. The maximum of copper content is limited to 2 % as higher contents reduce the hot ductility and can lead to precipitation hardening [7].

2.2.8 Tungsten

Tungsten has been added to duplex alloys up to 2 % to improve the pitting resistance, by extending the passive potential range. Also tungsten increases crevice corrosion resistance in heated chloride solutions [7].

2.3 Microstructure of SDSS

The microstructure of the SDSS is controlled by the alloying elements. In the modern raw material the balance between ferrite and austenite should be 50/50 for the optimum corrosion resistance, especially SCC resistance [1]. However it is generally accepted that the favourable properties of SDSS can be achieved with both ferrite or austenite in the 30 – 70 % range [3]. Figure 3 shows three different microstructures; ferritic, duplex and austenitic. By adding nickel which is an austenite stabilizer it clearly shows the transformation in the microstructure from ferritic, to duplex and finally to austenitic.

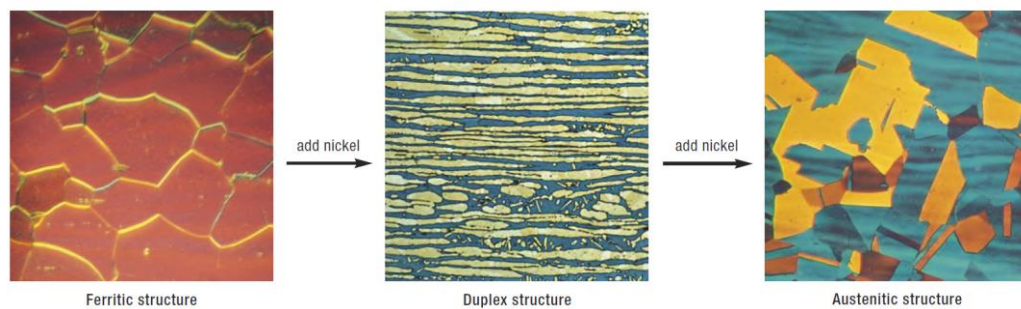


Figure 3: Different microstructures of steel [3]

The microstructure consists of a mix of roughly 50 % FCC austenite islands in 50 % BCC ferrite grains. This structure is achieved by having control of both the chemical composition and the annealing temperature.

There are different phase diagrams like Schaeffler diagrams available that show different phases at different temperatures and nickel and chromium additions [7]. To get an accurate result however, a computer program called ThermoCalc, which calculates the phase equilibria over a range of temperatures, is used. Figure 4 shows a calculated phase diagram for a SDSS alloy.

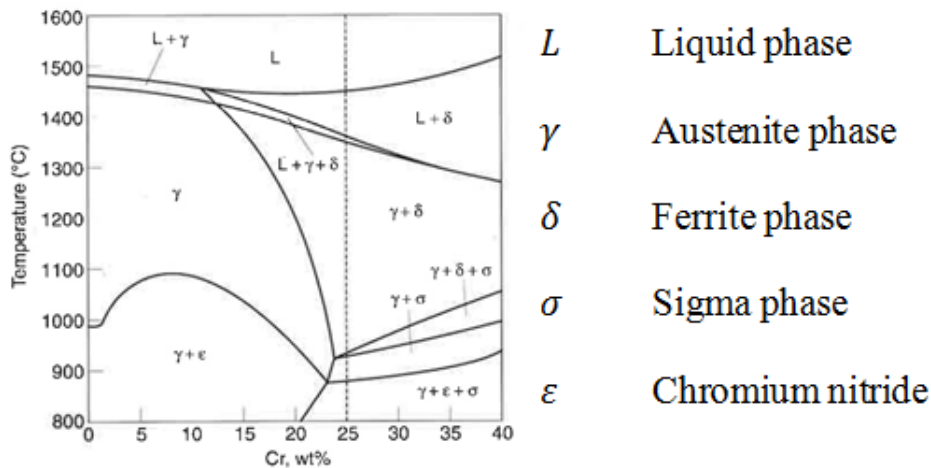


Figure 4: Thermocalc isopleth diagram showing the composition of a SDSS alloy at the dotted line [7]

The sigma and chromium nitride are intermetallic phases which will occur at different temperatures, depending on temperature, rate of cooling and the weight percent of the different alloying elements [7]. From these diagrams the temperatures when the different phases are stable can be determined.

2.3.1 Secondary phases

There are several undesirable secondary phases that occur in DSS during heat treatment. The phases may have an effect on both the mechanical properties and corrosion resistance, which again means they should be evaluated and checked for thoroughly. Usually time-temperature transformation (TTT) diagrams are used to show the heat treatment versus the rate of cooling [7]. Figure 5 shows a TTT diagram with three different SS solution annealed at 1050°C. The effect of quenching in regards to avoiding the detrimental secondary phases are obvious. The study of the secondary phases is performed either via a scanning electron microscope (SEM) or a transmission electron microscopy (TEM).

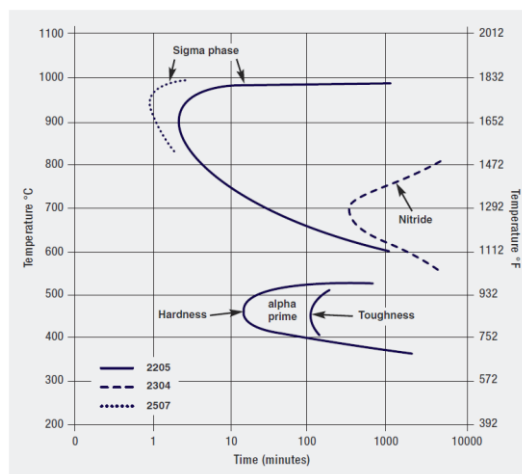


Figure 5: TTT diagram showing three different duplex steel grades 2205 (DSS), 2304 (lean DSS) and 2507 (SDSS) [3]

Modern manufacturing of DSS today have been designed to retard the formation of these phases. However if they are formed, the only way to remove them is solution annealing followed by quenching [7].

Sigma Phase

The high chromium content in SDSS means that the sigma phase is very common. The high amount of molybdenum will also increase the temperature range where the sigma phase is stable [9]. The sigma phase which is rich in both chromium and molybdenum will affect both hot ductility and room temperature ductility. In effect it is a hard embrittling precipitate [7].

The precipitation of the sigma phase usually occurs at triple junctions or at ferrite / austenite phase boundaries at the temperature range of 600 – 1000 °C [7]. Also the presence of sigma phase will decrease the pitting resistance due to the depletion of chromium and molybdenum from surrounding areas [3].

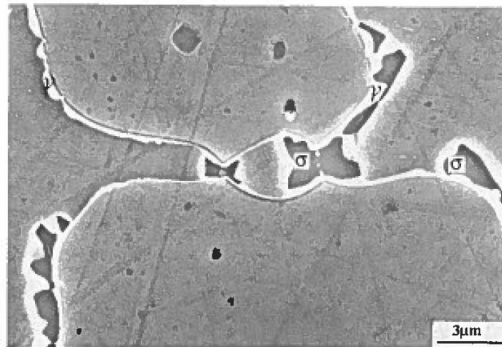


Figure 6: Microstructure of a SDSS SAF 2507 (UNS S32750) aged for 10 min at 850 °C. σ phase is shown at ferrite / ferrite phase boundaries and secondary austenite is visible in bright contrast between the primary austenite and ferrite (SEM) [9]

Secondary austenite

Secondary austenite (γ_2) can form very quickly as the decomposition of ferrite to austenite can occur over a wide temperature range [9]. This is due to the fact that the duplex is quenched from a higher temperature where the equilibrium fraction of ferrite is higher [9]. The secondary austenite formed at the ferrite / austenite phase boundaries has low chromium content, especially when Cr_2N precipitates are present. This means that these areas are more prone to pitting [9].

Chromium nitride

Chromium nitrides can be found both as CrN and Cr_2N . As nitrogen has become more used as an alloying element these nitrides are important to consider. During solution annealing the nitrogen solubility in ferrite is high. When quenching however the solubility drops, and intergranular precipitation of needle shaped Cr_2N occurs [7]. When Cr_2N is formed at

austenite/ferrite phase boundaries, it has an impact on the pitting corrosion resistance according to Nilsson [9].

Alpha prime

The secondary phases that forms at the lowest temperature range (300 – 525°C), is called alpha prime. These are the cause of the 475°C embrittlement which may occur in ferritic and duplex SS. According to Gunn [7] there has been some conflicting evidence as to the nature of this embrittlement, as alpha prime may precipitate together with Cr_2N where the needlelike Cr_2N is interspersed within a film of alpha prime.

2.3.2 Summary of secondary phases

Table 2 shows a summary of the secondary phases that can be found. As discussed these phases have a negative impact on both the corrosion resistance and the mechanical properties in regards to embrittlement.

Table 2: A summary of properties of some of the secondary phases present in SDSS [7]

<i>Phase</i>	<i>Composition (%)</i>			<i>Form. range (°C)</i>	<i>Lattice type</i>	<i>Preferred location</i>
	<i>Cr</i>	<i>Ni</i>	<i>Mo</i>			
Sigma	30	4	7	600 - 1000	Tetragonal	Inter ferrite/aust.
Secondary Austenite	27,4	8,7	4	650 - 900	FCC	Intra-ferrite
Chromium nitrides	72	6	15	700 - 950	Cubic	Intra-ferrite
Alpha prime	65	2,5	13	300 - 525	BCC	Intra-ferrite

2.4 Mechanical properties of DSS and SDSS

The mechanical properties of DSS are exceptional, and their room temperature yield strength is more than double of standard austenitic stainless steels [3]. The ultimate tensile strength is also very high with an elongation above 25 % [7].

The background for these properties is that several simultaneous mechanisms take place [7].

- Interstitial solid solution hardening (C, N)
- Substitutional solid solution hardening (Cr, Mo, Ni, etc.)
- Strengthening by grain refinement due to the presence of two phases
- Possible hardening due to the formation of secondary austenite (γ_2)
- Strengthening due to ferrite, since, for a similar composition these phases are harder than the austenitic structure

- Strain induced by differential contraction of the two phases on cooling from annealing temperatures

It is also important to consider the rolling direction of the material. The mechanical properties of wrought DSS are highly anisotropic. This means that the properties heavily depend on the orientation of the test sample [3]. As the material is rolled the grains will become elongated. The strength is therefore higher perpendicular to the rolling direction than in the rolling direction [7]. The anisotropy also increases as the plate thickness decreases [7].

Maximum and minimum hardness is also required in some standards. Normal solution annealed DSS have no problems being within these (approx. 277 - 321 HBW). Cold straining and / or intermetallic precipitation however will have an impact on the hardness [7]. This is also shown in Figure 7.

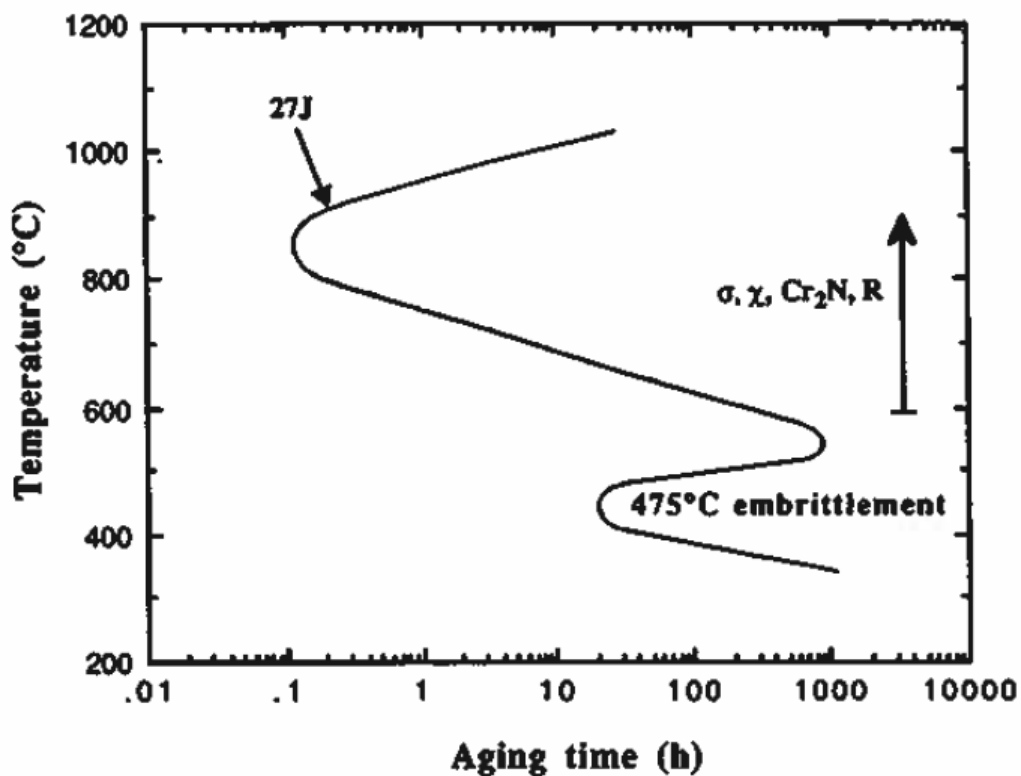


Figure 7: Time-temperature-transformation (TTT) diagram for SAF 2507 (UNS S32750 SDSS) with a curve corresponding to 27J impact toughness indicating rate of embrittlement [9]

The downside with the excellent mechanical properties of DSS is that machining will take more time and the wear and tear on the machining tools will be higher than with austenitic SS.

2.5 Corrosion theory

2.5.1 Background

There are several sources for what corrosion costs the society. According to Trethewey and Chamberlain [5], a number that is frequently used is around 4 % of a country's gross national product (GNP). Also Ahmad [10] reports the figures of 3 – 5 % of a country's GNP and that appropriate corrosion prevention measures could have saved 35 % of this cost. Corrosion has an impact in a lot of different ways and the six major reasons are listed below [5]:

- Lost production due to failure or shutdown
- High maintenance cost
- Environmental and customer regulations
- Loss of product quality due to contamination from corrosion
- Higher fuel / energy costs due to leaks from corroded piping
- Increased stocks of spare parts

Prevention of corrosion is therefore important and the different forms of corrosion need to be considered when choosing materials.

2.5.2 Basics of corrosion mechanics

According to Trethewey and Chamberlain [5] a fundamental definition of corrosion is described as:

Corrosion is the degradation of a metal by an electrochemical reaction with its environment.

To understand corrosion the basic principles of thermodynamics form the foundation.

The first law of thermodynamics [5]:

Energy cannot be created or destroyed

A variation of the second law of thermodynamics [5]:

Heat will not flow of its own accord from a cold place to a hot place

In a corrosion perspective, this energy comes from the chemical energy of a reaction.

A common way to explain corrosion is via the mixed potential theory proposed by Wagner and Traud in 1938 [10]. This theory separates the oxidation and reduction reactions in corrosion and states that the total oxidation rates equal the total reduction rates [2].

Corrosion occurs when a chemical process is made possible by a net release of free energy that goes across a metal or electrolyte interface [5]. This free energy is defined by Faraday as the work done in the corrosion process in terms of the potential difference and the charge transported as shown in equation (4) called Faraday's Law. This energy difference manifests as an electrical potential, which against means a tendency for corrosion [5].

$$\Delta G = (-zF) \times E \quad (4)$$

Where:

ΔG The work done

z The number of electrons involved in the corrosion reaction

F The Faraday constant (96494 coulombs per mole)

E The potential measured in volts

Further work by Nernst defines the potential according to equation (5).

$$E = E^0 - \frac{RT}{zF} \ln \frac{[products]}{[reactants]} \quad (5)$$

Where:

E The standard cell potential (Volt)

E^0 The cell potential at a given temperature (Volt)

R Universal gas constant ($8.3143 \text{ J mol}^{-1} \text{ K}^{-1}$)

T Temperature (Kelvin)

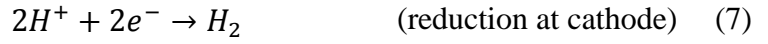
z Valence electrons (no unit)

$[products]$ Concentration of product (mol/liter)

$[reactants]$ Concentration of reactants (mol/liter)

The Nernst equation defines the non-equilibrium potential caused by the reaction for a given temperature and concentrations of the products and reactants [5].

In a corrosion cell four essential components needs to be present; anode, cathode, electrolyte and connections. All these components can be present by just having one piece of metal in an electrolyte as individual areas of the metals can act as anodes and cathodes due to differences in material or the electrolyte [5]. Multiple reactions will occur and if we consider when iron corrodes in a dilute acid we get the following equations [10]:



Equation (6) shows the oxidation of iron as it is exposed to the acid, equation (7) the formation of hydrogen gas and (8) the total equation. Using the Nernst equation at standard conditions (25 °C) for this chemical process ($\frac{RT}{F} = 25,693 \text{ mV}$) will give equation (9). By further including the valence electrons z as two and setting the concentration of $[H^{+}]$ and $[H_2]$ as 1 M gives equation (10). Finally inserting the iron ions concentration at 1 M produces equation (11).

$$E = E^0 - \frac{0.05916}{z} \log \frac{[\text{products}]}{[\text{reactants}]} \quad (9)$$

$$E = E^0 - \frac{0.05916}{2} \log [Fe^{2+}] \quad (10)$$

$$E = E^0 - \frac{0.05916}{2} \log [1] = E^0 \quad (11)$$

This means that the measured potential difference is the electrode potential under standard conditions, and that it is given by E^0 . As equation (6) is an oxidation reaction and equation (4) is larger than zero it indicates a spontaneous reaction. By using the electrochemical series [5], it will give a standard *reduction* potential of iron as $E^0 = -0.44V$ which gives $\Delta G > 0$. This agrees with the fact that iron dissolves spontaneously in acid.

2.5.3 Corrosion kinetics

As it is now clear how corrosion is a tendency of a system to corrode, the flow of current also needs to be considered. When the corrosion reaction is not in equilibrium, current will flow, and the relationship between the potential and this current flow is important to understand [5]. However, using only current in ampere would not account for the fact that a larger surface would corrode more than a small one [5]. This is accounted for by using current density as ampere per area. A positive or negative value of this current density will determine which way the current flows. Showing a variation of equation (6) in (12) and (13), it indicates this flow of current where i_a is the anodic current and i_c is the cathodic current.



When equilibrium arises we have that $i_a = i_c$ and this current cannot be measured as there is no net current flow.

2.5.4 Passive layer

The corrosion properties of a DSS are defined by the ability to maintain the passive layer in the given environment it is to operate. This state in which the stainless steel has a very low corrosion rate is called passivity [2]. Passivity is usually described by a polarization curve which is shown in Figure 8.

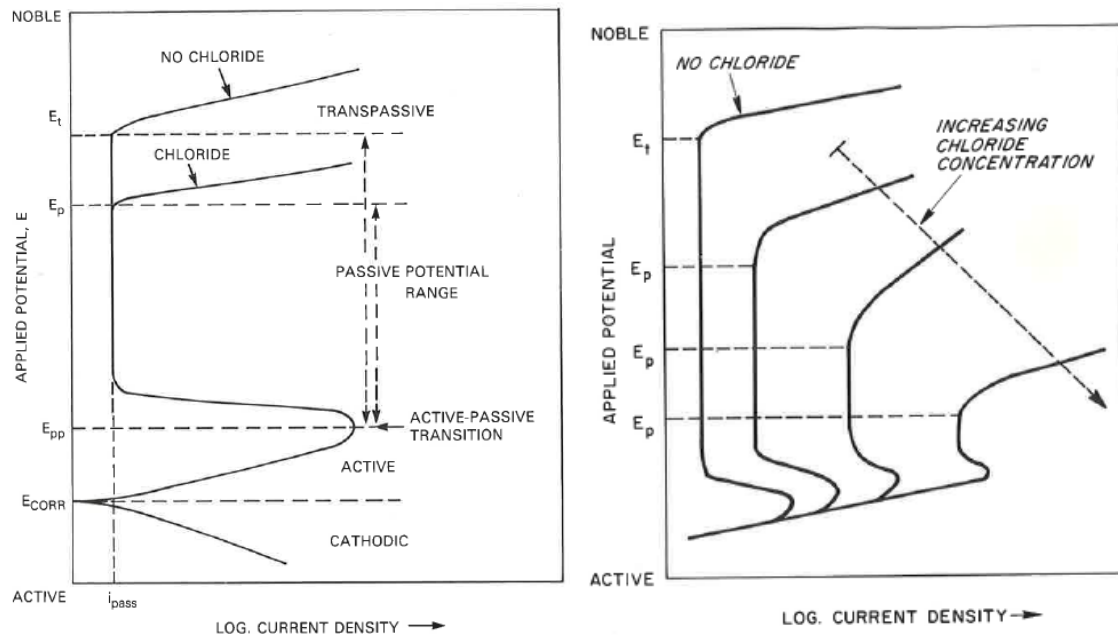


Figure 8: A polarization curve for a stainless steel in a sulfuric acid solution and also showing the pitting potential decreasing as the chloride concentration is increasing [2]

Several thresholds are defined, as well as the effect of chlorides on the passive region.

- E_t Transpassive potential, defines the end of the passive region and where gaseous oxygen evolves by electrolysis of water. This is the onset of the transpassive region
- E_p Pitting potential, defines a sudden increase in current density due to breakdown of the passive layer in chloride containing environment
- E_{pp} Primary passivation potential; defining where the active-passive transition begins
- E_{CORR} Corrosion potential, the compromise potential of the anode and cathode
- i_{pass} Passive current density; defining the minimum current to maintain the film in the passive range. Corrosion rates are usually very low in this region.

This means that the passive potential is defined between E_{pp} and E_p . The passive layer as shown in Figure 9, shows how it is both repaired and broken down. In the case of (a) and (a'), the metal ion (M) is captured by the passive layer and it is bridged together with the hydroxyl (OH^-) groups [2]. This means the layer is repaired and the corrosion resistance is maintained. In the case of (b) and (b') the environment contains chloride (Cl^-) ions, which has replaced some of the water molecules (OH_2). The bridging is then not possible which again causes a breakdown of the film.

These sites with a missing layer will be initiation sites for pitting corrosion [2].

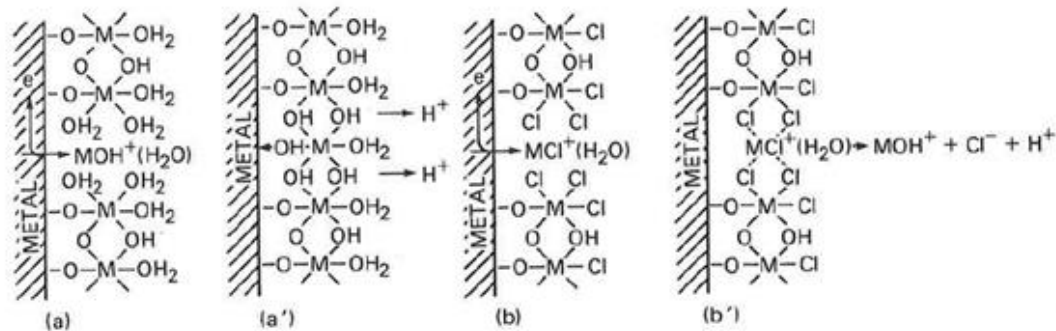


Figure 9: The passive layer is repaired in a', while destroyed in b' [2]

Metallurgical factors also needs to be considered on the metal on which the passive layer forms or is broken down on, as these are as important as the chemistry of the environment. As discussed earlier, the metal consists of several different alloying elements, secondary phases, carbides, nitrides etc. which will influence if the passive layer is able to maintain itself or not [2].

2.6 Corrosion of SDSS

The three most applicable types of corrosion for this thesis in regards to SDSS are pitting, crevice and SCC.

2.6.1 Pitting corrosion

Pitting is a form of localized corrosive attack that produces pits [2]. Metals with passive films are more susceptible to this type of corrosion. It is characteristic that these pits only form on small areas while the bulk of the surface is not affected, meaning the weight loss caused by this type of corrosion is minimal, but the result of the attack may cause major failures [10].

Conditions for pitting are listed below [10]:

- Breaks in the passive film or defects / injuries / lack of homogeneity in the metal surface
- Presence of halogen ions like Cl^-

- Stagnant conditions, no circulation of the electrolyte will increase the pitting

The mechanism of pitting [2]:

Pitting initiation

Breaks in the passive film are attacked and metal is dissolved as an anode while the rest of the surface acts as a cathode where oxygen forms into hydroxyl groups.

Pitting propagation

Accumulation of positive metal ions in the pit will cause a self-stimulating and self-propagating effect known as hydrolysis. The presence of Cl^- and H^+ ions will stop the metal from repassivating as seen in Figure 10 and the pH will become very low in the pit.

Pitting termination

When the pitting process has been ongoing for a while, the metal is perforated and the reaction is terminated.

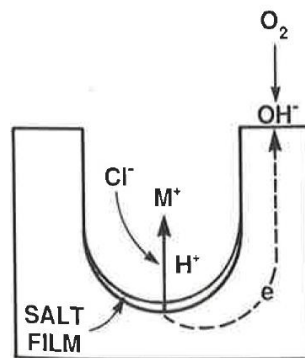


Figure 10: Illustration of the pitting mechanism [2]

The condition of the surface is important and heat treatment and cold working may have an impact here. The degree of cold work and environmental contamination like dust and salt particles will also have an effect [10]. Also grain size, inclusions and precipitation of secondary phases has an influence on the surface properties [7].

As discussed earlier, in a SDSS the addition of chromium and molybdenum will increase the pitting resistance, and the PREN is used to rank the pitting resistance of a given alloy.

To determine the severity of the pits the common weight-loss method is of little use.

Examination of the pits can be performed according to ASTM G46 which is described in chapter 3.1.3.

2.6.2 Crevice corrosion

Crevice corrosion is a form of localized corrosion that may occur within crevices or at shielded surfaces where a stagnant solution is present [5]. An important condition in regard to crevice corrosion is the formation of a differential aeration cell.

Crevice corrosion is highly associated with the geometry of structures such as riveted plates, gaskets, threaded components or depositions of sand or other particles [5].

The mechanism according to Trethewey and Chamberlain [5] can be described in the following steps:

- Corrosion initially is uniform over the surface and inside and outside of the crevice
- Consumption of dissolved oxygen results in the diffusion of more oxygen from electrolyte surfaces which are exposed to the atmosphere. There will be a lack of oxygen inside the crevice and the generation of hydroxyl ions will diminish.
- Production of excessive positive ions in the gap causes negative ions to diffuse into the crevice, and in the presence of chloride complex ions will be formed between the metal and chloride ions with water as shown in Figure 11. This will reduce the pH in the crevice and cause hydrolysis which again prevents the re-passivation.

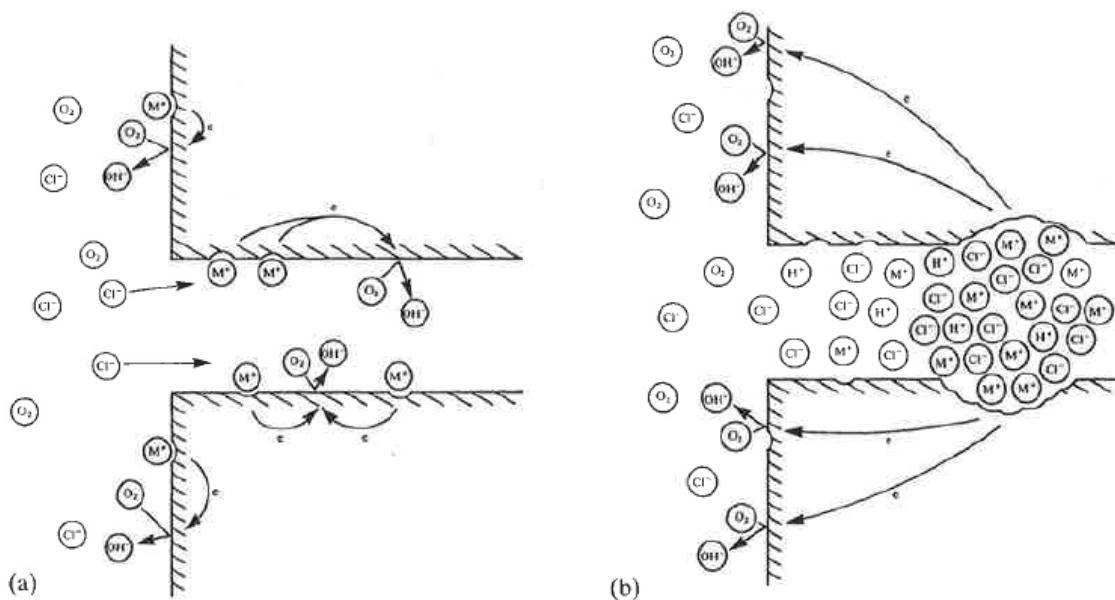


Figure 11: The Fontana-Green mechanism of crevice corrosion [5]

For stainless steels the crevice corrosion resistance can be related to pitting corrosion resistance. The critical crevice temperatures are roughly proportional to the critical pitting temperatures, however lower [7].

Testing for this type of corrosion is very difficult as the experimental parameters like surface condition, the material of the crevice formers like glass or plastic, and crevice width is very hard to control, which means that this type of corrosion will not be a high focus in this thesis. According to Gunn [7] it has been shown that SDSS grades are more resistant to crevice corrosion compared to 6 % superaustenitic alloys according to the fact that SDSS are more resistant to hydrochloric acid.

2.6.3 *Stress corrosion cracking*

SCC is when there is a failure due to the combined effect of stress and a chemical attack [10].

Conditions for SCC [10]:

- Susceptible metal
- Specific environment
- Tensile or residual stress

There are also different types of SCC classified according to if the environment contains chloride, sulfide or is caustic. This thesis will focus on chloride induced SCC. Other factors that will increase the risk of SCC is elevated temperature with high oxygen contents, high tensile stress compared to yield and presences of crevices or deposits [7].

An important feature of SCC is that it is much unexpected. Materials may fail in environments where they should be suited at stress levels below its normal fracture stress with little to no indication before failure [5]. Other important features that are of interest [5]:

- Alloys are more susceptible than pure metals
- Even if a metal is highly ductile, the SCC cracks will appear brittle.
- It is usually possible to define a threshold stress where SCC will not occur

DSS steels are all superior to the austenitic SS in regards to SCC, but they may suffer from SCC given high enough chloride concentration [7]. For austenitic alloys it also depends on the cation available with $Mg > Ca > Na$ in increasing order of aggressivity. This means that a solution of $MgCl_2$ is more aggressive in regards to SCC compared to a $NaCl$ solution [7].

The mechanism in which SCC works is complex and heavily dependent on environment and the type of material / alloy. It is generally accepted that there is no single mechanism for SCC [5]. Tables of alloy types in certain environments have been developed, but this is not a complete list as some combinations are still unknown. However it gives a good indication for a wide range of alloys [10]. Careful consideration needs to be taken when using these tables. This is due to the

fact that for example chloride levels due to seawater evaporation are hard to determine, and evaporated seawater may also deposit the aggressive *Mg* cations [7].

The cracking will generally occur in surface irregularities, corrosion pits or at the grain boundaries if these contain impurities. Further cracking is determined by the electrochemistry in the pit. In the pits the *pH* is of values as low as 2. This accelerates the dissolution process and also indicates that hydrogen is an important aspect in SCC [5]. The formation of a pit is therefore often the initiation phase of cracking. When the cracking begins, common fracture mechanics come into play. The crack growth will however not be examined in the experiments in this thesis, so this is not discussed further.

There have been several instances where chloride caused SCC has caused failure in the roof construction of swimming pools. Two types of mechanisms have been proposed for these failures. One considers the fact that a low *pH* chloride rich environment develops, while the other one considers that even higher chloride levels may be obtained at certain relative humidities [2]. There have been few studies on cases where solid salt deposits have been built up at lower relative humidities so it is not known how this affects SCC.

Due to the fact that DSS consist of both ferrite and austenite they have an advantage compared to austenitic steels. The ferrite will protect the austenite against SCC as ferrite has a lower corrosion potential in an acidified crack solution [7]. Meaning that when a crack in the austenite reaches ferrite, the mixed potential inside of the crack is depressed and the austenite is protected [7].

In DSS the cracking preferably occurs in the ferrite phase which is not expected due to the fact that ferritic steels are known for their increased resistance against this type of corrosion compared to austenitic steels. However the reason for this is that the ferrite in the duplex steel contains approximately 3 % nickel, compared to normal ferritic steels which are usually very low on nickel. The nickel therefore makes the DSS susceptible to SCC [7]. Figure 12 shows typical cracking in duplex steels in the ferrite and through both phases.

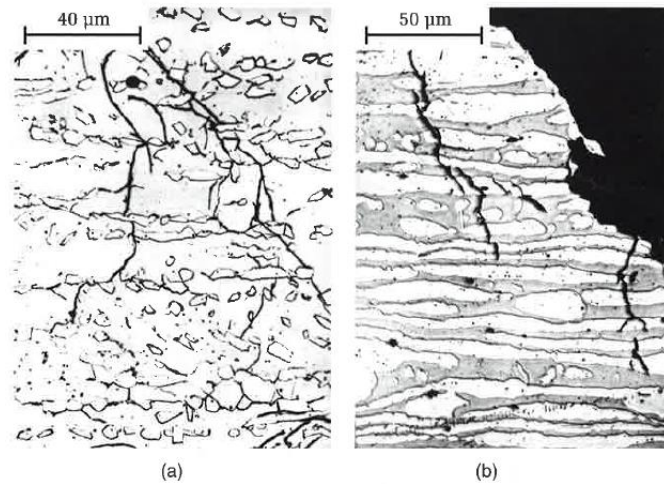


Figure 12: Examples of crack propagation where a) is showing cracking through the ferrite (500X) and b) is showing cracking through both phases (400X) [7]

2.7 Manufacturing methods of the materials used for the experiments

There are several methods used in the industry to enhance the properties of metals. In this thesis the two different processes used to obtain the required properties are solution annealing and cold straining. The two different manufacturing processes used for the materials in this thesis are described next.

2.7.1 Solution annealing

Solution annealing is a high temperature heating process performed on steels to avoid precipitation of intermetallic phases [1]. The purpose of this treatment is to keep the casting at a given temperature and time, long enough to bring the carbon in the steel into a solid solution. By quenching the steel in a specified medium, the carbon will be locked in the solid solution. Both the holding time and temperature depends on the material quality and the thickness of the casting. For SDSS it is very important to control the parameters to avoid intermetallic phases as discussed earlier.

2.7.2 Cold straining

Strain hardening is defined as the phenomenon where a ductile metal becomes harder and stronger as it is plastically deformed [11]. The reason this process is called cold straining or cold working is due to the fact that most metals strain hardens in room temperature. The change of mechanical properties is caused by dislocations, meaning linear defects in the lattice of atoms in a crystal [12]. Dislocations move under the influence of mechanical stress because of the shearing process that occurs when it is strained. During plastic flow the dislocations multiply and again their mutual interactions hinder their motions [13].

As seen in Figure 13, the effect of deforming the material increases the yield strength, but as a result it has a shorter elongation before fracture after the treatment.

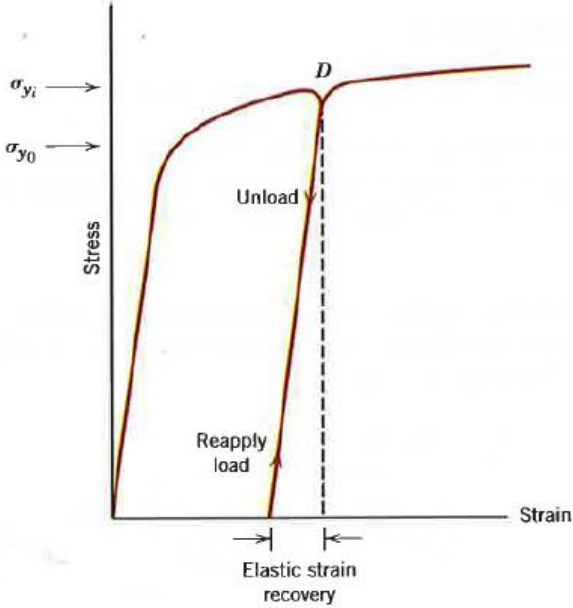


Figure 13: Stress-strain diagram showing the elastic strain recovery and strain hardening. Initial yield (σ_{y_0}) and yield (σ_{y_1}) after releasing the load D is shown [11]

The effect of cold work in regards to ultimate tensile strength (UTS) for different SS is shown in Figure 14.

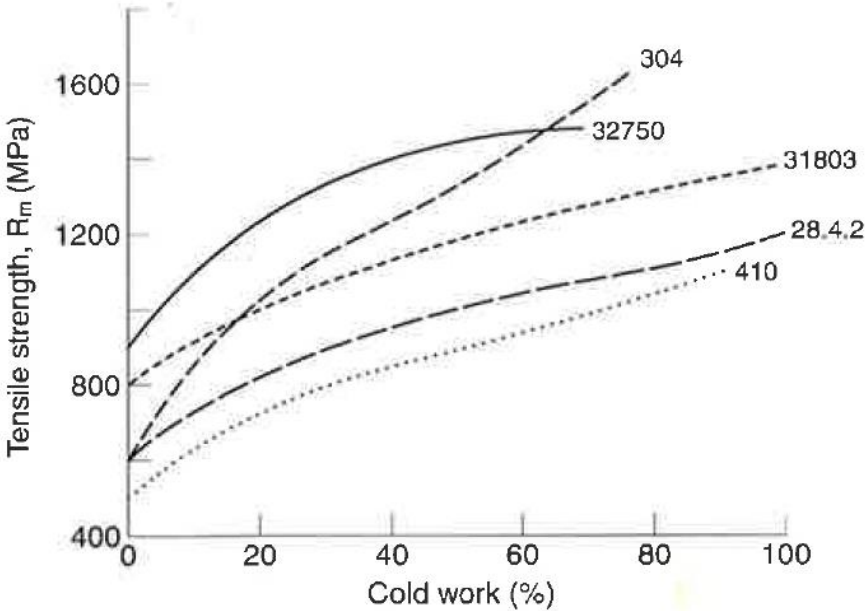


Figure 14: The effect of cold work in regards to UTS for several different SS [7]

2.8 Corrosion testing on SDSS in regards to SCC and pitting in chloride environments

Several earlier studies on SDSS and DSS in regards to SCC and pitting resistance have been reviewed to find the most suitable method of testing.

The influence of temperature and chloride concentration on the pitting resistance of a DSS was researched by Dong et al. [14]. The alloy was 2205 (DSS) and the environment was sodium chloride and iron chloride. The pitting experiments were performed according to the ASTM G48 [15] standard.

- The pitting resistance decreased when either the temperature or chloride concentration were increased.
- I_{corr} increases linearly with the concentration of $NaCl$
- Higher temperature and concentrations alter the shapes of the pits

Jin [16] studied the chloride induced SCC for a SDSS with different test methods. The ASTM G36 [17] standard for boiling magnesium chloride at 155°C was modified and it was decided to use calcium chloride instead due to the fact that magnesium chloride represents a too severe environment. As discussed earlier the type of cation highly affects the corrosion mechanism. A drop evaporation test was also used with droplets of sodium chloride at a concentration of 0,1M being applied at 6 drops/min. Finally an autoclave test were performed with oxygen content at 8 parts per million (ppm) and a pressure at 100 bar. The conclusions of this work were:

- SDSS steels possess a much higher SCC resistance than the austenitic AISI 304 or AISI 316
- Due to the mild nature of calcium chloride compared to magnesium chloride, calcium chloride is not deemed practical for lab testing due to the long lead time before fracture as 500 hours is not enough to time to develop SCC for highly alloyed SS.

Mietz and Isecke [18] discussed different test methods and the method of loading the specimens. There are three different methods for loading and they are classified as:

- Constant total elongation
- Constant load
- Slow strain rate

When constant load is used, the SCC sensitivity can only be assessed according to the following criteria:

- Fracture: yes / no
- Cracks: yes / no
- Depth and amount of cracks

Spaehn [19] did extensive work on SCC and corrosion fatigue cracking on several materials including the DSS UNS 32205. The experiments were performed in boiling magnesium chloride (35 %) at 125°C . The threshold stress for SCC was examined and compared with an austenitic SS 18Cr-9Ni. Also the effect of surface treatment in regards to SCC resistance was experimented on. Conclusions from this research:

- The threshold stress for SCC for an austenitic SS was about one third of the DSS
- A cathodic protection potential is found and this potential is similar for DSS and austenitic SS. A potential above $-0,12V$ decreased the resistance significantly in regards to SCC for both materials.
- The sigma phase lowered the resistance against anodic SCC.
- The surface treatment alters the SCC resistance. DSS that was pickled after grinding exhibited higher resistance than DSS that was only grinded and not treated.

2.9 Earlier studies on the manufacturing methods impact on corrosion resistance

There have been performed earlier experiments which have focused on the fact that the manufacturing method may affect the corrosion resistance in regards to both pitting and SCC for DSS. However the main focus has been to assess the difference of pitting corrosion between solution annealed and cold strained material, and there seem to be little available research on the difference in regards to SCC resistance. Also there is little research performed on SDDS, while the austenitic steels like AISI 304 or AISI 316 have received a lot of attention. Some of these earlier studies are discussed in this chapter.

2.9.1 Research on the effect of cold work on pitting corrosion resistance

As mentioned earlier the pitting resistance is measured by the PREN. A study performed by Rosso, Peter and Suani [1], focuses on the pitting resistance for solution annealed (SA) material versus cold strained (CS). Testing has been performed on diameters ranging from 14.3 - 47.62 mm. The alloy that was used for the experiments were the UNS S32760 SDSS. Four samples of both SA and CS material were tested and compared. The results show that both types of treatments give an acceptable $PREN > 40$, with the SA PREN being 41.48 and the CS PREN

being 41.39. There was a difference in the mechanical properties however, but this was most likely caused by the fact that the parameters for the SA were not optimized. These intermetallic phases, like sigma, then caused the material to be below the acceptance criteria in regard to the mechanical properties.

Work performed by Phadnis et al. [20], aimed to compare cold rolled (66 %) and heat treated AISI 304 in regards to the passive film. By analyzing the potentials and analyzing the film by X-ray photoelectron spectroscopy the differences was established. The main findings of this study are listed below.

- Rolled material shows a constant open circuit potential of -0.188 V while the heat treated is oscillating around -0.254 V
- Pitting potential of the rolled material was 0.25 V while it was 0.09 V in the heat treated
- The passive current density was $0.9 \times 10^{-6}\text{ A cm}^2$ for the rolled material while $1.5 \times 10^{-5}\text{ A cm}^2$ for the heat treated.
- Re-passivation of the pit occurred at 0.085 V in the rolled material while not at all in the heat treated material.
- The passive film formed on the rolled material is richer in chromium compared to the heat treated material. This is due to enhanced diffusion through the oriented grains in the rolled material.

Research on pitting corrosion resistance on CS AISI 316L with varying degree of nitrogen was performed by Mudali et al. [21]. The results showed that cold working up to 20 % enhanced the pitting resistance while a sudden decrease in pitting resistance were observed at 30 % and 40 % cold work. The main results from this study:

- Increased nitrogen content from 0.05 % to 0.22 % significantly decreased the pitting corrosion resistance of AISI 316L.
- Cold work from 0 – 20% increased the pitting resistance and this was more significant when the nitrogen content increased as well.
- Cold work from 30 – 40% decreased the pitting resistance and the decrease was higher with increasing nitrogen content.

A study performed by Peguet, Satpati and Muthe [22], on AISI 304 and AISI 430 also aims to determine the influence of cold work on the pitting corrosion resistance. According to Peguet et al. [22], earlier studies in this field are not conclusive if the pitting potential is higher or lower with CS compared to SA material. This is also true for the re-passivation. The conclusion of this research is the following:

- It may not be the strain induced martensite that is the main factor governing the sensitivity to corrosion.
- The highest pit dissolution is found at 20 % CS.
- The re-passivation ability decreases as the CS rate increases.

Renton, Elhoud and Deans [23] performed research on the corrosion behavior of a SDSS in regards to plastic deformation. As duplex steels contains two phases the cold work affects duplex steels in another way than the single phase austenitic steels. Work performed by Johannsson and Oden [24] discuss the load sharing between the austenite and ferrite in DSS. This shows that comparing the CS studies for austenitic stainless steels may not be applicable for DSS. The conclusions from Renton et al. [23] were:

- Cold work of 4 – 16 % plastic strain has positive effect on the pitting potential for a SDSS, and two critical levels of plastic strains at 8 and 16 % were detrimental for the pitting potential.
- Plastic deformation of austenite and ferrite develops in a nonlinear fashion with increasing plastic strain.
- The nonlinear relationship between pitting potential and plastic strain is caused by the changing surface area ratio of the cathodic austenite and the anodic ferrite which affects the strength of the galvanic couple between them.

Work performed by Elhoud, Renton and Deans [25] focuses on the manufacturing variables such as cold work, heat treatment and surface condition and their effect on the corrosion resistance. This work must be seen in context with the study performed by Renton et al. [23] as the authors are the same. The conclusions from Elhoud et al. [25] support Rentons et al. [23] work.

- Cold work improved the pitting resistance of the polished sample until a certain critical amount of plastic strain (approx. 15 %).
- The samples that were not polished and maintained their surface defects had increasing pitting resistance with increasing cold work, but had a critical level at 8 % plastic strain. The pitting resistance also decreased after 16 % like the polished samples.

It is obvious from these studies that there are many variables affecting the pitting corrosion resistance and that there still is research to perform. Conflicting results and small sample sizes also suggest that no definitive conclusion can be taken. The research however seem to agree that a degree below 15 – 20 % is beneficial for the pitting resistance, but the surface condition of the material also needs to be considered for this to hold true.

2.9.2 Research on the effect of cold work on stress corrosion cracking resistance

Research performed by Takizawa et al. [26] looks into different types of DSS's to determine the effect of cold work in regards to the SCC resistance. The materials have ferrite contents at 23, 51, 61 and 80 % which is obtained by adjusting the amount of nickel. The experiments were performed in boiling magnesium chloride and the times to failure were logged at the different amounts of cold work. The specimens were u shaped and bend to apply stress. The conclusions from this work are:

- The susceptibility of SCC was lowest for the sample which contained 51 % ferrite compared to the others.
- Extended time held at the SA temperature made the ferrite and austenite grains coarser and as a result the material became more susceptible to SCC. Especially the ferrite grain diameter had an effect in regards to cracking and increasing the size of the grains gave a remarkable effect on the SCC susceptibility.
- After cold working the SCC susceptibility became higher for the high in ferrite content materials, while it became lower for the materials high in austenite. The material containing 51 % ferrite remained pretty stable.

Mietz et al. [18] also performed research on the cold works influence on SCC resistance of a austenitic stainless steel of the type 1.4529 (UNS N08926/N08367) and a DSS of the grade 1,4462 (UNS S31803/ S32205). The experiments were performed with u-bent specimens with saturated $MgCl_2$ salt spots. The conclusion of these experiments:

- No indication is found in regards to that cold work increases the SCC susceptibility
- Cold straining at both 5 % and 20 % showed no significant difference in SCC susceptibility compared to SA material

Work performed by Bauernfeind et al. [27] on austenitic SS's in chloride media uses constant load and slow strain as well as testing in boiling magnesium chloride solution. Four different degrees of cold work were used between 14 – 50 %. Conclusions of this work:

- Cold work does not have an effect on the threshold stress for SCC initiation.
- As the cold work highly enhances the mechanical properties the relative relationship between threshold stress and yield stress however shows a sharp decline with higher amount of cold work.

In the work of Leonard et al. [28] the effects of severe cold work on the microstructure and SCC resistance is looked into. Anomalous microstructure was created in the specimens by making a

groove. The test environment was chloride with Na cations and the stress applied was at yield. The main findings:

- No SCC was found associated with the damage microstructure except for one instance.
- Chloride induced SCC was observed for the areas with the highest damage to the microstructure.
- The surface defects are very important to control or repair in order to avoid later SCC from damaged microstructure due to cold working.

The consensus from the research in this field suggests that the effect of cold work has no effect on the SCC resistance. There is however very few studies specifically for DSS or SDSS.

2.9.3 Research on the effect of temperature and chloride concentrations on stress corrosion cracking resistance

A summary of earlier studies on SCC resistance for DSS by Manchet, Fanica and Lojewski [29], gives a good overview of what to expect from different load setups and chloride concentrations. Analyzing the results from testing with different concentrations of chloride and loading setups they compiled the results into a graph shown in Figure 15. The blue line indicates a chloride concentration of approximately 26 %. It clearly shows the relationship between temperature and chloride concentration. Also fracture happens at very high chloride concentrations above 40 %. The constant load and strain tests were performed until fracture or 720 hours .

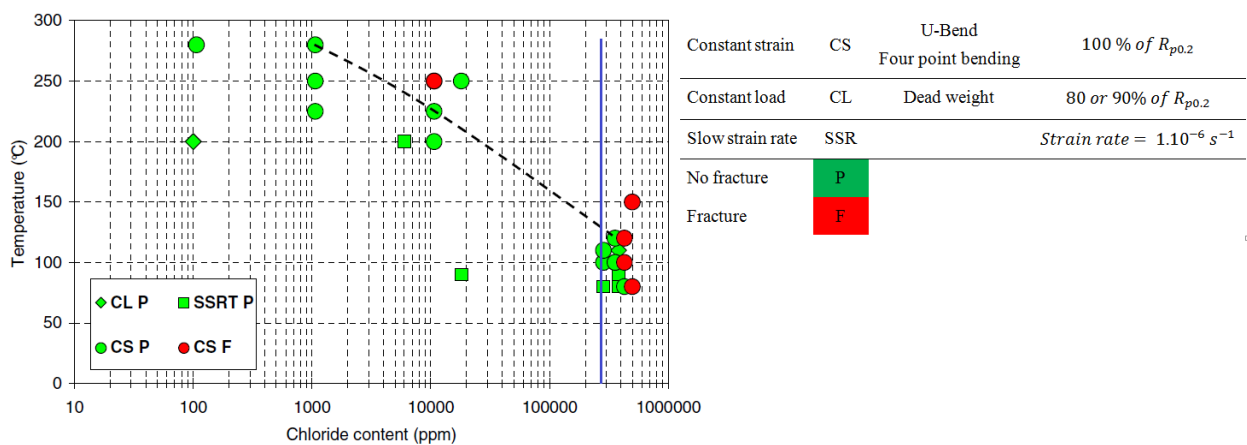


Figure 15: Summary of several studies on a SDSS with varying temperature and chloride concentrations [29]

According to Bernhardsson quoted in Gunn [7], the super duplex alloy UNS S32750 is immune to SCC in a 3 % NaCl solution up to 250 °C . The tests were performed for 1000 hours.

However duplex alloys will suffer from SCC given a high enough chloride concentration [7].

Johansson and Prosek [30] investigated SCC for a lean DSS according to G36 [17], and all the specimens failed within 24 hours. The cracks were through the whole thickness and there were also no signs of pitting attacks.

3 Testing

3.1 Standards

According to today's practice the only corrosion testing performed on bolts delivered according to NORSOK M-630 [31] is the ASTM G48 Method A [32].

There are several standards for SCC and a good summary can be found in the ASTM G30 standard [33]. Based on earlier research the ASTM G36 [17] and ASTM G44 [34] standards are the basis for the experiments in this thesis.

Also to review the results in regards to pitting there are several options. In this thesis the ASTM G46-94 [35] was used to some extent for the visual inspection. The SCC results were determined according to the criterion of fracture or no fracture.

The parameters for the experiments are discussed in chapter 3.6.

3.1.1 *ASTM G36 Standard practice for evaluating Stress-Corrosion-Cracking Resistance of Metals and Alloys in a Boiling Magnesium Chloride Solution*

The ASTM G36 [17] standard describes SCC testing of metals in a boiling magnesium chloride solution. It is applicable to SS and alloys of wrought, cast and welded quality and the susceptibility of the materials to chloride stress corrosion is determined by this standard.

Important aspects of this standard:

1. Careful examination should be performed to differ between pitting and stress corrosion
2. The specimens should be prepared according to ASTM G1 [36] and ASTM G30 [33]
3. Use of glass foundations when submerged to avoid any direct contact between the test specimens and the heating source.
4. Reagent grade chemicals and water should be used for preparing the test solution
5. The solution should be changed every 7 days
6. Loss of water by evaporation will lead to a large increase in the boiling point. This may accelerate the SCC, and it is therefore important to minimize the loss of water through evaporation by adding water during the testing.
7. Safety precautions need to be taken when heating magnesium chloride. Use gloves and eye protection when handling magnesium chloride.

3.1.2 ASTM G44, Standard Practice for Exposure of Metals and Alloys by Alternate Immersion in Neutral 3,5 % Sodium Chloride Solution

The ASTM G44 [34] standard describes the alternate immersion method which can be used for different metals and alloys. It can also be used for several different corrosion tests like SCC, uniform, pitting, intergranular and galvanic corrosion.

The purpose of this method of testing is that the test specimen is immersed for a given period before drying in air. By having a cycle of 10 minutes submerged and 50 minutes in air drying, the specimen will accumulate salt in certain areas like crevices or surface defects. After a while the concentrations of salt will be very high on localized spots, which again can induce SCC or pitting due to the passive layer being broken down. A typical test period for a 3,5 % sodium chloride (*NaCl*) solution is 20-90 days depending on the resistance of the alloy to corrosion in the test medium.

Important aspects of this standard:

1. Careful examination should be performed to differ between pitting and stress corrosion
2. The time it takes from the test specimen is fully immersed or removed from the solution shall be maximum two minutes.
3. The mechanism used to immerse and take out the specimen from the solution should not contain any materials than can contaminate the test solution.
4. Make sure the rate of drying is equal for all the test specimens and that the drainage of the specimens does not affect each other
5. If two different materials are tested, use separated test solutions
6. Refill with water regularly to keep a constant volume of the test solution
7. The solution should be changed every seven days
8. Relative humidity of the surrounding air should be kept at 45 ± 10 % and the temperature should be maintained at 27 ± 1 °C.

3.1.3 ASTM G46 Standard Guide for Examination and Evaluation of Pitting Corrosion

The ASTM G46 [35] describes different methods for examination and evaluation of pitting corrosion. In short there are several methods, both destructive and nondestructive and their different applications. For this thesis the simplest visual inspection will be performed. This requires a magnifying glass, good lightning and a steel brush. Important aspects of this standard are listed below:

1. Examine the surface with a magnifying glass before cleaning any of the corrosion products away. Also take pictures to compare it to the cleaned surface.
2. Clean the surface with a steel brush according to G1 [36] and also look for undercutting pits.
3. Use a microscope at 20X for a more detailed examination .
4. Determine the size, shape and density of the pits.
5. To more accurately count the pits, a plastic grid with 3 or 6 mm squares can be used.

3.2 *Properties of bolted assemblies and necessary considerations*

The most common way to determine the preload of a bolt is to specify the torque required. The typical equation for this is described by Dahlvig, Christensen and Strømsnes [37] in equation (14) and (15).

When torquing a bolt, the friction and pitch in the threads (M_v) needs to be considered, and when a sufficient load has been achieved, the friction against the surface (M_s) will also counteract the torque. Therefore the sum of equation (14) and (15) will give the total torque for the desired load in the bolt.

$$M_v = F * \frac{d_2}{2} * \tan \left(\left(\frac{\mu}{\cos(\alpha)} \right) + \left(\frac{P}{(\pi * d_2)} \right) \right) \quad (14)$$

$$M_s = \mu' * F * \frac{s + d_h}{4} \quad (15)$$

The input required for these equations are determined from the type of bolt in question. The middle diameter (d_2), the pitch (P), the angle of the threads (α), and the width across the flats (s) can easily be found for a given bolt. Also the diameter of the hole is determined and should be readily available.

The required input is then the required force (F) that the bolt should be torqued at, and two friction coefficients, μ for the threads and μ' between the surface and bolt head or nut.

According to Dahlvig et al. [37], the values of these coefficients are:

$$\mu = 0,18 - 0,35 \quad \text{without lubricant}$$

$$\mu = 0,14 - 0,26 \quad \text{with lubricant}$$

$$\mu' = 0,19 - 0,35 \quad \text{without lubricant}$$

$$\mu' = 0,08 - 0,18 \quad \text{with lubricant}$$

As seen in appendix A the variation of friction will have a great impact on the required torque for a given force. In this thesis lubricant is used, but if one considers max and min values of

friction with lubricant for a given force of 10 *kN* on a ½ inch bolt, the max torque is 295,7 *Nm*, while the minimum torque is 130,7 *Nm*. This shows that relying on friction for the experiments in this thesis is not reliable and that a different method should be chosen.

In the case of gaskets or in cases where the flange or plate where the bolt is going through is thin, the deformation of the gasket, plate, washer or flange also needs to be considered.

Using a tensile testing machine to determine the strain at yield is a good method to determine the elongation at yield which again can be measured when torquing the bolts. The downside of this method is that it is a destructive testing method. Also measuring elongation at a high accuracy may be difficult, meaning it will be beneficial to have the bolts as long as possible.

Another method to determine the torque at yield could be to use a load cell, like for example a tensile testing machine as hold back while tensioning the bolts to the required force. This could be achieved by having a plate with a hole in the same material as the flange, as well as having the same surface properties. Then the required torque for a given force could be determined for this actual case with the same surface properties and lubricant that are to be used in the experiment. This would presumably give an accurate torque for the given materials and the lubricant. However as there was limited time available, and this method would require extra machining, this method was not chosen.

A fourth method to determine the yield in the bolts is to use strain gauges. Then the strain can be measured accurately while torquing the bolts. This will require a clean and smooth surface when fixing the strain gauges.

The final method that was considered was using a hydraulic tensioning system. This system will prestress the bolt at the desired force by jacking it up against the surface. Friction between the surface and in the threads can then be ignored. This is however not easily attainable equipment and requires competent personnel and hydraulics.

A summary of methods to determine that the bolts are stressed at a certain limit with advantages and downsides can be found in Table 3.

Table 3: Summary of methods for determining stress in a bolt

<i>Method</i>	<i>Advantages</i>	<i>Downsides</i>
Use torque from tables	Easy, fast, nondestructive	High uncertainty in regards to friction
Tensile testing machine	Accurate, standard procedure	Need to manufacture holders, time consuming, need access to tensile testing machine, destructive
Determine the torque for the given friction from lubricant and surface	Accurate	Need machining of components, not straight forward, method needs to be established, destructive
Strain gauges	Accurate, nondestructive	Need high accuracy when fixing strain gauges, need smooth surface, access to strain gauges and other accessories
Hydraulic tensioning	Accurate, nondestructive	Expensive equipment, need access to hydraulics and competent personnel

The chosen method will therefore need to consider the following:

- Access to a laboratory / equipment
- Access to workshop for machining
- Amount of specimens available in regards to destructive testing
- The surface geometry of the bolts and the bolt length

An interesting aspect in regards to bolted assemblies is where the fracture will occur. There are three different cases to consider as shown in Table 4.

Table 4: Fracture modes for bolt and nut [38]

<i>Relationship between bolt and nut strength</i>	<i>Place of failure</i>
Nut stronger than bolt	At the root of the bolt threads
Bolt stronger than nut	At the root of the nut threads
Nut and bolt equal strength	At the pitch line

It is preferred that the fracture will occur in the bolt rather than the nut, as the bolt shaft in many cases can be inspected, while a fracture in the nut may be unnoticeable. So for the scenarios where the nut is stronger or of equal strength as the bolt, this can be achieved by enough thread

engagement. This consideration however needs to account for the fact that the load distribution in the threads is not uniform. As the first thread will take a higher percentage of the load than the next, the maximum height of the nut is usually around one diameter for carbon steel [37]. The equation to calculate the strength of the threads is given in (16) and (17). The threads will fail by shear and not tension, so this is based on the shear strength (S_u) of the nut and bolt [38].

$$F = S_u \times A_{ts} \quad (16)$$

$$A_{ts} = \pi \times n \times L_e \times D_{smin} \times \left(\frac{1}{2n}\right) + 0.57735 \times (D_{smin} + E_{nmax}) \quad (17)$$

When the test materials (see chapter 3.4) arrived, it became obvious that tensile testing was the most efficient and accurate method to establish the elongation at a given stress. The studbolts were fully threaded which excluded the use of strain gauges. Also there were enough specimens to allow for destructive testing. Determining the torque for the given surfaces and lubricant were deemed to complex compared to the readily available tensile testing machine at Hydro Karmøy Aluminium R&D. The availability of a hydraulic tensioning system was also investigated, but it was found that it would not be possible in the given timeframe. Also the flange that was delivered to serve as a test jig had a thickness of 36 mm which allowed for easy measuring of elongation while torqueing as the bolts were around 74 mm.

3.3 Tensile testing

The purpose of obtaining the stress-strain curve is to be able to determine the elongation when the bolts are at a certain stress level. By analyzing the graph produced by the tensile testing machine, the strain at yield is determined. Then by measuring the length of the bolts when torqueing, one can easily tighten the bolt to the wanted stress level. As there was a small quantity of studbolts available for all the experiments, the goal was to use as few bolts as possible for this destructive testing method. To simulate the scenario of the bolts when mounted on the flange, the length of the gap between the holders were set at the flange thickness which is 36 mm. This is shown in Figure 16. To ensure that the bolts would get minimum friction while mounting them in the holders the lubricant Gleitpaste was used. The MSDS for this lubricant can be found in Appendix B. This grease contains silver, and from earlier experiences from offshore personnel this grease works well with SS.

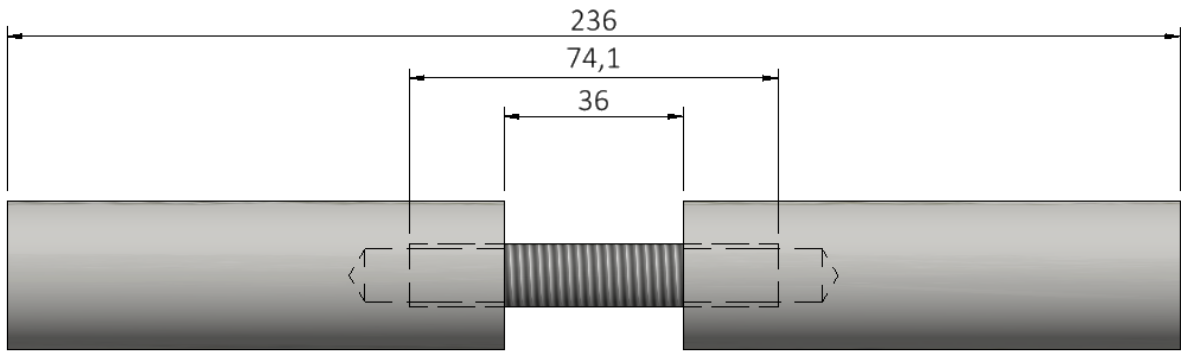


Figure 16: Sketch of the holder setup with the bolt mounted

The results from the tensile testing are logged as tensile stress versus strain. To be able to determine the Young's modulus which is the gradient, the equation for the linear part of the curve was found by use of Excel. This was offset 0.2 % to be able to find the offset yield and the corresponding strain. An example of this procedure is shown in Figure 17 for the first test on 316L.

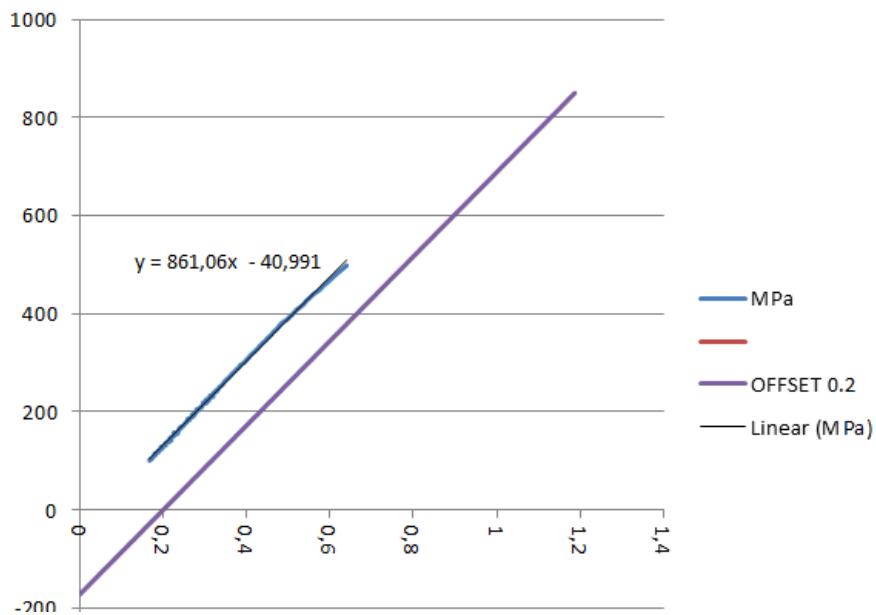


Figure 17: Linear part of the stress-strain curve

This linear offset yield was plotted in the stress strain curve and the offset yield point was found together with the strain at this given point as shown in Figure 18. It also shows that the slope for the start of the curve is not linear, which is caused by the tolerance in the threads of the holders.

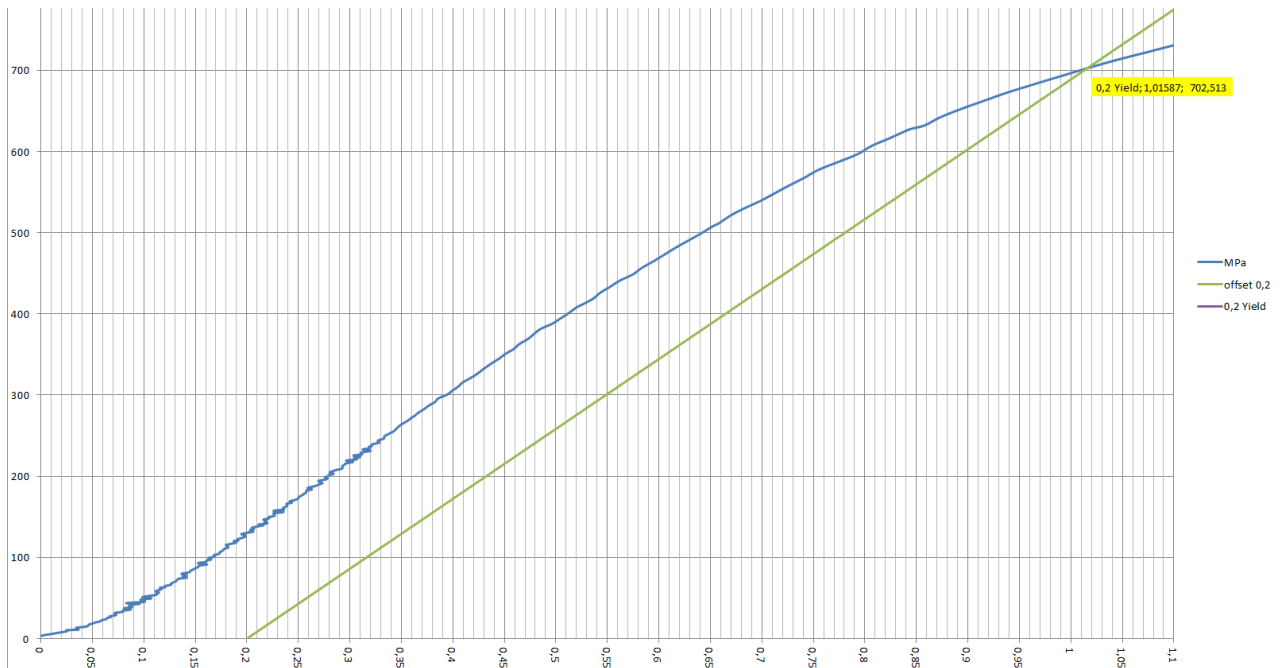


Figure 18: Offset yield stress and strain determined from the curve

An interesting result was discovered when tensile testing the bolts. The Young's modulus was significantly lower than what was expected. In the case of SDSS the Young's modulus was logged as 85 – 98 GPa which does not agree with the expected 199 GPa [39]. There were no available literature to explain this, but it was obvious that the threads in some way were responsible for this.

An ANSYS analysis was performed and while it did not produce the same results as the tensile testing in regards to elongation it agreed with the fact that the Young's modulus changed when the force increased. It did not however produce the same Young's modulus as the tensile testing. The setup for the ANSYS analysis is shown in Figure 19.

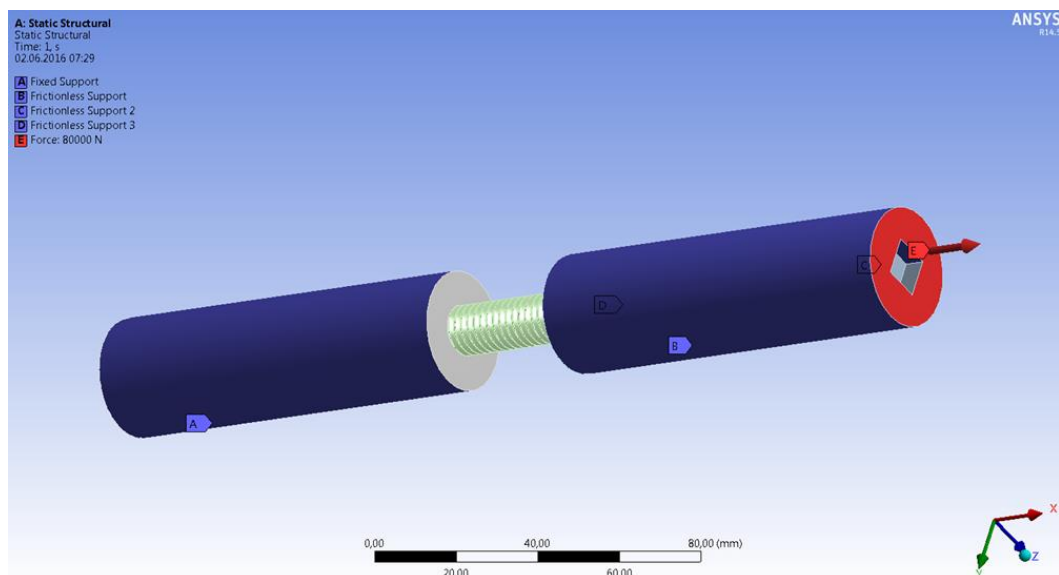


Figure 19: ANSYS setup for verifying the tensile results

Figure 20 shows that the deformation is different in the outer part of the threads compared to the inner part of the thread, and this might explain the lower Young's modulus experienced in the tensile testing.

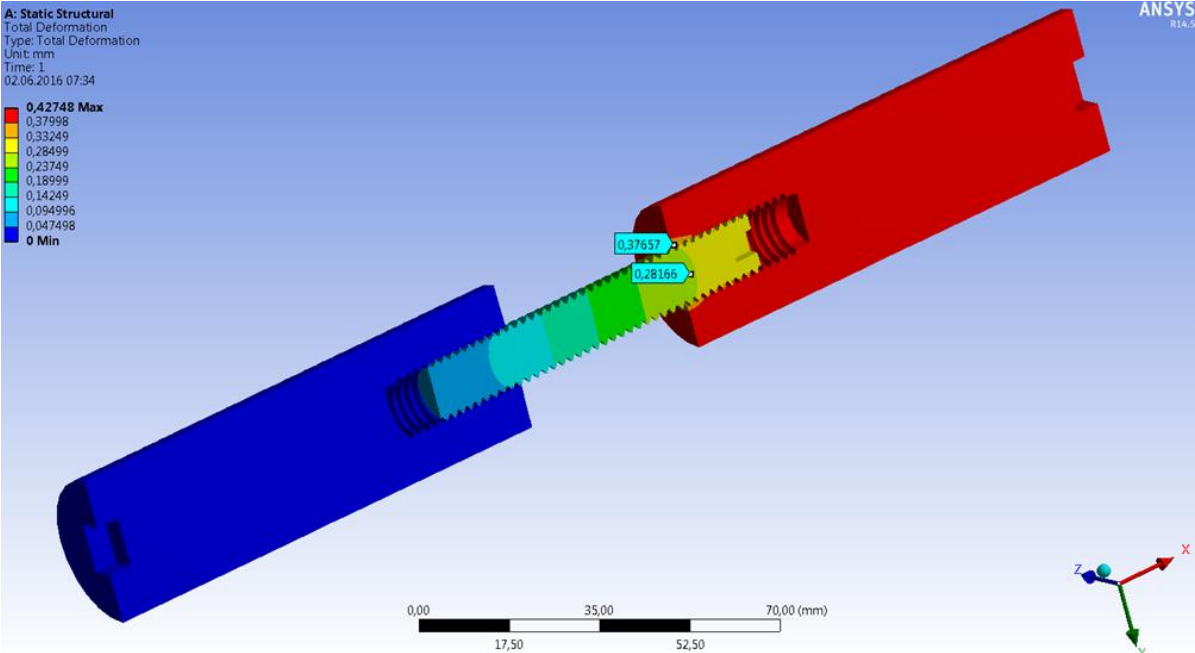


Figure 20: ANSYS result that shows the difference of deformation in the outer and inner parts of the threads

3.3.1 The use of tensile testing test results for the experiments

To account for the fact that the measuring is performed directly on the total bolt length, while only the middle part of the bolt between the nuts is strained, the elongation Δk (shown in Figure 21) is calculated as shown below in equation (18):

$$\epsilon_{yield} = \frac{\Delta l}{l_0} = \frac{\Delta k}{k_0}$$

$$\Delta k = \epsilon_{yield} \times k_0$$

$$\Delta k = \epsilon_{yield} \times ((k_0 + \Delta k) - \Delta k)$$

$$\Delta k = \epsilon_{yield} \times (T - \Delta k)$$

$$\Delta k = \frac{\epsilon_{yield} \times T}{1 + \epsilon_{yield}} \tag{18}$$

Where:

- ϵ_{yield} Strain at yield
- Δl Elongation during the tensile testing
- l_0 Initial length before tensile testing

Δk	Elongation from torquing the bolt
k_0	Theoretical initial length before torquing the bolt during assembly
T	Thickness of flange and distance between the holders during tensile testing
K_0	Initial length of bolt

This means that the total length of the bolt after torquing is defined as equation (19):

$$K_1 = K_0 + \Delta k \quad (19)$$

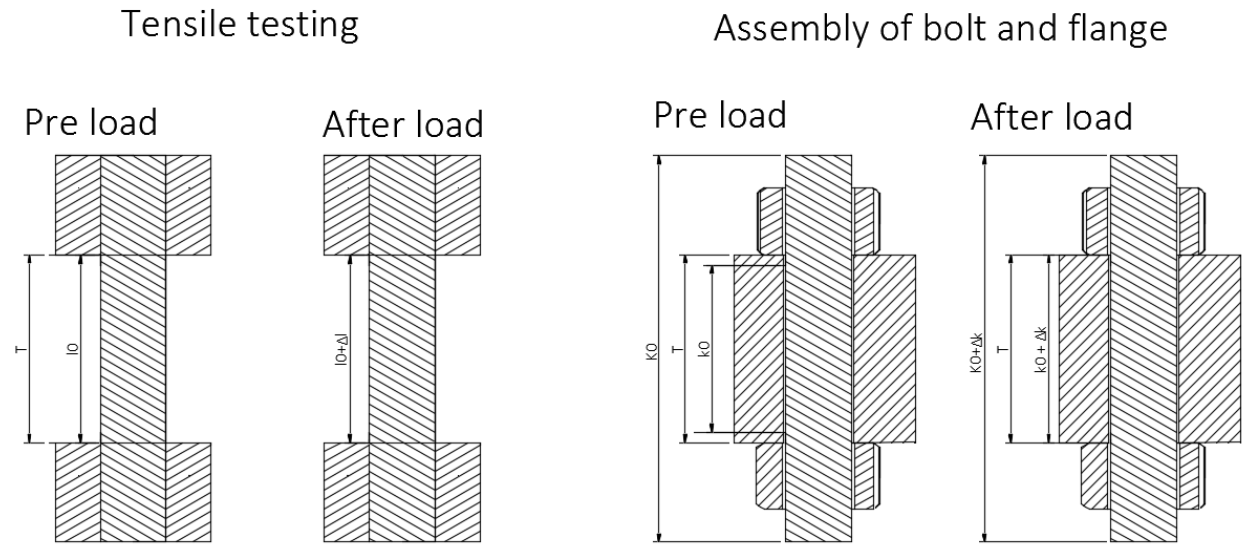


Figure 21: Sketch of tensile testing and assembly of bolt and flange

By calculating the strain at yield from the tensile testing results the percent of yield in the bolt during torquing can be controlled.

Also this means that the length between the holders in the tensile testing should be equal to the thickness of the flange (T).

3.4 Test materials

This chapter describes the test materials used for the experiments and their dimensions and conditions. A summary of the chemical composition and the mechanical properties can be found in Table 5 and Table 6.

3.4.1 SDSS flanges

To avoid any galvanic corrosion in the test jig, it was decided to use flanges of SDSS UNS S32760 material quality. A total of six flanges were delivered from SFF, but only three were modified and used for the testing. Having the bolts and flanges in the same material is also beneficial when heating the materials as the thermal expansion is similar. The flanges material

certificate is attached as appendix C and they are manufactured and delivered according to Norsok M-630 MDS 54 [31].

The flanges were received in used condition from SFF AS, and were cleaned with acid in an ultrasonic cleaner. Before and after pictures can be seen in Figure 22. The flanges had holes of 25,5 mm which did not fit the ½ inch bolts that were delivered, meaning that machining had to be performed. Details for this are discussed in chapter (3.6.2).



Figure 22: Before and after picture of flanges after cleaning and machining

3.4.2 Solution annealed (SA) bolts (D60)

The bolts were received in new condition from Ome Metallurgica via Tools Randaberg, and manufactured according to NORSOK M-630 [31] and ASTM A1082 / A1082M [40]. A total of 16 bolts were delivered in the SA condition. The alloy was a SDSS of the type UNS S32760 and they were delivered with a 3.1 material certificate (MDS) which can be found in appendix D. The SA bolts are specified as L001 in the MDS

The specification is given as: *ANSI B16.5 ½ × 70 P 13 UNC 2A*. This specification indicates a diameter of ½ inch, a threaded length of 70 mm with 13 threads per inch (TPI) and unified coarse (UNC) threads of tolerance class 2. The length of the bolts was measured to be around 74,1 mm.

The heat code is stamped on each SA bolt as 75 and the heat treatment is solution annealing performed at 1125 °C with quenching in water. The bolts were tested for corrosion with the ASTM G48 Method A [32] with acceptable results and a weight loss of 0,027 g/m². Also no intermetallic or other detrimental phases are observed.

3.4.3 Cold strained (CS) bolts (D59)

The bolts were received in new condition from Ome Metallurgica via Tools Randaberg, and manufactured according to NORSOK M-630 [31] and ASTM A1082 / A1082M [40]. The alloy was a SDSS of the type UNS S32760 and they were delivered with a 3.1 MDS which can be found in appendix D. A total of 16 bolts were delivered in the CS condition and the CS bolts are specified as L003 in the MDS

The specification is given as: *ANSI B16.5 ½ × 70 P 13 UNC 2A*. This specification indicates a diameter of ½ inch, a threaded length of 70 mm with 13 TPI and UNC threads of tolerance class 2. The length of the bolts was measured to be around 74,0 mm. The heat code is stamped on each CS bolt as **94** and the heat treatment by solution annealing is performed at 1100 °C with a heating up time at 4,5 hours and a holding time of 2,5 hours before quenching in water.

According to the cold straining procedure from the Ome Metallurgica, the maximum cold deformation is set at 10 %. Also, according to the procedure the maximum yield for topside studbolts is 970 MPa, while studbolts for subsea use should have a maximum yield of 900 MPa [41]. The supplied bolts have an offset yield of 1004 MPa which means they cannot be used for either topside or subsea.

The bolts were tested for corrosion with the ASTM G48 Method A [32] with acceptable results and a weight loss of 0,089 g/m². Also no intermetallic or other detrimental phases are observed.

3.4.4 Solution annealed nuts (for both D59 and D60)

The nuts were received in new condition from Ome Metallurgica via Tools Randaberg, and manufactured according to NORSOK M-630 [31] and ASTM A1082 / A1082M [40]. The alloy was a SDSS of the type UNS S32760 and they were delivered with a 3.1 MDS which can be found in appendix D. A total of 32 nuts were delivered and the SA nuts are specified as L002 in the MDS. Having only a total of 32 nuts and 32 SDSS bolts may force reuse of the nuts if all the bolts are to be tested.

The specification is given as: *ANSI B18.2.2 – Tab. 10 ½ C 22,22 H 12,8 P 13 UNC 2B*. This specification indicates a diameter of ½ inch, a nut height of 12,8 mm with 13 TPI and UNC threads of tolerance class 2. It is also stated that the nuts have been pickled and passivated.

The heat code is stamped on each nut as **502** and the heat treatment is solution annealing performed at 1100 °C for 3643 seconds with quenching in water for 702 seconds.

The nuts were tested for corrosion with the ASTM G48 Method A [32] with acceptable results and a weight loss of $0,02 \text{ g/m}^2$. Also no intermetallic or other detrimental phases are observed.

3.4.5 B8M Cl. 2 bolts (CS)

The bolts were received in new condition and manufactured according to ASTM A320/A320M – 15a [42] in the quality B8M cl. 2, and they were delivered with a 3.1 MDS which can be found in appendix E. Class 2 means the bolts are cold strained. This material is equivalent to AISI 316L and is referred as such for the rest of this thesis.

The specification is given as: *STUDBOLT B8M CL.2 ½" L75 mm*. This specification indicates a diameter of ½ inch, a threaded length of 75 mm with 13 TPI and UNC threads of tolerance class 2. The length of the bolts was measured to be around 79,7 mm.

The heat code is stamped on each bolt as **6D** and the heat treatment is carbide solution annealing before strain hardening.

No information is given in regards to microstructure, degree of cold straining or ASTM G48 testing in the MDS.

3.4.6 B8M nuts

The bolts were received in new condition and manufactured according to ASTM A194/A194M – 16 [43] in the quality Gr. B8M, and they were delivered with a 3.1 MDS which can be found in appendix E

The specification is given as: *HEX NUT ½" Gr. 8M*. This specification indicates a diameter of ½ inch and the height of the nut is measured to be 12,2 mm.

The heat code is stamped on each bolt as **S** and the heat treatment is carbide solution annealing. No information is given in regards to intermetallic phases or ASTM G48 testing in the MDS.

Also there is no information in regards to yield. Only that the proof load is given as 11350 pound force in the material certificate. However the minimum offset yield ($R_{p0.2}$) according to ASTM A194 [43] is 80ksi or 551,6 MPa.

3.5 Summary of test materials

The chemical composition of the test materials is listed in Table 5, and the mechanical properties can be found in Table 6.

Table 5: Chemical composition of the different test materials in weight %

<i>Part</i>	<i>Cr</i>	<i>Mo</i>	<i>Ni</i>	<i>N</i>	<i>Cu</i>	<i>Mn</i>	<i>C</i>	<i>W</i>	<i>PREN</i>
SDSS Flanges	25,19	3,77	6,76	0,26	0,56	0,68	0,016	0,63	41,79
SDSS SA bolts	25,55	3,47	7,50	0,26	0,56	0,58	0,023	0,54	41,16
SDSS SA nuts	25,36	3,62	7,03	0,23	0,56	0,53	0,019	0,54	41,00
SDSS CS bolts	25,60	3,50	7,20	0,26	0,58	0,60	0,024	0,54	41,23
316L bolts	16,60	2,00	10,00	0,03	0	1,72	0,027	0	23,74
316L nuts	16,85	2,02	10,10	0,03	0	1,81	0,023	0	24,06

Table 6: Mechanical properties of the different test materials

<i>Part</i>	$R_{p0.2}$ (MPa)	R_m (MPa)	<i>Elong.</i> (%)	<i>ROA</i> (%)	<i>HBW</i> ^a	<i>Fer. cnt.</i> (%)	<i>Heat Code</i>
SDSS Flanges	638	827	31,4	57,5	254	52	32
SDSS SA bolts	662	877	42,0	84,0	278	55	75
SDSS SA nuts	581	814	45,1	87,5	266	55	502
SDSS CS bolts ^b	588	830	47,0	80,0	254	52	
SDSS CS bolts	1004	1075	23,4	77,1	N/A	52	94
316L bolts	655	775	32,5	68,4	277	N/A	6D
316L nuts	552 ^c	N/A	N/A	N/A	281	N/A	S

^a Maximum hardness listed

^b Before cold straining

^c Minimum value from ASTM A194

3.6 Test setup

The parameters for the tensile testing and the torquing are discussed as well as the building and design of the test jig. Also the parameters for the corrosion aspect of the experiments which were based on the G36 [17] and G44 [34] standards will be determined. It was decided to perform experiments in two different setups. One test setup is based on G36 [17] with heated magnesium chloride and the other one based on G44 [34] with alternate immersion. However some parameters from these standards have been altered due to the equipment that was available, and to try and accelerate the testing due to limited time available. Also to verify the alternate immersion setup four 316L bolts were tested.

3.6.1 Tensile testing setup

The tensile testing was performed at Hydro Aluminium Karmøy R&D with a tensile testing machine of the model Zwick 1475 that had a capacity of 10 tonnes. One initial test was performed at the laboratory at UIS with a tensile testing machine capable of 250 kN to verify the test setup.

To ensure that the tensile testing was performed in a safe way it was important that the holders for the bolts were able to take the load when the bolts fractured. The easiest way of ensuring this was to find a material with higher or equal UTS as the nuts.

Calculations were performed to ensure that the SA nuts and holders would be able to withstand the load from the CS bolts when tensioned to UTS. Equation (16) was used with the shear strength taken as 0,6 of the UTS according to Von Mises. Calculations are attached in appendix F. The length of the thread engagement would be longer in the case of the holder. Also the outer diameter of the holders was important so that they would fit in the tensile testing machine. The thickness of the flange where the bolts are to be mounted is 36 mm so the gap between the holders is also set at 36 mm.

The design parameters for the holders were therefore:

- Cylinder shaped
- Maximum outer diameter 30 mm and maximum length of cylinder to be 100 mm
- Hole with ½ inch UNC threads with 13 tpi
- Minimum thread engagement in the holder to be 20 mm
- Material with UTS higher than the SA nut which is 814 MPa

The material chosen for the holders was S165M, which had UTS of 985 MPa. The MDS is attached as appendix G. Olufsen Skipsservice manufactured them at no cost according to the

fabrication drawing that can be found in appendix H. The finished manufactured holders assembled with a bolt in the tensile testing machine are shown in Figure 23.

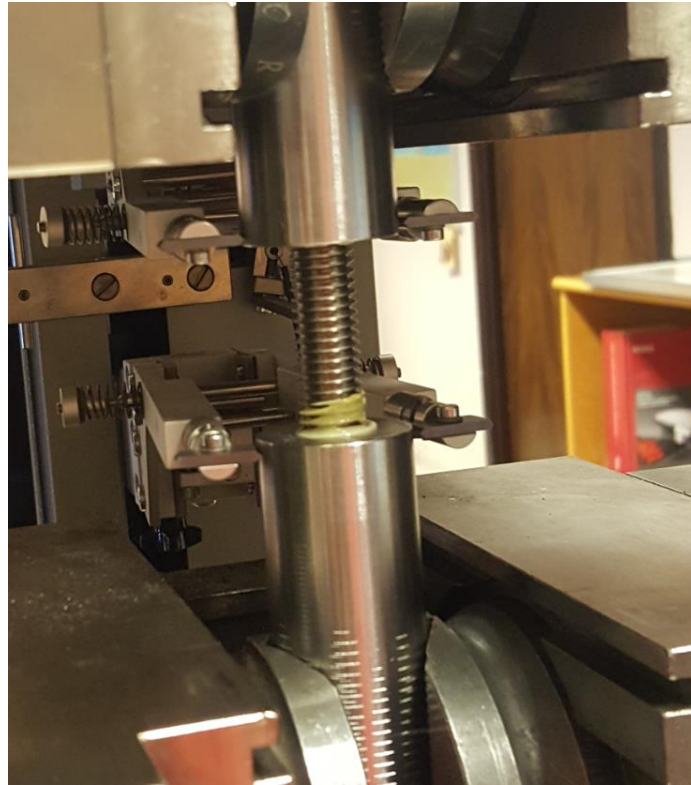


Figure 23: Holders with a bolt mounted in the tensile testing machine

As the extensometer is not suited to be placed on the threads, as they are sloped, they are placed on each holder as shown in Figure 23. However in test 4 in which the threads were machined, the extensometer was placed directly on the bolt shaft.

According to Table 6, the offset yield point for the materials is known. This means that the theoretical strain at yield is possible to calculate.

From Hooke's law we have that:

$$\varepsilon = \frac{E}{\sigma} \quad (20)$$

Where E is the Young's modulus, ε is the strain and σ is the tensile stress.

The Young's modulus is not specified in the MDS, but sources give them as 199 GPa for UNS S32760 [39], and 193 GPa for 316L [44] at room temperature.

Since the strain at the offset yield point is 0,2 % this needs to be added to the strain found from equation (20). Detailed calculations are attached as appendix I. The theoretical elongation at yield is listed in Table 7 for the length of 36 mm.

Table 7: Theoretical strain and elongation

<i>Material</i>	<i>Offset yield point (MPa)</i>	<i>Offset yield strain</i>	<i>Theoretical el. at offset yield (mm)</i>
316L	655	0,0054	0,194
SA SDSS	662	0,0053	0,192
CS SDSS	1004	0,0071	0,254

3.6.2 Torqueing of bolts

It was decided to perform the experiments on the as received condition of the bolts. As the bolts received were ½ inch diameter, they would not fit in the holes already in the flanges. Machining was performed to be able to use them. It was decided to have four holes drilled in each flange with a diameter of 13,5 mm. The hole should be as wide as possible to allow for the fluid to surround the bolt, but too big of a hole would not be practical when tightening the nut, so 13,5 mm was decided as ideal.

Vision of the bolts after they had been torqued was also important, meaning a slit was cut on the edge of the flange. The width of this slit was set at 6 mm so that it gave enough vision without removing too much material under the nut. However in retrospect, the slit could have been wider if it had not gone all the way from top to bottom, and left enough material underneath the nut. Also the edges of the slit were chamfered and grinded to avoid a sharp edge underneath the nut that could increase the friction. The machining was performed by Mecan, at short notice and at no cost, according to the fabrication drawing found in appendix J. Three flanges were machined and available for the experiments. Figure 22 shows the flanges after machining.

As discussed earlier, the amount of stress applied to the bolts is directly affecting the time it takes to initiate SCC. Therefore it was decided to torque the bolts to 100 % of yield. The calculations performed earlier showed that the SA nuts would be able to take the load even from the CS bolts in yield.

To determine the elongation at yield, the equation (19) was used. The strain values used in this equation were from the results from the tensile testing. As the elongation was very small a micrometer was used to measure the length, and as the torque were performed in short increments, measuring was done between each torqueing.

It was also decided that the lubricant would be the same as for the tensile testing, e.g. Gleitpaste. Even though the Gleitpaste contains silver, the potential of SDSS and silver is so close that

galvanic corrosion is not found problematic. The silver will also be encapsulated in the grease, and all excess grease is cleaned with an electro cleaner.

3.6.3 Preparation of magnesium chloride test solutions

As the test solution was chosen to be magnesium chloride some parameters regarding concentration and mixing needed to be determined. Magnesium chloride was chosen for both the immersed heating and the alternate immersion as the Mg cation is more aggressive as discussed earlier.

Since there was no laboratory grade magnesium chloride available, the magnesium chloride used for the testing was acquired from Felleskjøpet in the form of magnesium chloride hexahydrate. This means that for each magnesium chloride molecule there are six water molecules. The MDS can be found in appendix K. The added water is tap water and not lab grade water as specified in the standard.

There are two temperatures that will be applied for these experiments:

- Room temperature at 23 – 27 °C
- Heated solution of a temperature of 90 °C

The solubility for magnesium chloride is [45]:

- 54,3 g per 100 ml water at 20 °C
- 72,6 g per 100 ml water at 100 °C

Since the temperature is slightly above 20 °C , extra magnesium chloride hexahydrate needs to be added until it precipitates to verify that the solution is saturated. This also means the concentration in reality will be slightly higher than calculated. Detailed calculations for the concentrations can be found in appendix L. Table 8 shows the details of the test solutions used.

Table 8: Test solutions with magnesium chloride

	Added quantity			Concentration	
	$MgCl_2 \cdot (H_2O)_6$	Water	Total volume	$MgCl_2$	Cl^-
20 °C	116 gm	38,35 gm	119 mL	35 wt. %	26 wt. %
100 °C	155 gm	18,00 gm	120,3 mL	42 wt. %	31 wt. %

From this table the test solutions were mixed. It was obvious through trial and error that mixing smaller batches was the easiest as the magnesium chloride hexahydrate consisted of big crystals that needed a lot of stirring to fully dissolve. Also for the heated solution it was found easiest to incrementally add magnesium chloride hexahydrate as the temperature increased.

3.6.4 Setup for immersed test with heating (G36)

It was obvious that performing experiments with boiling magnesium chloride was difficult with the given circumstances, especially since the bolts are tested in as received condition instead of preparing test specimens according to G1 [35] and G30 [33]. A modified version of G36 [17] will be applied in this thesis. The experiments were performed in an empty office at DeepOcean.

The design criteria for this setup were:

- Room enough to handle the flange assembly with dimensions being $80\text{mm} \times \text{Ø}160\text{mm}$ while being fully immersed in magnesium chloride solution
- Obtain as high temperature as possible
- No metal must come in contact with the test solution and flange assembly
- Safe during use over a period of approx. 1 month
- Being able to remove the assembly for inspection

Several different ways of doing this were evaluated. However when it came to obtain at temperature of 155°C , all of the available methods came short. As it was not possible to just use a metal container and heat it up due to galvanic corrosion and pollution of the test solution, something else was needed. Also most normal water heaters like heating coils and similar were made of metal, and also not safe to leave in the test solution for longer periods of time. Available aquarium heaters for use in for example a glass or plastic container were only able to maintain at temperature of maximum 36°C .

The best solution to reach a high temperature was to use a slow cooker. This can maintain a temperature of 90°C , as well as deemed safe to operate for longer periods of time. However, as no suitable place for it was found to have the slowcooker operating at night time, it was decided to use alternating heating. In effect that means the assembly will be heated for 16 hours to a steady temperature of 90 degrees and kept at room temperature for the remaining 8 hours. As the inner container is of ceramics, there is no risk of pollution or galvanic corrosion. It also comes with a lid, which stops most of the evaporation.

To avoid direct contact between the ceramic container and the flange assembly in regards to heat exchange, a glass plate was placed on the bottom of the container. Also when the flange assembly was in the container, roughly 2 liters of solution was required to keep the assembly fully submerged. Ropes were attached to the assembly to allow for removing the assembly for inspection. See Figure 24 for the setup.

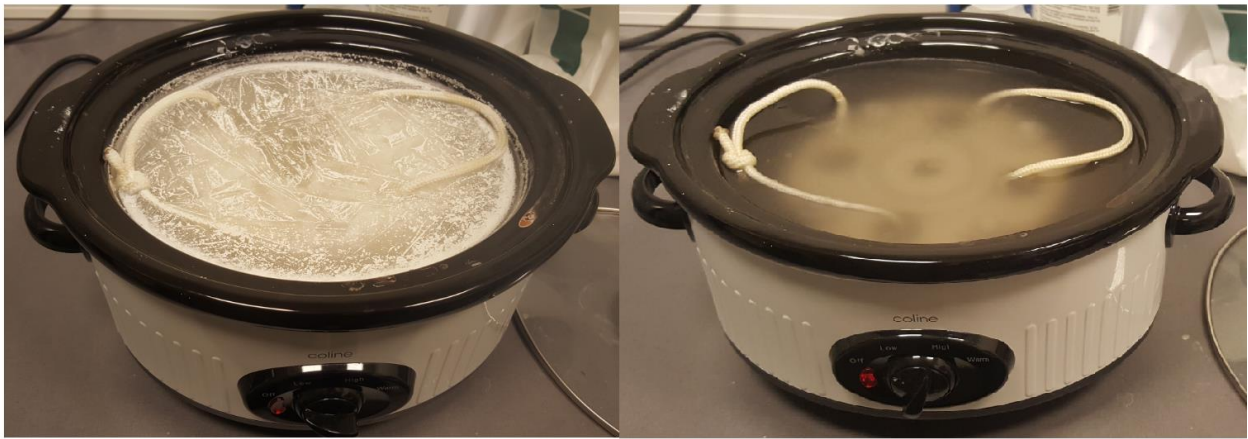


Figure 24: Setup for immersed testing with the left showing the solution at room temperature and the right one showing the temperature at 90 °C

As seen from Figure 24, the solution solidifies at room temperature due to the lower solubility.

The failure criterion is fracture in regards to SCC, and for the pitting resistance a visual inspection will be performed.

3.6.5 Setup for alternate immersion testing (G44)

To try to accelerate the SCC a modified version of the G44 [34] is applied. The bolts are tested in as received condition and on the same bolt assembly as described earlier.

The design criteria are given from the G44 [34] for most of the parameters. However to be able to accelerate the SCC a test solution of magnesium chloride is used instead of the recommended 3,5 % sodium chloride solution. Due to the fact that the alternate immersion runs on an interval of 10 minutes in the solution and 50 minutes in air, an automatic test jig needed to be designed and constructed. To be able to verify the test setup, bolts of 316L were also tested in this jig. As the test solution should not contain more than one alloy, there needs to be two containers of test solution. In the case of 316L the flange was still SDSS so there might be a risk of galvanic corrosion. The experiments were performed in an empty office at DeepOcean.

Design criteria for jig and environment:

- Automatic and reliable setup
- Be able to run for a long period of time, approx. 2 months.
- Maximum time to fully immerse specimens 2 minutes
- Run parallel tests
- Maintain a relative humidity of approximately 35 – 55 %
- Maintain a temperature of 27 °C
- Take the load of the flange assembly which is 6 kg

Several methods were evaluated to obtain the necessary requirements. However it became obvious early on that programming of some sort was required to have the test jig be fully automatic. In regards to the environmental conditions the humidity and temperature needed to be controlled. As the weight of the bolt assembly was 6 kg it also limited the options regarding the test setups. This meant that something more heavy duty was required. The following test setup was there for decided on.

By acquiring a second hand electrical linear actuator shown in Figure 25 that could maintain the weight and was fast enough to fully submerge the test specimens within two minutes, allowed for constructing the test jig. The actuator came with a remote control which had in and out direction controls. Also the specification on the actuator gave the pull load as 300 kg and the push load as 700 kg. The easiest way would then be to mount the actuator in the vertical position which meant that it would be lowering the bolt assembly when going in the *out* direction and lifting the assembly when going in the *in* direction.

The remote control functions by pushing the in or out button for 29 seconds to fully extend or retract the shaft. Also the shaft of the actuator can extend for 31 cm so this needs to be taken into account in regards to the height of the jig when building the frame on which the actuator will be mounted.

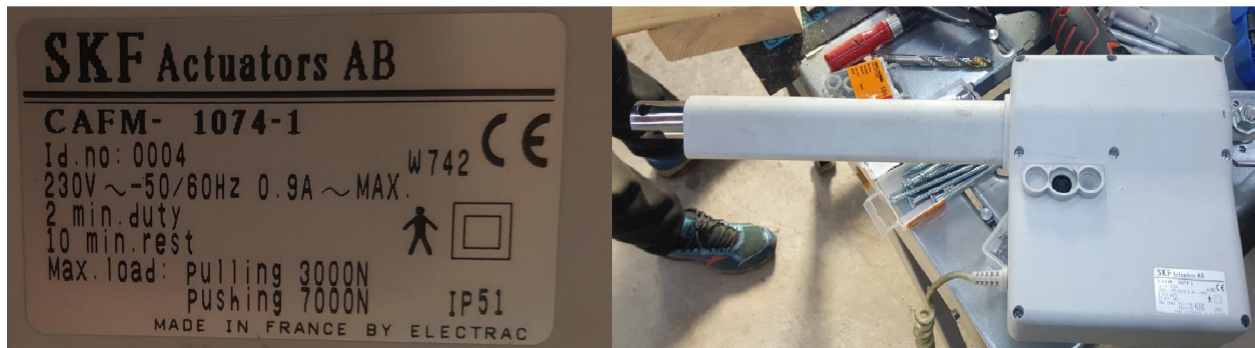


Figure 25: Electrical linear actuator with specifications

As the lifting device was settled, it needed to be programmed to automatically lower and lift the bolt assembly at the given interval of 10 minutes in the test solution versus 50 minutes in air.

To be able to control the in and out directions on the remote control separately, one relay for each function as well as a programmable card was required. The card chosen was Arduino, due to its simplicity in regards to programming. The Arduino card was then connected via USB to upload the code and to a 12 V power supply.

A part list for the setup:

- Electrical linear actuator of the model CAFM 1074-1
- Relay card of the model Songle Relay
- Arduino UNO 3 rev 3
- Power supply of the model Mascot 12-30 V DC

The sketch program for Arduino was used and the following parameters were coded:

- Turn on relay 1 for 29 seconds, which makes the actuator fully extend
- Turn off relay 1 and delay for 10 minutes
- Turn on relay 2 for 29 seconds, which makes the actuator retract
- Turn off relay 2 and delay for 50 minutes
- Loop this indefinitely

As the Arduino code had problems with delays longer than 300.000 milliseconds, the delay was divided in to smaller portions of delay. There was some inaccuracy during testing of the setup, but it was only 30 seconds off the total sync in seven days, so this was not an issue in regards to the testing. The full code can be found in appendix M.

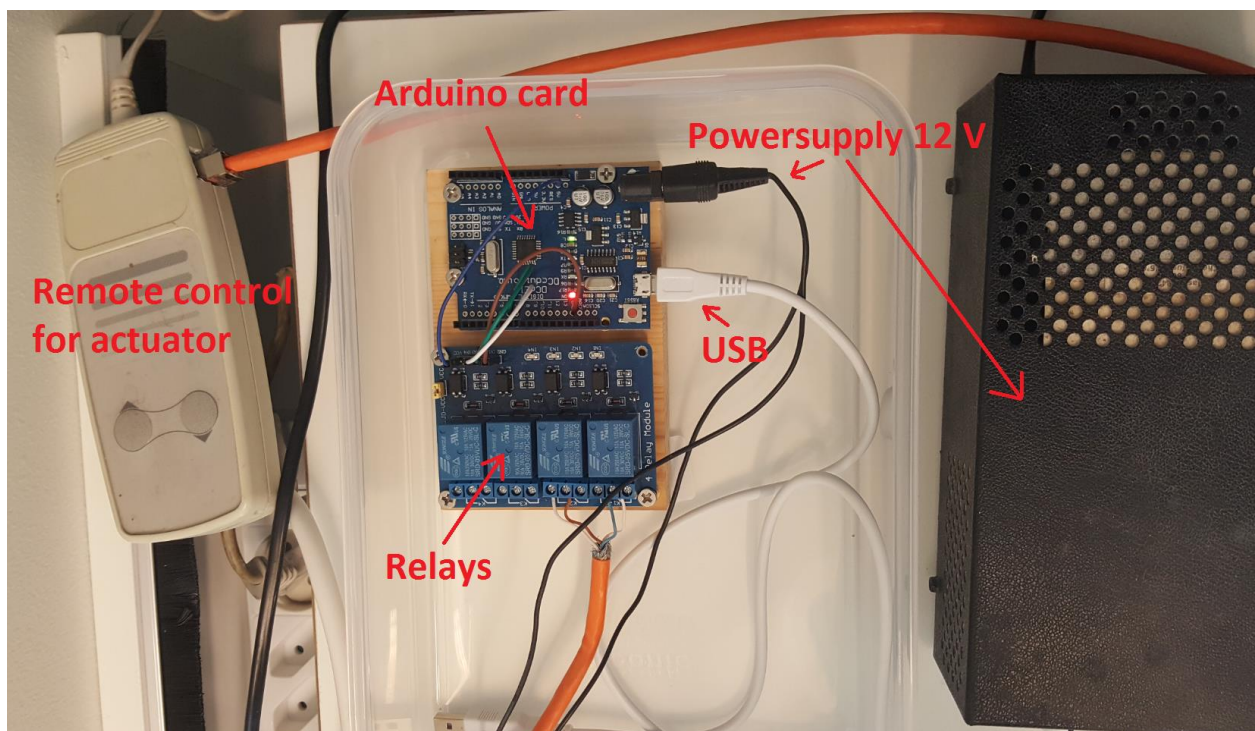


Figure 26: Overview of Arduino setup

Figure 26 shows the main setup. The power supply provides 12 V to the Arduino card. The micro USB is for uploading the code to the Arduino, and the remote control is connected to the relays. Relay 1 controls the out direction, while relay 2 controls the in direction.

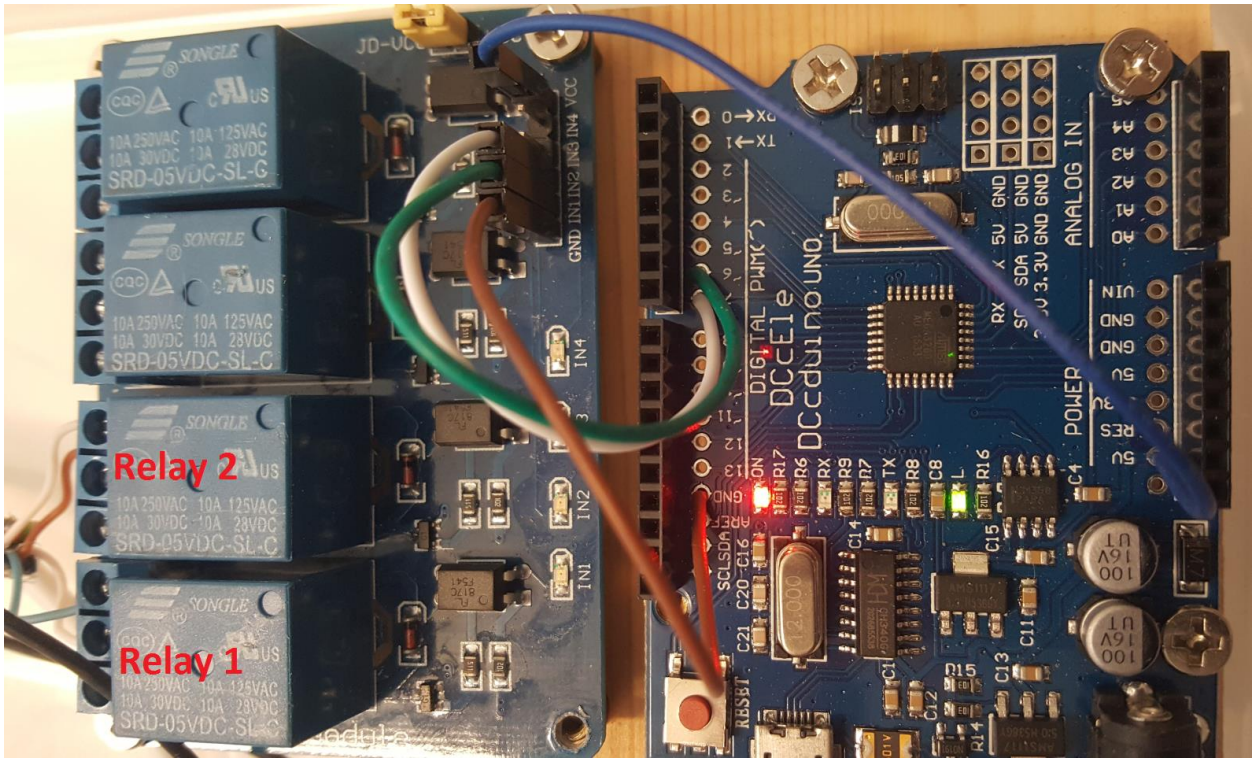


Figure 27: Close up of wiring

Figure 27 shows the connections between the Arduino and the relays. The wiring is setup in the following way:

- Blue wire Supplies 5 V from the Arduino to the relays
- Brown wire Ground between the Arduino and the relays
- Green wire Pin 6 on the Arduino to relay 1
- White wire Pin 7 on the Arduino to relay 2

After the programming and initial testing was performed, the jig for this was constructed. A frame work of four $36\text{ mm} \times 68\text{ mm}$ was connected by a $50,8\text{ mm} \times 152,4\text{ mm}$. It was bolted together to be able to easier move it. The jig was covered by plastic to increase the relative humidity in the air within. Also it was setup for parallel testing where one flange assembly consisted of four 316L bolts while the other assembly has 2 CS and 2 SA SDSS bolts. This is show in Figure 28 and the test solution for each bolt assembly is therefore separated. The black container was also filled with water to increase the humidity. The two plastic containers held approximately four liters each of test solution. Securing the bolted assemblies with rope ensured that no contamination by any metal would occur in the test solution.



Figure 28: Framework with actuator and bolt assemblies

The failure criterion is fracture in regards to SCC, and for the pitting corrosion a visual inspection will be performed.

3.6.6 Processing of results

According to G46 [35], a visual inspection of the bolts after testing will be performed. However as there was not a microscope easily available an inspection jig was created to be able to magnify and photograph the results. This homemade microscope was created by turning the lens of a web camera (PS3 eye) upside down as seen in Figure 29. When this wide angle lens is switched the other way it will work as a powerful magnifying glass with the benefit that it can save and store pictures and videos of the results. The light arrangement was made out of LED strips to get as bright light as possible when taking pictures. According to the scaling of pictures taken, the magnification is approximately 10X. The fact that most of the pitting occurred in the thread roots also made it hard to obtain a larger magnification without machining the threads away with the current setup. This will of course not give a detailed view of the very small pits, but the ones around 0,5 mm were easily identifiable. Counting the pit density and depth was difficult and not included due to the crude nature of the microscope as well as the thread geometry made it difficult to get a detailed inspection of the side of the threads.

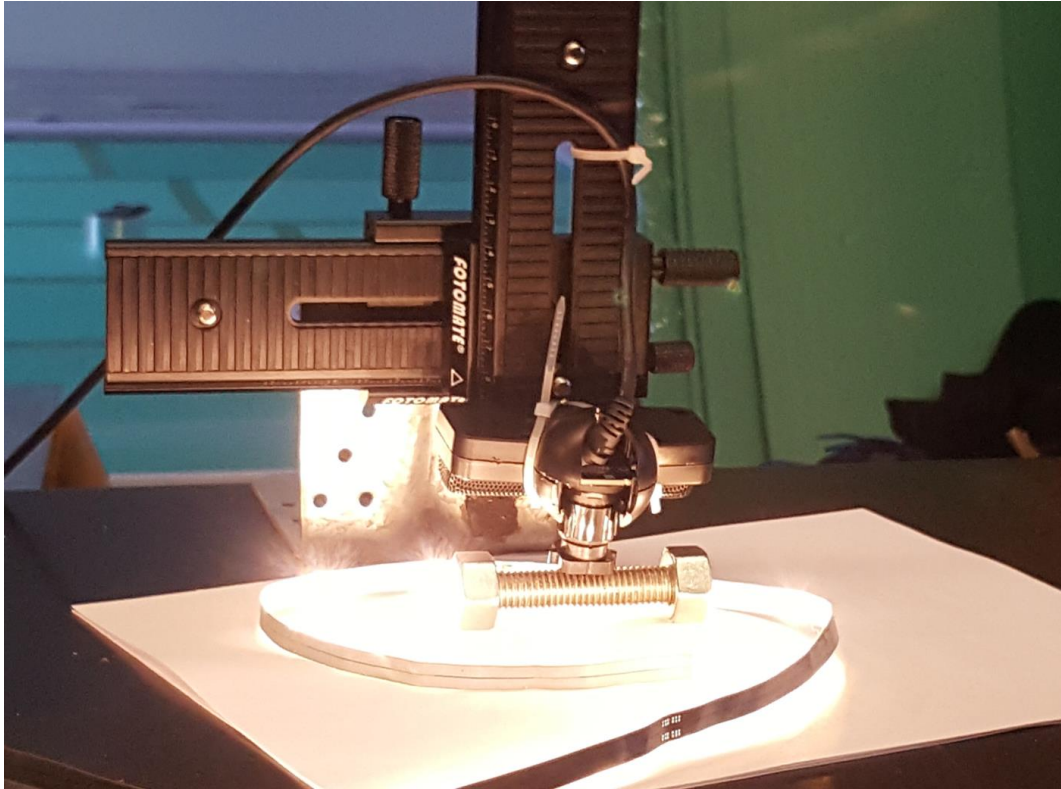


Figure 29: Inspection jig for visual inspection of bolts

3.7 Experimental

Several experiments are performed in this thesis:

- Tensile testing of AISI 316L, SDSS SA and SDSS CS bolts
- Torqueing of AISI 316L, SDSS SA and SDSS CS bolts
- Alternate immersion on four AISI 316L, two SDSS SA and two SDSS CS bolts
- Immersed heating testing
 - Test 1: two SDSS SA and two SDSS CS bolts
 - Test 2: two SDSS SA and two SDSS CS bolts

The actual testing took place from 15th of April till 6th of June. Details regarding the different experiments are described in the next subchapters.

3.7.1 Tensile testing

The testing was performed at Hydro Aluminium Karmøy R & D center with assistance from competent personnel. Also one initial test was performed in University of Stavanger's workshop.

The tensile testing machine measured the stress versus the elongation and the output was a text file that could be imported in Excel for post processing. As there were some uncertainties in regards to how the studbolts would react to tensile testing, the initial tests were performed on the cheaper 316L bolts to verify the setup.

A tensile testing machine of the model Zwick 1475 with a capacity of 10 kN was used for the experiments at Hydro, and a tensile testing machine with 25 kN of the model Instron 5900 series was used at UIS. The holders that were manufactured were able to fit in both tensile testing machines.

The following test procedure was prepared and used during testing:

1. Grease the section of the bolts going into the holder with Gleitpaste lubricant
2. Assemble the holders and the bolts together with a gap of 36 mm and make sure that the bolt has entered an equal length in each holder
3. Safely secure the assembly in the tensile testing machine
4. Place extensometer on each holder
5. Input on diameter is set at 10,823 mm based on tensile area $0,92 \text{ cm}^2$ [37]
6. Monitor the stress-strain curve to fracture
7. Save the results
8. Test another bolt of the same type
9. Compare the results of the two tests
 - a. If small variation stop testing
 - b. If high variation test another bolt of the same type
10. Compare the results and take the average of the test values
11. Determine the strain from the curve at yield
12. Calculate the elongation required for yield

A total of four 316L bolts, two SA SDSS bolts and two CS SDSS bolts were tested. One of the 316L bolts had the threads machined off to check for the effect of threads versus no threads. In this case the extensometer was placed directly on the bolt shaft instead of on the holders.

3.7.2 Torqueing of bolts

The torqueing of the bolts was performed at the DeepOcean offshore base at Killingøy with assistance from DeepOcean personnel. The flanges are prepared and ID accordingly.

- Flange 1: 316L:1, 316L:2, 316L:3, 316L:4
- Flange 2: SA:1, SA:2, CS:1, CS:2
- Flange 3: SA:3, SA:4, CS:3, CS:4
- Flange 4: SA:5, SA:6, CS:5, CS:6

The torquing of the bolts were performed in a work bench where the flange was locked in place. The equipment required to tighten the bolts were a torque wrench (max. 300Nm), wrench, micrometer and grease.

To avoid any excess friction in the threads and between the nut and the flange, the grease used was Gleitpaste as in the tensile testing. All excess grease was cleaned off with an electro cleaner spray and pressured air when the torquing was finished.

The length after torquing was determined from the tensile testing results. As each bolt had a different initial length, the bolts were torqued to different final lengths as well. In Table 9 the different test numbers and their specifications are listed. The final length column contains the final length the bolts should theoretically have after torquing with the given elongation at yield obtained in the tensile testing.

Table 9: Identification and specification on the bolts

<i>Material</i>	<i>Test no.</i>	<i>Initial length (mm)</i>	<i>Elongation at yield (mm)</i>	<i>Final length (mm)</i>
316L	316L:1	79,19	0,35	79,54
	316L:2	79,11	0,35	79,46
	316L:3	79,14	0,35	79,49
	316L:4	79,09	0,35	79,44
SDSS	SA:1	74,10	0,33	74,43
	SA:2	74,39	0,33	74,72
	SA:3	73,96	0,33	74,29
	SA:4	74,16	0,33	74,49
	SA:5	74,10	0,33	74,43
	SA:6	74,05	0,33	74,38
SDSS	CS:1	74,08	0,39	74,48
	CS:2	74,15	0,40	74,55
	CS:3	74,12	0,40	74,52
	CS:4	74,22	0,40	74,62
	CS:5	74,21	0,40	74,61
	CS:6	74,20	0,40	74,60

The following test procedure was used for the torquing:

1. Secure the flange in the work bench so it is not able to move during torquing
2. Grease the bolt and the surface of the nut that are laying against the flange with Gleitpaste lubricant
3. Assemble the bolt and nuts on the flange
4. Mark and log the position and material of the bolt in question
5. Measure the initial length of the bolt with a micrometer
6. Find the final length of the bolt from Table 9
7. Start torquing with a low initial value as the friction in both the threads and between the nut and the flange is uncertain
8. Measure and increase the torque as required
 - a. Increase the torque gradually ($2 - 5 Nm$), with smaller and smaller increments when close to the final length.
9. When the final theoretical length has been achieved proceed to the next bolt
 - a. The next bolt of the same material can however be torqued with an initial higher torque as the torque at yield is determined on the first test. However it should still be started minimum 20 Nm below this torque due to uncertainty regarding friction on each bolt
10. Clean the surface with electro cleaner and pressured air to remove all excess grease on the threads and surfaces

3.7.3 Immersed test in heated magnesium chloride

The immersion testing was performed at an empty office at DeepOcean. A slowcooker of the model Coline was used, and this was able to maintain 90 °C on average.

The following test procedure was used:

1. Prepare the test solution according to appendix L for 100 °C
2. Place a glass plate on the bottom of the slow cooker to isolate between the bolt assembly and the ceramic pot
3. Add a rope to the bolt assembly to allow for lifting
4. Place the bolt assembly in the ceramic pot
5. Pour the test solution into the pot
6. Turn on the device
7. The device is turned on for ideally 16 hours and off for 8 hours each day

8. Inspect visually four times every day by lifting the bolt assembly out of the solution and gently torque the nut with a wrench
9. Add water if evaporation occurs
10. Change the test solution if corrosion products develop, or once a week
11. Change test solution between each test

The criterion for success or failure was fracture or no fracture in regards to SCC. Pitting will be evaluated by visual inspection.

3.7.4 Alternate immersion

The alternate immersion testing was executed using the test jig designed and constructed for this thesis. The main goal of this thesis is to compare the SDDS CS and SA bolts, however for the alternate immersion a bolts assembly with four 316L bolts were also tested to verify the setup.

The testing was performed in an empty office at DeepOcean and the temperature was kept constant at 27 degrees. Also the relative humidity was originally only 10 – 15 % in the office. Wrapping the jig in plastic increased this to a relative humidity at 25 – 27 %.

The following test procedure was used:

1. Prepare the test solution according to appendix L for 20 degrees
2. Add extra magnesium chloride hexahydrate until precipitation
3. Pour the test solution into two separate containers
4. Prepare the bolt assemblies for testing by attaching a rope to each one
5. Secure the bolt assemblies to the horizontal spreader beam attached to the actuator
6. Turn on the device
7. The device is running uninterrupted for the whole duration of the experiment
8. Inspect every day by visual examination and try to unscrew the bolts by hand
9. Add water regularly if evaporation occurs
10. Change the test solution if corrosion products develop, or once a week

The time available for the immersed testing was 39 days or until fracture. The criterion for success or failure was fracture or no fracture in regards to SCC. Pitting will be evaluated by visual inspection.

3.8 Results

3.8.1 Tensile testing

The tensile testing results were surprising as the Young's modulus was logged as below half of what was expected of the given material quality. This also causes the elongation to be longer than what was expected. This effect was encountered in the tensile testing machine at both UIS and Hydro Aluminium Karmøy R&D. A total of eight bolts were tested in the tensile testing machine, and the average of the tests were used when torqueing the bolts. It should be noted that it was not possible to stress the SDSS CS bolts to fracture due to the max capacity of the tensile testing machine only being 10 tonnes. To establish the effect of the threads, one specimen (Test 4) was machined down to 5,7 mm in diameter and the extensometer was placed directly on the shaft instead of the holders. A summary of the results is presented in Table 10, and the average values and input for torqueing is listed in Table 11.

Table 10: Summary of tensile testing results

<i>Test ID</i>	<i>Material</i>	<i>Elongation (%)</i>	<i>0,2 Yield (MPa)</i>	<i>E modulus (GPa)</i>
Pre-test UIS	316L	N/A	N/A	71,4
Test 1	316L	1,016	702,5	86,1
Test 2	316L	0,973	680,5	88,0
Test 3	316L	0,619	395,0	93,1
Test 4 ^a	316L	0,704	760,5	150,8
Test 5	SA SDSS	0,943	699,7	94,2
Test 6	SA SDSS	0,934	717,0	97,7
Test 7	CS SDSS	1,240	885,3	85,1
Test 8	CS SDSS	1,002	703,7	87,7

^a Test 4 is machined to a diameter of 5,7 mm

Table 11: Average values from tensile testing

<i>Material</i>	<i>Elongation (%)</i>	<i>0,2 Yield (MPa)</i>	<i>0,2 Yield (MPa) from MDS</i>	<i>Elongation at 0.2 Yield to be used for testing^b(mm)</i>
316L ^a	0,994	691,5	655	0,3545
SDSS SA	0,938	708,4	662	0,3347
SDSS CS	1,121	794,5	1004	0,3991

^a Only test 1 and 2 were used for the average for 316L

^b Elongation is based on a length of 36 mm according to equation (19)

By comparing the elongation of the theoretical elongation using the yield from the MDS, it is clear that the elongation is higher in the experiments. This is caused by the fact that the tolerance in the threads will cause a delay before the linear part of the gradient occurs. And as the Young's modulus is lower than expected this affects the slope of the stress-strain curve, which again means the elongation will be higher. The testing is performed by torqueing the bolts with a nut on each side of a flange, meaning the delay caused by the threads will also occur during torqueing of the bolts. Also the theoretical values use the Young's modulus from available literature, while the testing produced significantly lower Young's modulus. A comparison of the theoretical and experimental values is listed in Table 12.

Table 12: Comparing theoretical elongation versus elongation from experiments

<i>Material</i>	<i>Theoretical el. at offset yield (mm)</i>	<i>Elongation from experiments (mm)</i>	<i>Deviation (%)</i>
316L	0,194	0,3545	55 %
SA SDSS	0,192	0,3347	57 %
CS SDSS	0,254	0,3991	64 %

Figure 30 shows the test specimens after testing and the stress-strain curves for each test can be found in appendix N.



Figure 30: Bolts after tensile testing

3.8.2 Torqueing of bolts

The results from torqueing the bolts were as expected and there were no problems in regards to tearing of the threads. Of course there might be some small errors when measuring, as the bolts did not have machined ends and it was difficult to measure on the exact same spot after each torque increment. There were also a few occurrences of where increasing the torque gradually produced very little elongation, before the final torqueing pulled it too far.

Five bolt assemblies were prepared for testing and referred to as:

- Flange 1: 316L:1, 316L:2, 316L:3, 316L:4
- Flange 2: SA:1, SA:2, CS:1, CS:2
- Flange 3: SA:3, SA:4, CS:3, CS:4
- Flange 4: SA:5, SA:6, CS:5, CS:6

The results from the tensile testing were used and the final lengths and the required torque values can be found in Table 13.

Table 13: Measured values during testing

<i>Material</i>	<i>Test no.</i>	<i>Initial length (mm)</i>	<i>Final length (mm)</i>	<i>Final measured length (mm)</i>	<i>Torque required (Nm)</i>
316L	316L:1	79,19	79,54	79,53	142
	316L:2	79,11	79,46	79,47	130
	316L:3	79,14	79,49	79,50	135
	316L:4	79,09	79,44	79,47	142
SDSS	SA:1	74,10	74,43	79,44	150
	SA:2	74,39	74,72	74,72	172
	SA:3	73,96	74,29	74,31	155
	SA:4	74,16	74,49	74,51	150
	SA:5	74,10	74,43	74,67	140
	SA:6	74,05	74,38	74,40	145
SDSS	CS:1	74,08	74,48	74,50	215
	CS:2	74,15	74,55	74,56	210
	CS:3	74,12	74,52	74,51	215
	CS:4	74,22	74,62	74,61	210
	CS:5	74,21	74,61	74,66	215
	CS:6	74,20	74,60	74,62	210

3.8.3 Immersed test in heated magnesium chloride

The results from the immersed testing setup were a success in terms of provoking SCC. The first experiment, test 1, however had some issues. The visual inspection that was performed two times a day meant that the assembly was lifted out of the magnesium chloride and checked visually. This could only be done when the solution had been heated for around 4 – 6 hours, as the solution solidified when cooled. Also the grease between the nut and the flange functioned as an adhesive that secured the nut to the flange. The magnesium chloride did also not fully dissolve in some cases, due to the alternate heating, so this worked as an adhesive as well. When the flange was lifted out of the solution the magnesium chloride cooled off in the air and formed a film on the whole surface. It was when the whole assembly was retracted from the solution and cleaned in tap water, meaning the magnesium chloride and grease loosened up, that the fractures

were discovered in test 1. This means that the exact moment of fracture is impossible to determine for test 1, and the results only show that all the bolts experienced failure in this test. When test 2 was initiated, a better inspection system was developed to determine the time of fracture. This was performed by torquing each nut with a wrench gently by hand four times a day when the solution had liquefied. This also prevented the same degree of salt buildup that occurred in test 1.

In regards to alternate heating, it was not possible to maintain the 16 hours on, 8 hours off interval. However the heating cycles were documented for each test. It also needs to be taken into account that when turning the slowcooker off, the ceramic bowl preserved the heat for some time after. Meaning that when it was only turned off for 8 hours it was still lukewarm in the morning when turned on again. This means the average temperature for the whole test period is somewhere between 23 – 90 °C .

Test 1 results

The heating cycle was logged and is presented in Table 14.

Table 14: Details on heating and cooling for heated experiment test 1

<i>Day</i>	<i>1</i>	<i>2</i>	<i>3</i>	<i>4</i>	<i>5</i>	<i>6</i>	<i>7</i>	<i>8</i>	<i>9</i>	<i>10</i>	<i>11</i>	<i>12</i>	<i>13</i>	<i>14</i>	<i>Total</i>
Heating (h)	6	12	0	16	16	15	16	24	16	12	10	11	8	4	166
Cooling (h)	18	12	24	8	8	9	8	0	8	12	14	13	16		150
															316

Pitting was not observed on any bolts by visual inspection at 10 X.

The results from test 1 showed fracture in both CS bolts and in one of the SA bolts. The other SA bolt had a crack in both nuts however and the largest crack went all the way through to the inside of the nut. The fractures appear as brittle as expected from SCC. Also all the fractures are at approximately 45 degree angles. The surface of the fractures is of a dull grey color. Pictures with details are shown in Figure 31, Figure 32 and Figure 33.

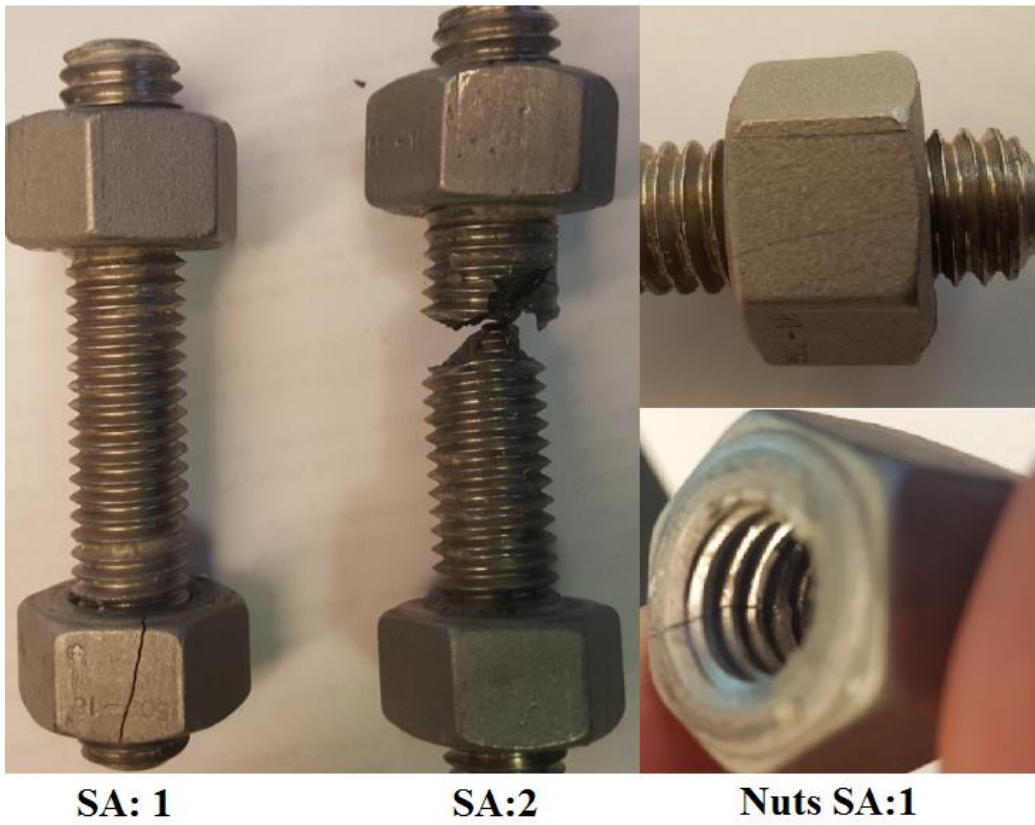


Figure 31: Details of SA bolts from test 1 of immersed testing at 90 °C

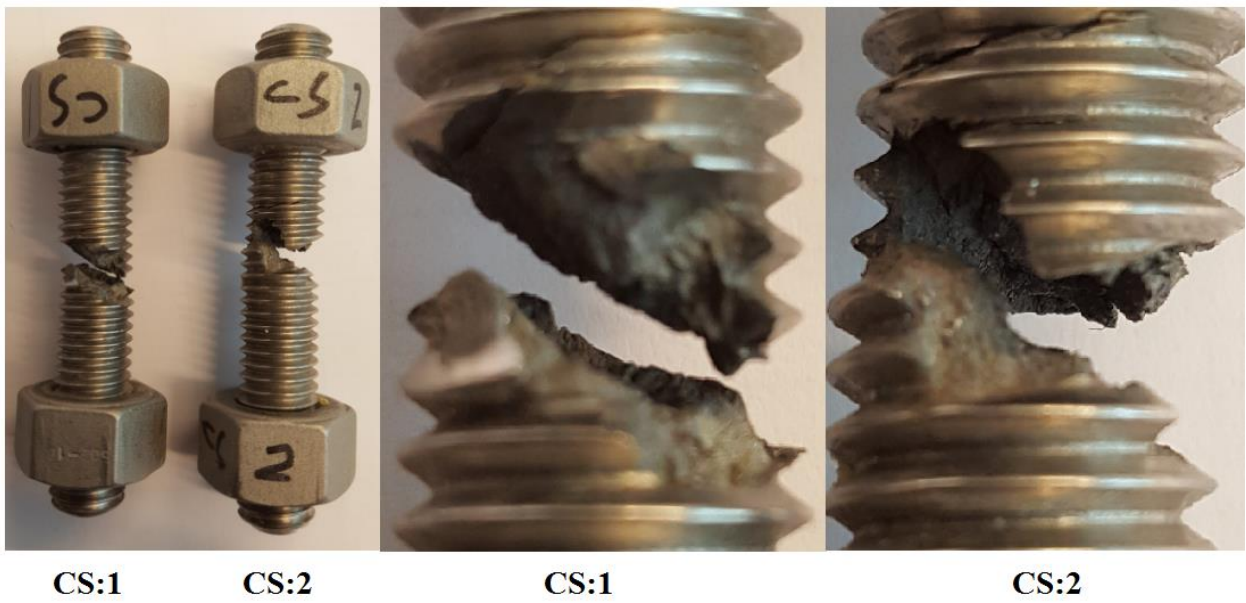


Figure 32: Details of CS bolts from test 1 of immersed testing at 90 °C

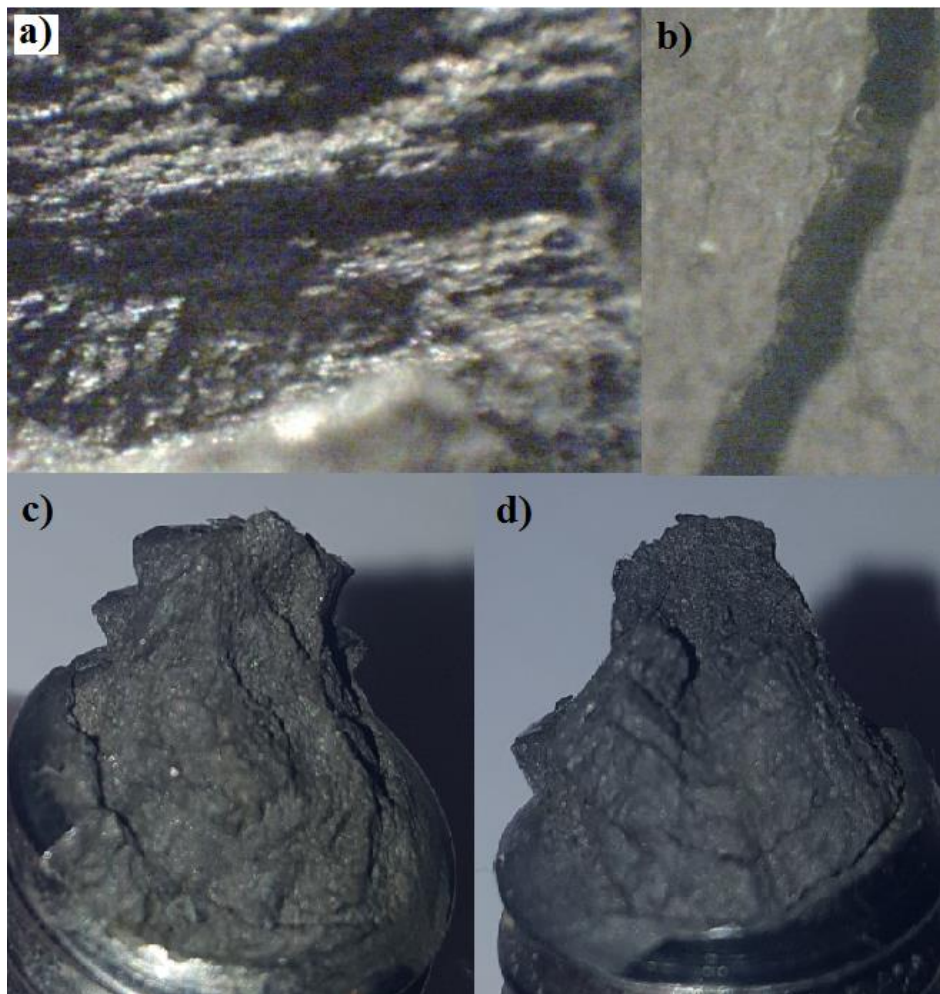


Figure 33: Details of the fractures. a) showing the surface of the fracture (10X), b) showing the crack in the nut for SA:1 (10X), c) the surface of the fracture for SA:2 and d) showing the surface of the fracture for CS:2

Test 2 results

For test 2, the amount of heating and cooling is logged before fracture and shown in Table 15

Table 15: Results from immersed heating test 2

<i>Bolt ID</i>	<i>Heating (h)</i>	<i>Cooling (h)</i>	<i>Total time in solution (h)</i>	<i>Fracture</i>
SA:5	33	15	48	YES
SA:6	100	56	156	NO
CS:5	29	8	37	YES
CS:6	44	15	59	YES

Pitting was not observed on any bolts by visual inspection at 10 X.

Both of the CS bolts and one SA bolt fractured after a short time in the solution. However the SA bolt (SA:5) that fractured was torqued to 120 % of yield according to the calculations as too

much torque was applied. The other SA bolt (SA:6) did not show any signs of cracking after 156 hours in the test solution.

The resulting fractures are shown in Figure 34. The deformation in SA:5 occurred when trying to torque the bolt with a wrench and it suddenly gave in at a small amount of force.

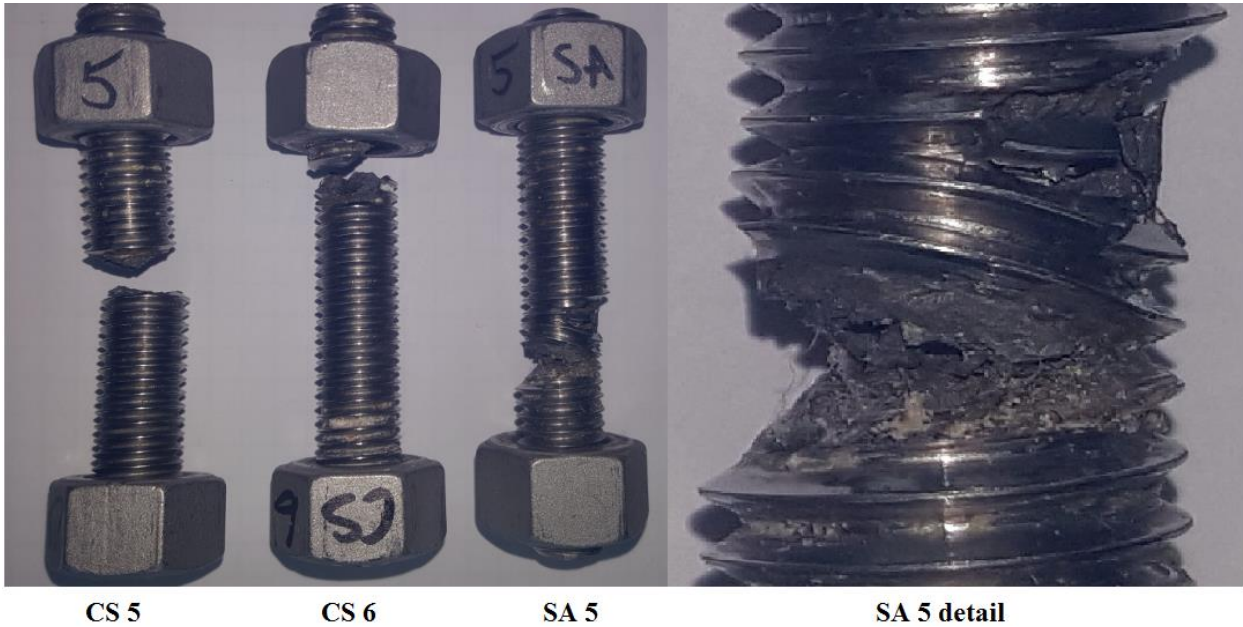


Figure 34: Details of CS bolts from the immersed testing at 90 °C

Figure 35 shows the SA:6 bolt which did not fracture in test 2.

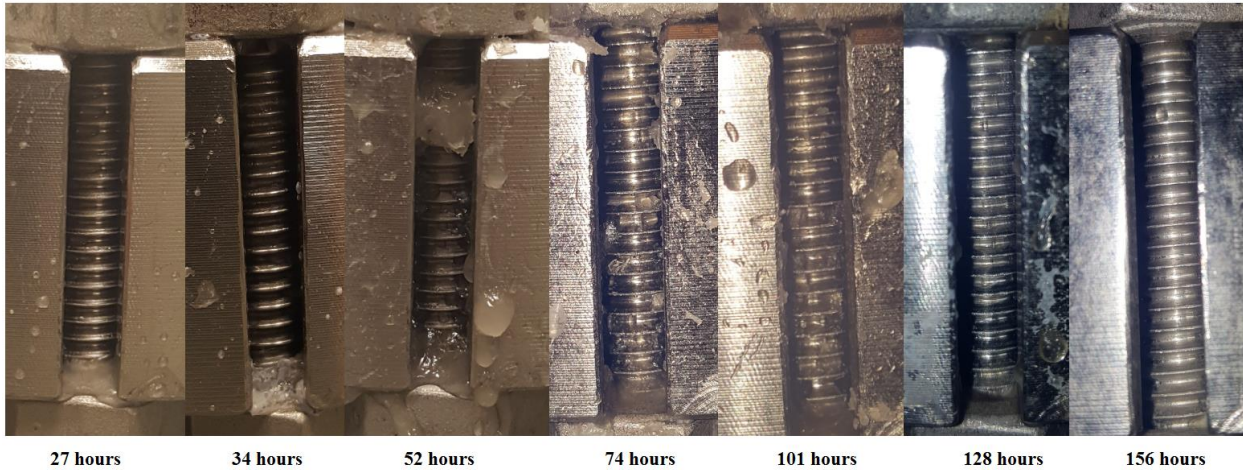


Figure 35: Progress pictures of the SA:6 bolt with hours in the test solution

The SA:6 bolt was examined with a visual inspection with 10X magnification and no cracks or pits were observed.

3.8.4 Alternate immersion testing

The results from the alternate immersion were as expected with obvious pitting on the 316L bolts while there was significantly less pitting observed on the SDSS bolts.

In regards to SCC, none of the tested bolts in 316L or SDSS quality experienced fracture in the alternate immersion testing. One of the 316L bolts had a crack from the top of the thread going towards the root. If this is due to SCC or if it was already there before the corrosion testing is not possible to determine without further detailed examination. Determining micro cracks by use of for example metallographic was not possible in the short time frame after the testing was finished as there was limited access to a laboratory.

The alternate immersion experiment was terminated after 936 hours, which again means that the bolt assemblies have been dipped in test solution 936 times. The test jig worked exceptionally well and had no issues running for the whole experiment.

316L results

For the 316L bolts the pitting gradually increased and Figure 36 shows the progress over time. The last picture in Figure 36 shows the bolt after it had been removed from the flange and cleaned in tap water.

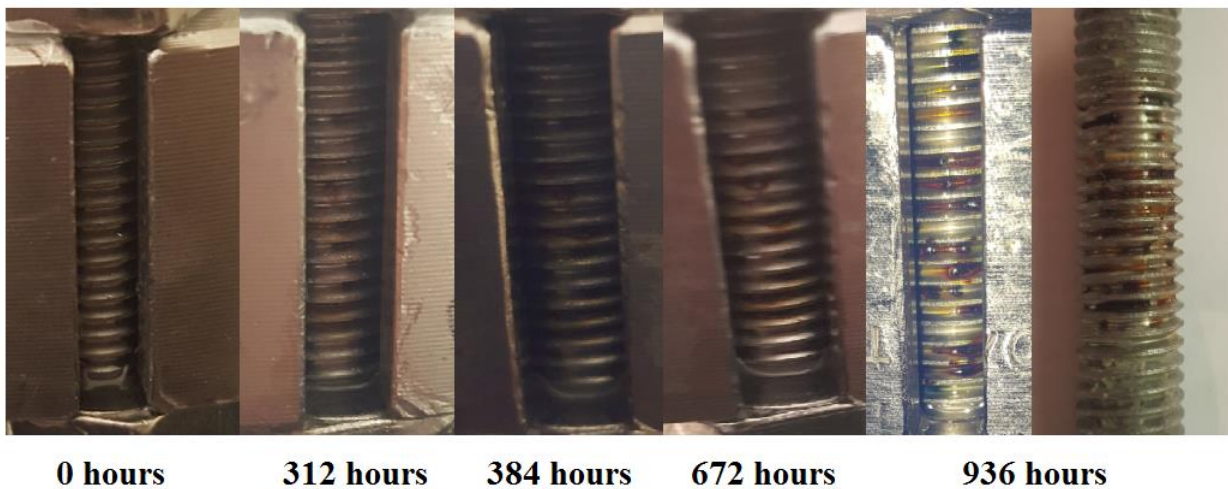


Figure 36: Progress pictures of the 316L bolts alternate immersion experiment for 936 hours

As seen from Figure 37, where the corrosion products have been cleaned away with a plastic brush and water, the pits are clearly visible. As the 316L bolts were mainly used to verify the setup, a more detailed investigation of the pits in regards to density etc. was not performed. Pictures of the pits at 10X are shown in Figure 38.



Figure 37: 316L bolts from alternate immersion testing after cleaning

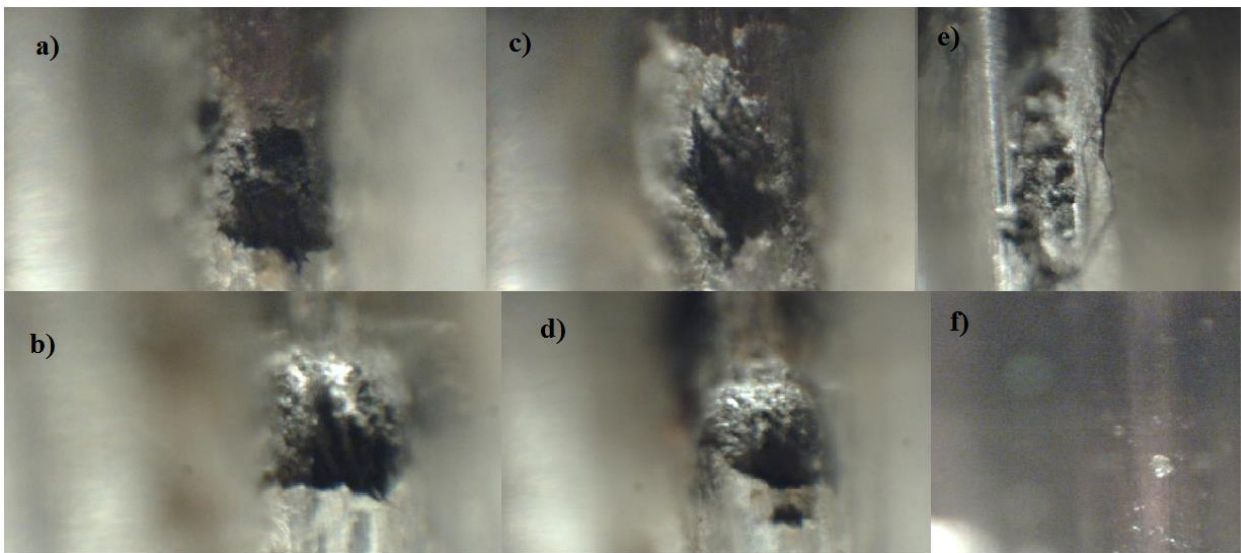


Figure 38: a), b), c) and d) showing pits at the root of the threads at approx. 10X. Picture e) shows a crack going from the top of the thread towards the root and f) shows the root before the experiment.

SDSS SA and CS results

Only minor corrosion products were observed during the testing as shown in Figure 39. However after around 500 hours, there were a few pits that started producing corrosion products in the CS bolts. The worst case of pitting is shown in the last picture in Figure 39 at the top of the shaft of CS:4.

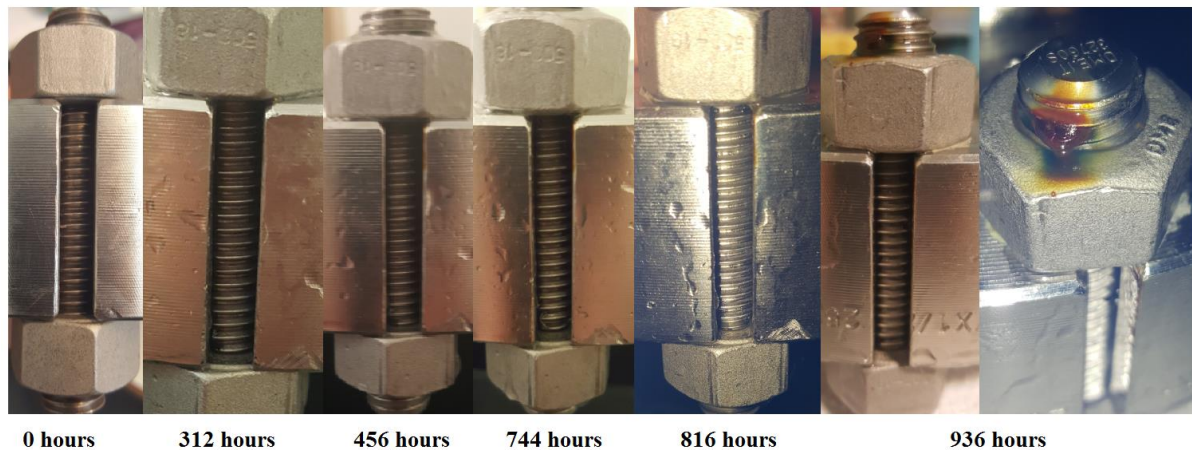


Figure 39: Progress pictures of the SDSS CS:4 bolt in the alternate immersion experiment for 936 hours

The CS bolts had obvious pitting with corresponding corrosion products. Visual inspection of the SA bolts did show any pitting on the surface at all. The pits are either too small for the 10X magnification to pick up or non-existing.

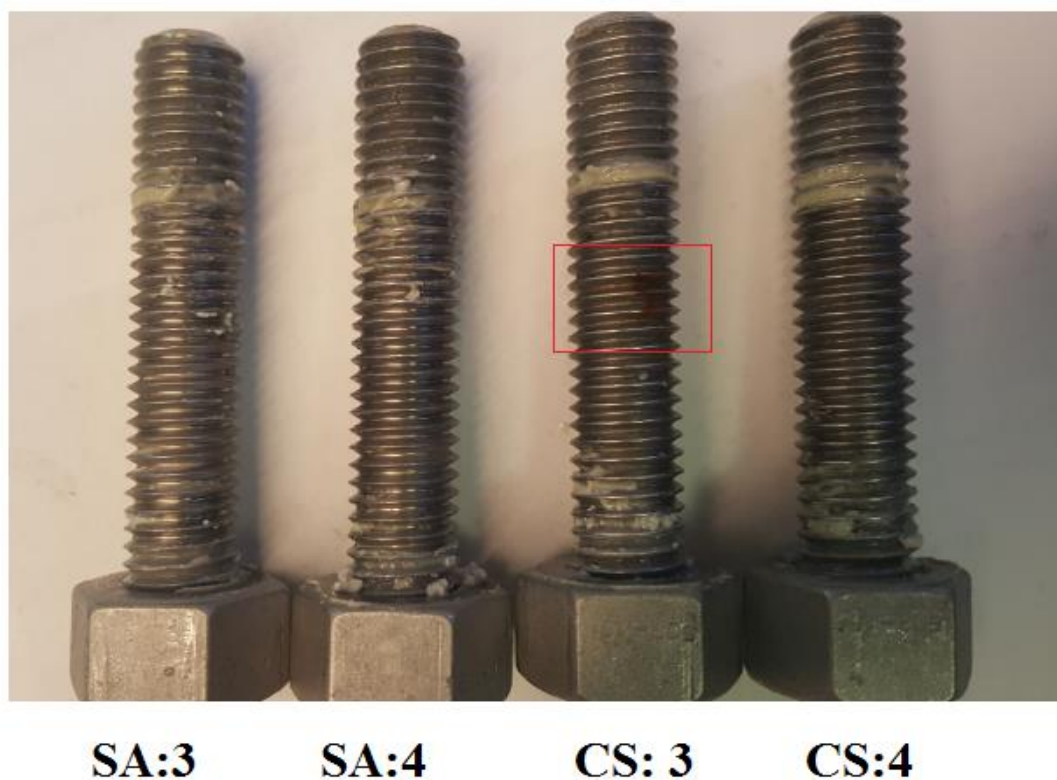


Figure 40: The SDSS bolts after alternate immersion testing for 936 hours

Figure 40 shows the SDSS bolts after the testing and before cleaning. The two major pits were found, one at the middle of the shaft of CS:3 as indicated with the red box, and one on the top of the shaft at CS:4 shown in the last picture of Figure 39. A detailed view of the two major pits on the CS bolts are shown in Figure 41.

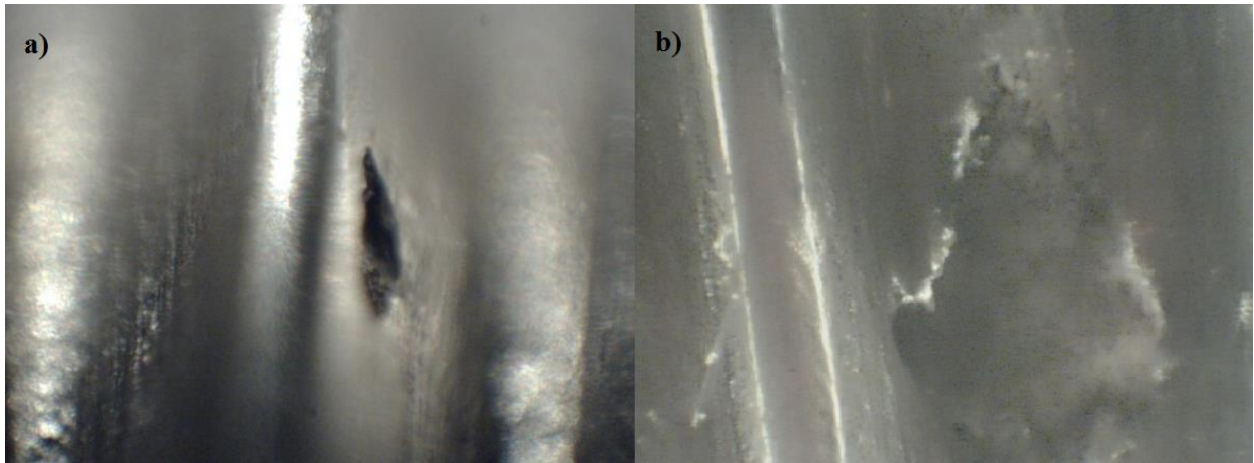


Figure 41: Details of the pitting on the CS bolts. a) shows the pit on the top of the bolt (CS:3) on the side of the thread and b) shows the pit in the center of the bolt (CS:4) at the root of the thread

(Page intentionally left blank)

4 Discussion

4.1 Tensile testing and torquing of bolts

During the tensile testing it became obvious that this method might have some inaccuracies. The offset yield was however determined and they were above the minimum values in the MDS in regards to the 316L and the SA SDSS bolts. However the results from the CS SDSS bolts did not match the MDS and were significantly lower than expected. This might be caused by the limited capacity of the tensile testing machine as it had only 10 T_e capacity so the CS bolts were not pulled to fracture. This lack of capacity might have caused the yield to be appear lower and thereby also causing the elongation at yield to be less. In effect this means that there is a possibility that the elongation used in the corrosion testing might be lower than it should be for the CS bolts. And hence the percentage of yield might be less than 100 %.

It was also obvious that the holders had some spring effect, meaning that some elongation is caused due to the tolerance in the threads. By looking at the stress-strain curves this effect occurred in all the tests at varying degree, but for test 4 where the bolt was machined down to a smaller diameter and the extensometer was placed directly on the bolt shaft, this effect was eliminated also indicating that the threads affect the Young's modulus.

Also for test 4 an expected Young's modulus was registered at 151 MPa. The Young's modulus for the other tests were all below half of what literature states it should be. As this happened at two different tensile testing machines something with the setup or some unexpected effect causes this. Nothing was found in the literature to explain this phenomenon. An ANSYS analysis was performed to try and replicate the effect using frictionless constraints. This agreed with the fact that the Young's modulus was altered when threads were present when increasing load was applied.

However when assembling the bolts on the flange they are in the same setup as for the tensile testing, with the holders being replaced with nuts. There is of course more thread engagement in the holders, but as discussed earlier there is limited value of having a very long thread engagement as the first threads take most of the load. There might be some inaccuracy in regards to the elongation at yield caused by these effects, but it was decided that these values were accurate enough to use for torquing the bolts for the corrosion experiments. Also the strain from the testing was higher than the theoretical strain, meaning the bolts in theory should be torqued to yield or higher, at least for the SA bolts, which needs to be considered when analyzing the results from the SCC testing.

The torquing of the bolts had no issues but seeing as the length of the stressed part of the bolts was only 36 mm, there is a higher risk of inaccuracy. It would have been ideal to have bolts delivered with a higher length causing the elongation to be higher and again it would be easier to measure. Also measuring with a micrometer, on a surface that is not machined will have caused some inaccuracy as it is hard to hit the exact spot when measuring between the torquing intervals.

In retrospect tensile testing with measuring the resulting elongation may not be as accurate as expected. This is due to the uncertainties in regards to both the Young's modulus and the risk of error when measuring the elongation, especially when the lengths of the bolts are as short as for the ones used in these experiments. If possible, acquiring only partly threaded bolts and using strain gauges on the smooth part of the shaft may be a better solution to exactly measure the strain when torquing.

4.2 Immersed test with heating

This experiment had some issues in regards to not having the ability to be switched on for the whole test. As the method of alternating heating between approximately 23 – 90 °C was used, the magnesium chloride solidified when cooled as it was supersaturated at room temperature. The next heating cycle therefore had a thick crust above the magnesium chloride solution for the first hours of the next heating cycle which prevented inspection.

The improved inspection regime for test 2 was very successful. There is of course impossible for this method to exactly determine the time of fracture, but it was determined it would be good enough in regards to not disturbing the test solution too much.

In regards to the difference of the SCC resistance for SA compared to CS, one of the SA bolts (SA:6) seemed to show a very high resistance to SCC compared to the two CS bolts and the other SA (SA:5) bolt tested. It was discovered that the SA:5 bolt had been torqued at a stress level approximately 120 % of yield, which is probably the reason for this bolt fracturing earlier than SA: 5 which was torqued to 100% of yield. This shows that torquing while measuring elongation is difficult, when a small increase in torque can suddenly produce a lot of elongation due to a sudden decrease in friction. However as there are a limited amount of bolts tested, as well as the testing has been performed on as received materials instead of test specimens according to a standard, there are a lot of variables that may affect the results.

As discussed earlier the torquing of the bolts may not have been as accurate as expected. And in the case of the CS bolts where the offset yield is 1004 MPa and the UTS is 1075 MPa, a small error in the torquing may be crucial. This makes the CS bolts a lot more sensitive to errors in

torqueing compared to the SA bolts which has a difference of 215 *MPa* between offset yield and UTS.

The surface properties and the micro structure is very important in regards to SCC resistance, and there might be some minor difference in each test specimen. The environment in the testing is also very severe and adjusting either the temperature or chloride concentration could have been beneficial when comparing SA against CS to extend the time of testing. With such an aggressive environment it was hard to determine the exact time of fracture without inspecting the specimens at a very high frequency, which again would disturb the test solution and potential pitting and SCC initiation.

It is also important to acknowledge the fact that the material cost of testing directly on the as received bolts is very high compared to making small test specimens from for example a plate.

To better determine the exact time of fracture some modifications can be implemented:

- Varying the three main variables one by one or together
 - Temperature
 - Chloride concentration
 - Stress levels
- A built in load cell in the flange that would register the exact moment when the load is relieved and fracture occurs

4.3 *Alternate immersion testing*

The test setup worked as intended and was very reliable. The humidity was increased after some modifications to the jig. The required relative humidity requirement of minimum 35 % was not possible with the current setup, and it was kept steady around 24 – 26 %. This might have had an effect as the relative humidity is important to develop a corrosive environment. Also at the start of the experiment there were some issues with supersaturated test solutions. This caused a thin film of magnesium chloride to form on the surface of the solution. Every time the specimens were dipped a new layer of salt was formed on the whole flange. After a few days long stalactites were formed as seen in Figure 42. This was handled by adding a small amount of water while stirring.

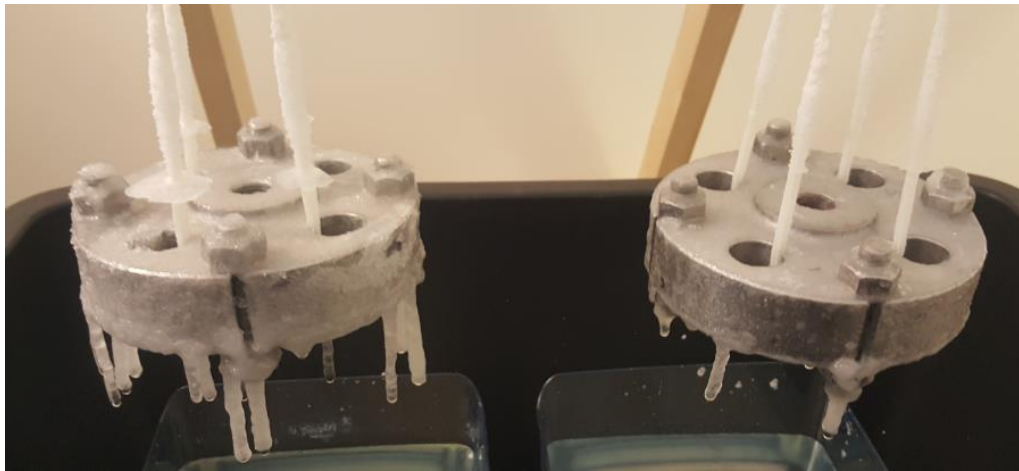


Figure 42: Supersaturated test solutions produced stalactites

The pitting on the 316L bolts were as expected with serious pitting and corrosion products. No fractures occurred meaning all the 316L bolts passed the alternate immersion test criterion in regards to SCC. One crack however was found in one of the 316L bolts, but as the bolts were not visually inspected at 10X before the testing it is not possible to conclude that this came from the testing. It was not possible to determine if there are any other cracks with 10X magnification, meaning that metallographic testing needs to be performed to further investigate the degree of cracking.

In the case of comparing SDSS SA against CS bolts, the CS bolts had obvious pitting with corrosion products compared to the SA bolts which did not have any pits that visual inspection at 10X magnification could discover. Both the SA and CS bolts exhibited high resistance against pitting compared to the 316L bolts after 936 hours which was as expected.

This test exchanged the recommended sodium chloride described in G44 [34] with magnesium chloride for the test solution, but it is difficult to determine the significance of this without further examination of the bolts in regards to cracks.

In regards to SCC, this method does not seem very applicable for lab testing as the time aspect might be an issue.

There are several things that could accelerate the experiments. Increase the magnesium chloride concentration by heating the test solution would provide a more severe environment. Also increasing the relative humidity by using an air humidifier could be a possible enhancement for the testing. In regards to the stress levels, the bolts were torqued to 100% of the offset yield. There is of course the option to stress the bolts to above yield, but this would not be recommended unless there is a very accurate method used.

As the number of bolts tested were so few it is possible that minor differences in the test specimens used will skew the results in one or the other direction, meaning that it is impossible to conclude that the pitting resistance is higher for SA compared to CS bolts. The magnification used to visually inspect the pits was only 10X. This means that in theory the CS bolts may have produced a few larger pits while the SA bolts may have produced a lot of smaller ones that can only be detected with metallographic testing or with a SEM / TEM. This however seems unlikely.

This test however showed an indication of higher resistance to pitting in the SA bolts compared to the CS bolts.

4.4 Further work

As there was not enough time to performing experiments on a high number of bolts, further work should continue testing too see if the results can be recreated. Especially the immersed testing is easy to setup and works well for a lab environment in regards to the time aspect. With better equipment and more specimens, the indications of a higher pitting and SCC resistance of the SA bolts compared to the CS bolts could be confirmed or not.

It would also be interesting to test regular standard specimens in the same environment that has been used in this thesis to compare the difference on testing directly on a bolt compared to a standard specimen.

(Page intentionally left blank)

5 Conclusion

This thesis has been performed using modified standards, which again can make it hard to compare the results directly to earlier research. Also the testing was performed directly on the bolts in as received condition compared to earlier research that use standard test specimens. However the setups of the test equipment and the actual experiments have been documented so it should be possible to recreate the results or use the information gained from this thesis to do further research on the subject. To provide a definite conclusion on the experiments is not possible due to the amount of specimens tested and the extra variable coming from not performing the experiments in a laboratory with the proper equipment for logging, lab grade chemicals and using the parameters set in the standards. However some recommendations for further research are provided as well as the experience gained from this thesis.

The tensile testing of the bolts provided an unexpected result for the Young's modulus, and this should be investigated with more testing if the method of measuring elongation to determine the stress level is to be used again.

The alternate immersion testing setup worked flawlessly and using an Arduino card to control the system was relatively easy to set up in regards to the coding. Also the alternate immersion experiment provided some expected results with the 316L bolts exhibiting a high degree of pitting. The SDSS SA and CS bolts did exhibit a difference in pitting resistance. The CS bolts had clearly visible pits while the SA did not show any signs of pitting. This should be investigated further as only two of each type of bolts was tested and this is not enough to provide a definite conclusion. Also earlier research shows that there is not any difference between pitting resistance for SA or CS material, so the results from the experiments performed in this thesis might be an anomaly.

Only one crack in the 316L bolt was found by visual inspection at 10X of the bolts from the alternate immersion testing. However this does not mean that micro cracks are not present meaning further examination of the bolts needs to be performed to assess the effect on SCC from the alternate immersion testing.

The immersed heating experiment was successful in regards to provoking SCC. In test 1 all of the specimens experienced fractures. In test 2 which was more closely supervised, it showed an indication that the SA bolts have a higher resistance in regards to SCC compared to the CS bolts. But as with the alternate immersion testing, too few specimens were tested to conclude on this and further testing needs to be performed.

In regards to pitting, there were no pits on either the SA or CS bolts in the immersed heating tests that could be discovered with 10X magnification.

6 References

1. Rosso, M, Peter, I, and Suani, D., (2013) *About heat treatment and properties of Duplex Stainless Steels*, Journal of Achievements in Materials and Manufacturing Engineering, Vol: 59 Issue 1. Available at: <http://www.journalamme.org/>
2. Sedriks, A.J., (1996) *Corrosion of stainless steels 2nd Ed*, John Wiley & sons, New York
3. *Practical Guidelines for the Fabrication of Duplex Stainless Steel*, (2014), International Molybdenum Association, Third Edition, London. Available at: <http://www.imoa.info/molybdenum-media-centre/downloads/practical-guidelines/fabrication-series.php> Last accessed: 11.05.2016
4. Liljas M., (2010) *80 Years with Duplex Steel, a Historic Review and Prospects for the Future*, Acom 4th ed, pp 28-34. Available at: <http://www.outokumpu.com/SiteCollectionDocuments/Outokumpu-corrosion-management-news-Acom-4-edition-2010.pdf> Last accessed: 01.05.2016
5. Trethewey, K., and Chamberlain, J., (2001) *Corrosion for Science and Engineering 2nd Ed*. Pearson Education, Print on Demand Edition.
6. Gunn, R.N., (1993) *The weldability and Properties of Duplex and Superduplex Stainless Steels*, Proceedings of the Third International Offshore and Polar Engineering Conference, Singapore 6-11th June, pp. 228-234
7. Gunn, R.N., (1997) *Duplex Stainless Steels*, Woodhead Publishing Ltd., Suffolk
8. Charles, J., (2007) *Duplex Stainless steels, a review after DSS '07 held in Grado*, Duplex '07, Grado, Available at: <http://journals.cambridge.org/> Last accessed: 03.04.2016
9. Nilsson, J.O. (1992) *Super duplex stainless steels*, Material Science and Technology Vol: 8, pp. 685-700. Available at: https://www.researchgate.net/profile/J-O-Nilsson/publication/233551448_Super_duplex_stainless_steels/links/0046352a97dbff0849000000.pdf/download?version=vtp Last accessed: 11.04.2016
10. Ahmad, Z., (2006), *Principles of Corrosion Engineering and Corrosion Control*, Butterworth-Heinemann, Great Britain
11. Callister, W.D., (2007), *Materials Science and Engineering an Introduction*, 7th Ed. John Wiley & Sons, Versailles, KY
12. El-Azab, A., (2008), *The statistical Mechanics of Strain-Hardened Metals*, Science, Vol: 320, pp.1729-30, DOI: 10.1126/science.1160003
13. Devincere, B., Hoc, T., and Kubin, L., (2008), *Dislocation Mean Free Paths and Strain Hardening of Crystals*, Science Vol: 320, pp.1745-8, DOI: 10.1126/science.1156101

14. Dong, C., Luo, H., Xiao, K., Sun, T., and Li, X., (2011), *Effect of Temperature and Cl⁻ Concentration on Pitting of 2205 Duplex Stainless Steel*, Journal of Wuhan University of Technology-Mater. Sci. Ed., 2011, Vol.26 (4), pp. 641-647, DOI: 10.1007/s11595-011-0283-4
15. ASTM G48 – 11, (2015), *Standard Test Methods for Pitting and Crevice Corrosion Resistance of Stainless Steels and Related Alloys by Use of Ferric Chloride Solution*, West Conshohocken, ASTM International, www.astm.org
16. Jin, L.Z., (1995), *The Chloride Stress-Corrosion Cracking Behavior of Stainless Steels under Different Test Methods*, Journal of Materials Engineering and Performance, Vol 3 (6), pp. 734-739, DOI: 10.1007/BF02818373
17. ASTM G36-94, (Reapproved 2000), *Standard practice for evaluating Stress-Corrosion-Cracking Resistance of Metals and Alloys in a Boiling Magnesium Chloride Solution*, West Conshohocken, ASTM International, www.astm.org
18. Mietz, J., and Isecke, B., (1999) *Assessment of test methods for evaluation stress corrosion cracking susceptibility of prestressing steels*, Materials And Corrosion-Werkstoffe Und Korrosion, Vol.50 (5), pp.273-281, Available at: <http://onlinelibrary.wiley.com> , Last accessed: 04.05.2016
19. Spaehn, H., (1990), *Stress Corrosion Cracking and Corrosion Fatigue of martensitic, Ferritic and Ferritic-Austenitic (Duplex) Stainless Steels*, Environment-Induced Cracking of Metals, EICM Houston, Texas pp. 449-487 Available at: <http://oai.dtic.mil/oai/oai?verb=getRecord&metadataPrefix=html&identifier=ADA228834> Last accessed: 12.05.2016
20. Phadnis, S.V., Satpati, A.K., Muthe, K.P., Vyas, J.C., and Sundaresan R.I., (2003), *Comparison of rolled and heat treated SS304 in chloride solution using electrochemical and XPS techniques*, Corrosion Science 45, pp. 2467-2483, DOI: 10.1016/S0010-938X(03)00099-4
21. Mudali, U.K., Shankar, P., Ningshen, S., Dayal, R.K., Khatak, H.S., and Raj, B., (2002) *On the pitting corrosion resistance of nitrogen alloyed cold worked austenitic stainless steels*, Corrosion Science Vol 44, pp.2183-2198, DOI: 10.1016/S0010-938X(02)00035-5
22. Peguet, L., Malki, B., and Baroux, B., (2007), *Influence of cold working on the pitting corrosion resistance of stainless steels*, Corrosion Science 49, pp. 1933-1948, DOI: 10.1016/j.corsci.2006.08.021
23. Renton, N.C., Elhoud, A.M., and Deans, W.F., (2011) *Effect of Plastic Deformation on the Corrosion Behavior of a Super-Duplex Stainless Steel*, Journal of Materials Engineering and Performance Vol 20 (3), pp. 436-444 DOI: 10.1007/s11665-010-9688-z

24. Johansson, J., and Oden, M., (2000), *Load sharing between austenite and Ferrite in a Duplex Stainless Steel during Cyclic Loading*, Metallurgical and material transactions, Vol 31 (6), pp. 1557-1570, DOI: 10.1007/s11661-000-0166-3
25. Elhoud, A.M., Renton, N.C., and Deans, W.F., (2011), *The effect of manufacturing variables on the corrosion resistance of a super duplex stainless steel*, International journal of advanced manufacturing technology Vol 52 (5), pp. 451-461, DOI: 10.1007/s00170-010-2756-6
26. Takizawa, K., Shimizu, Y., Yoneda, E., and Tamura, I., (1981), *Effects of Cold Work, Heat Treatment and Volume Fraction of Ferrite on Stress Corrosion Cracking Behavior of Duplex Stainless Steel*, Tetsu-to-haganè (Journal of the Iron and Steel Institute of Japan), 67 (2), pp. 353-361, Available at: http://ci.nii.ac.jp/vol_issue/nels/AN00151251_en.html Last accessed 12.05.2016
27. Bauernfeind, D., Haberl, J., Mori, G., and Falk, H., (2006), *Influence of Cold Deformation on Stress Corrosion Cracking Resistance of Highly Alloyed Austenitic Steels in Chloride Media*, Corrosion Vol 61, NACE paper No. 06504, Available at: <http://www.nace.org/> Last accessed: 06.04.2016
28. Leonard, A.J., Martin, J.W., Davis, A.P., Ueda, M., and Kimura, S., (2010) *Effect of Severe cold work on the microstructure and SCC resistance of Superduplex Stainless steel downhole tubulars*, NACE paper no. 10289 Available at: <http://www.nace.org/> Last accessed: 13.04.2016
29. Manchet, S.L., Fanica, A., and Lowjeski, C., (2013), *Resistance to Stress Corrosion Cracking of Duplex Stainless Steels*, NACE paper no. 2086 Available at: <http://www.nace.org/> Last accessed: 31.05.2016
30. Johansson, E., and Prosek, T., (2007), *Stress Corrosion Cracking Properties of UNS 32101 – A New Duplex Stainless Steel With Low Nickel Content*, NACE paper no. 07475 Available at: <http://www.nace.org/> Last accessed: 01.06.2016
31. Standards Norway, NORSOK M - 630, (2013), *Material data sheets for piping*, 6th ed., Standards Norway, Available at: <https://www.standard.no/>
32. ASTM G48 - 03, (2003), *Standard Test Methods for Pitting and Crevice Corrosion Resistance of Stainless Steels and Related Alloys by Use of Ferric Chloride Solution*, ASTM International, West Conshohocken, PA, www.astm.org
33. ASTM G30 - 97, (Reapproved 2003), *Standard Practice for Making and Using U-Bend Stress-Corrosion Test Specimens*, ASTM International, West Conshohocken, PA, www.astm.org

34. ASTM G44 - 99, (1999), *Standard Practice for Exposure of Metals and Alloys by Alternate Immersion in Neutral 3,5 % Sodium Chloride Solution*, ASTM International, West Conshohocken, PA, www.astm.org
35. ASTM G46 – 94, (Reapproved 2003), *Standard Guide for Examination and Evaluation of Pitting Corrosion*, ASTM International, West Conshohocken, PA, www.astm.org
36. ASTM G1 – 03, (2003), *Standard Practice for Preparing, Cleaning, and Evaluating Corrosion Test Specimens*, ASTM International, West Conshohocken, PA, www.astm.org
37. Dahlvig, G., Christensen, S., and Strømsnes, G., (2000), *Konstruksjonselementer*, 2nd ed, Gyldendal, Aurskog
38. Fastenal and Engineering & Design Support, (2009) *Screw thread design*, Fastenal and Engineering & Design Support, rev 3-4-09, Available at: <https://www.fastenal.com/content/feds/pdf/Article%20-%20Screw%20Threads%20Design.pdf> Last accessed 05.05.2016
39. Langley Alloys, (2011), *Super Duplex S32760*, Available at: <http://www.langleyalloys.com/ALLOYS32760.php> Last accessed 18.05.2016
40. ASTM A1082 / A1082M-15, (2015), *Standard Specification for High Strength Precipitation Hardening and Duplex Stainless Steel Bolting for Special Purpose Applications*, ASTM International, West Conshohocken, PA, www.astm.org
41. OME Metallurgica (2015) , *Qualification Test Record*, QTR No.: 1301, Rev 3
42. ASTM A320 / A320M-15a, (2015), *Standard Specification for Alloy-Steel and Stainless Steel Bolting for Low-Temperature Service*, ASTM International, West Conshohocken, PA, www.astm.org
43. ASTM A194 / A194M-16, (2016), *Standard Specification for Carbon Steel, Alloy Steel, and Stainless Steel Nuts for Bolts for High Pressure or High Temperature Service, or Both*, ASTM International, West Conshohocken, PA, www.astm.org
44. Davies, J.R., (1994), *Stainless Steels*, ASM International, pp. 489
45. Wikipedia, (2016), *Magnesium chloride*, Available at: https://en.wikipedia.org/wiki/Magnesium_chloride Last accessed: 18.05.2016

7 Appendices

Appendix A: Torque calculations

Torque calculations on bolt and nut

Torque on threads

Axial force:	$F := 98.9 \text{ kN}$
Pitch of threads	$P := 1.9538 \text{ mm}$
Middle diameter:	$d_2 := 11.43 \text{ mm}$
Middle radius of thread:	$r_m := \frac{d_2}{2} = 5.715 \text{ mm}$
Friction coefficient in threads	$\mu_1 := 0.1 \quad \mu_2 := 0.2$
Angle of threads UNC	$\alpha := 30 \text{ deg}$
Friction angle	$\varepsilon_1 := \text{atan}\left(\frac{\mu_1}{\cos(\alpha)}\right) \quad \varepsilon_2 := \text{atan}\left(\frac{\mu_2}{\cos(\alpha)}\right)$
Angle of pitch	$\phi := \frac{P}{\pi \cdot d_2}$
Torque with friction 0,1	$M_{v1} := F \cdot r_m \cdot \tan(\varepsilon_1 - \phi) = 34.266 \text{ N} \cdot \text{m}$
Torque with friction 0,2	$M_{v2} := F \cdot r_m \cdot \tan(\varepsilon_2 - \phi) = 98.507 \text{ N} \cdot \text{m}$

Torque between nut and surface

Axial force:	$F := 98.9 \text{ kN}$
Friction between nut and surface	$\mu' := 0.1 \quad \mu'_2 := 0.2$
Diameter of hole	$d_h := 13 \text{ mm}$
Width across flats	$s := 22 \text{ mm}$
Radius of friction area	$r'_m := \frac{s + d_h}{4} = 8.75 \text{ mm}$
Torque with friction 0,1	$M_{s1} := \mu' \cdot F \cdot r'_m = 86.538 \text{ N} \cdot \text{m}$
Torque with friction 0,2	$M_{s2} := \mu'_2 \cdot F \cdot r'_m = 173.075 \text{ N} \cdot \text{m}$
Total torque with friction 0,1:	$M_{tot} := M_{v1} + M_{s1} = 120.803 \text{ N} \cdot \text{m}$
Total torque with friction 0,2:	$M_{tot} := M_{v2} + M_{s2} = 271.582 \text{ N} \cdot \text{m}$

Appendix B: MSDS Gleitpaste

MATERIAL SAFETY DATA SHEET 91/155/EEC, §14 GefStoffV, TRGS 220

Date of issue: 10.03.2003

Version 01 of 01.12.2002 Revison 0

EMB-Gleitpaste Special White Grease Paste

Seite 1/4

1. SUBSTANCE-/PREPARATION AND COMPNY IDENTIFICATION

- 1.1 CHEMICAL NATURE /APPLICATION/CHARACTER: White lubricating grease paste for industrial use
1.2 ADDRESS OF PROCUCER/SUPPLIER: EMB Eifeler Maschinenbau GmbH
Kolumbusstraße 54
D-53881 Euskirchen

2 COMPOSITION / INFORMATION OF INGREDIENTS

- 2.1 MATERIAL:
2.2 CAS-Nr.:
2.3 FORMULATION: X
2.4 CHEMICAL CHARACTER: Lubricating grease based on severe treat mineral oil, synthetic oil, solid lubricants, thickener and additives
2.5 DAINGEROUS INGREDIENT This product is not hazardous to health as defined by the EC Dangerous Substance/Preparations Directives.

3 HAZARDS IDENTIFICATION

This health hazard assessment is based on a consideration of the composition of this product. This product is not hazardous to health. Nevertheless, normal hygiene rules by working with chemical products should be considered.

4 FIRST AID MEASURES

- 4.1 CONTACT WITH SKIN Remove contaminated clothing. Wash skin with soap and water. If symptoms develop, obtain medical attention. Use a skin creme for receiving the natural skin film.
4.2 CONTACT WITH EYE If substance has gone into the eyes, immediately wash out with plenty of water until medical assistance is provided. Retract eyelids often. Contact a doctor.
4.3 INGESTION Wash out mouth with water. Obtain medical attention immediately.
4.4 INHALATION Not expected to be a problem.
Remove patient from exposure, keep warm and at rest. Obtain medical attention if ill effects occur.
4.5 ADDITIONAL INFORMATION High pressure accidental injection through the skin requires immediate medical attention for possible incision, irrigation and / or debridement.

5 FIRE-FIGHTING MEASURES

- 5.1 SUITABLE EXTINGUISHING MEDIA Not classed as flammable. If involved in a fire, it may emit noxious and toxic fumes.
Foam, CO₂, dry chemical or water fog
5.2 UNSUITABLE EXTINGUISHING MEDIA Water in beam-form
5.3 SPECIAL DANGER In case of fire and/or explosion do not breath fumes.
5.4 SPECIAL PROTECTION EQUIPMENT Product may give off toxic fumes in a fire. Firefighters must wear breathing apparaturs.
5.5 FURTHER INFORMATION Water may be used to cool closed containers to prevent pressure build up.

Date of issue: 10.03.2003

Version 01 of 01.12.2002; Revision 0

EMB-Gleitpaste Special White Grease Paste

Seite 2 / 4

6 ACCIDENTIAL RELEASE MEASURES

- 6.1 PERSONAL PRECAUTIONS Avoid contact with eyes and skin. Avoid breathing vapours.
- 6.2 ENVIRONMENTAL PRECAUTIONS Do not release to the environment
- 6.3 METHODS OF CLEANING/ BESEITIGUNG Absorb spillages in sand, earth or any suitable absorbent material. Transfer to a container for disposal. In case of bigger quantities inform public authority
- 6.4 FURTHER INFORMATIONS ----

7 HANDLING AND STORAGE

- 7.1 HINTS FOR HANDLING Normal security rules for organic products with a flash point higher than 100°C. Avoid eye and skin contact. High pressure injection under the skin may occur due to the rupture of pressurized lines. Always seek medical attention.
- 7.2 HINTS FOR STORAGE Do not store in open or unlabelled containers. Store away from strong oxidizing agents or combustible material.
- 7.3 REQUIREMENTS TO STORAGE ROOMS-/CONDITIONS see 7.2
- 7.4 HINTS FOR CONNECTING-STORAGE see 7.2
- 7.5 FURTHER INFORMATION none

8 EXPOSURE CONTROLS / PERSONAL PROTECTION EQUIPMENT

- 8.1 TECHNICAL PROTECTIVE MEASURES No special requirements under ordinary conditions of use and with adequate ventilation.
- 8.2 EXPOSURE CONTROL LIMITS
- 8.2.1 MAK-VALUE none
- 8.2.2 COMPANY-INTERNAL LIMITS none
- 8.3 RESPIRATORY PROTECTION No special requirements under ordinary conditions of use and with adequate ventilation.
- 8.3.1 SKIN-PROTECTION If prolonged or repeated skin contact is likely, oil impervious gloves must be worn. Good personal hygiene practices should always be followed.
- 8.3.2 EYE-PROTECTION General eye contact is unlikely with this type of material. If eye contact is likely, safety glasses with side shields or chemical type of goggles should be worn.
- 8.3.3 INHALATION-PROTECTION General inhalation is unlikely with this type of material.
- 8.3.4 WEAR as usual by working with organic chemical products
- 8.4 FURTHER INFORMATION none

Date of issue: 10.03.2003

Version 01 of 01.12.2002; Revision 0

EMB-Gleitpaste Special White Grease Paste

Seite 3 / 4

9 PHYSICAL AND CHEMICAL PROPERTIES

9.1	<u>PHYSICAL STATE:</u>		grease-paste	
9.2	<u>COLOUR</u>		white / beige-coloured	
9.3	<u>ODOUR</u>		weak	
9.4	<u>CHANGE IN PHYSICAL STATE</u>	MELTING POINT BOILING POINT/RANGE DROPPING POINT	not determined not determined 190 °C	
9.5	<u>FLASH POINT</u>		> 220 °C	DIN 51376
9.6	<u>IGNITION TEMPERATURE</u>		not determined	
9.7	<u>EXPLOSION LIMITS</u>	LOWER UPPER	not determined	
9.8	<u>VAPOUR PRESSURE</u> (20°C)		not determined	
9.9	<u>DENSITY</u> (20°C; 1bar)		appr. 1,1 g/cm ³	
9.10	<u>SOLUBILITY IN WATER</u> (20°C)		negligible	
9.11	<u>pH-VALUE</u> (20°C)		not determined	

10 STABILITY AND REAKTIVITY

10.1	<u>THERMAL DECOMPOSITION</u>	Stable. Avoid extreme heat.
10.2	<u>CONDITIONS TO BE AVOIDED</u>	Extreme heat
10.3	<u>MATERIALS TO BE AVOIDED</u>	None known
10.4	<u>HARZARDOUS DECOMPOSITION PRODUCTS</u>	None known. By normal using no decomposition. In case of decomposition different decomposition products developed. The composition of these products depends on exact decomposition conditons.
	<u>IN CASE OF FIRE</u>	CO ₂ /CO, elemental oxides, metal oxides and other undefined decomposition products
10.5	<u>FURTHER INFORMATIONS</u>	none

11 TOXICOLOGICAL INFORMATIONS

11.1	<u>ORAL TOXICITY LD50</u>	Practically non-toxic (LD 50: greater than 2000 mg/kg; based on testing of similar products)
11.2	<u>SKIN IRRITATION</u>	Practically non-irritating (Primary Irritation-Index: greater than 0,5 but less than 3; based on testing of similar products)
11.3	<u>SKIN SENSIBILITY</u>	no datas available
11.4	<u>EYE IRRITATION</u>	Practically non-irritating (Draize score: greater than 6 but less 15; based on testing of similar products) Irritating to eye, no datas available
11.5	<u>INHALATION</u>	Under ordinary conditions of not applicable
11.6	<u>FURTHER INFORMATION</u>	none available

12 ECOLOGICAL INFORMATION

12.1	<u>AKUTE FISH-TOXICITY</u> (LC50/96 h)	> 100 mg/l (base-oil; OECD 203)
12.2	<u>EFFECT-CONCENTRATION</u> (EC50/24 h)	> 10 g/l (base-oil; DIN 38412, p. 8)
12.3	<u>READY BIODEGRADABILITY</u>	no information available
	<u>FURTHER INFORMATIONS</u>	This product is expected to be inherently biodegradable. There is no evidence to suggest bioaccumulation will occur. It may be harmful to aquatic organisms.



MATERIAL SAFETY DATA SHEET 91/155/EWG, §14 GefStoffV, TRGS 220

Date of issue: 11.03.2003

Version 01 vom 01.12.2002; Revision 0

EMB-Gleitpasten Special White Grease Paste		Seite 4 / 4
13 DISPOSAL CONSIDERATIONS		
13.1	<u>PRODUCT</u>	Dispose in accordance with local and state regulations
13.1.1	<u>WASTE IDENTIFICATION NUMBER</u>	120112 (greases)
13.2	<u>CONTAINER</u>	
13.2.1	<u>WASTE IDENTIFICATION NUMBER</u>	150199 (plastic containers with harmful rests)
14 TRANSPORT INFORMATIONS		
14.1	<u>UN-NR:</u>	Not regulated
14.2	<u>GGVS/ADR:</u>	Not regulated
14.3	<u>GGVE/RID</u>	Not regulated
14.4	<u>GGVBinSch/ADNR:</u>	Not regulated
14.5	<u>GGVSEE / IMDG - CODE</u>	Not regulated
14.6	<u>ICAO / IATA - DRG</u>	Not regulated
14.7	<u>FLASH-POINT</u>	220°C
14.8	<u>TECHN. NAME STREET TRANSPORT</u>	NOT RERSTRICTED
14.9	<u>ADDITIONAL INFORMATIONS</u>	Not classified as hazardous for transport. EU labelling not required
15 REGULATORY INFORMATIONS		
15.1	<u>MARKING TO EEC REGULATIONS</u>	No marking required
	<u>PRODUCT CONTAINS</u>	
15.2	<u>NATIONAL REGULATIONS</u>	
	<u>VbF - CL:</u>	not flammable
	<u>TA - LUFT:</u>	no informations available
	<u>WGK</u>	1 (in accordance to VCI), slightly hazard to water
16 FURTHER INFORMATIONS		
16.1	<u>EDITOR</u>	Marketing department
16.2	<u>VERSION REPLACES VERSION :</u>	

Appendix C: MDS SDSS Flanges

		23813 Cortenova (Lecco) ITALY Largo De Vecchi 11 P.o. box 11 Tel. 0341.98341 Fax 0341.983496 - 983497 lno.uberli@melesi.it		CERTIFICATO DI COLLAUDO WORKS CERTIFICATE CERTIFICAT D'ESSAIS		N. 78248 DATA/DATE 31/01/12 SHEET/PAGE 1/1						
FLANGE E FORGIATI		ORDINE/ORDER/C.DE F/64589/00 DATA/DATE 16/11/11 COMMESSA 47610		FLANGEFITT STAINLESS LTD RAWLEY'S LANE, HARRINGTON CHESHIRE WA2 8JB GB								
N. RIF.	ITEM	N / QUANTITY	DESCRIZIONE / DESCRIPTION / DESIGNATION			NOTE						
SI113	037	45	A182F55 1" WN 2500 RJ XS/808			P107						
SI113	039	65	A182F55 1" x 1/2" THR 2500 RJ			P107						
N.	MATERIALE / MATERIAL / MATERIEL	HEAT / COULÉE	ACCIAIERIA / STEEL PLANT / ACIERIE			ORIGIN. CERT. / CERT. D'ORIGINE						
SI113	ASTM A182 F55 09a	529632	SANDVIK Refining method A.O.D.			A/11-187220						
N. RIF.	ANALISI CHIMICA / CHEMICAL ANALYSIS / COMPOSITION CHIMIQUE											
	C	Mn	Si	S	P	Cr	Ni	Mo	N	W	Cu	PRE
SI113	0,016	0,680	0,230	0,000	0,023	25,190	6,760	3,770	0,260	0,630	0,560	41,791
N. RIF.	PROVE MECCANICHE / MECHANICAL TESTS / ESSAIS MECANQUES											
	#	SO	LU	RS-YIELD	R-TENSILE	A. %-ELONG.	C. %-REDUCT.	RESILLENZA / IMPACT TEST / RESILIENCE			HARDNESS / DURETE	
	mm	mm.2	mm.	LMITE	RUPTURE	ALLONGEM.	STRICTIO	MEDIO / AVERAGE	MINIMO	TIPO	TEMP.	R R C
				MPA	MPA	2"		Joule	Joule		°C	max. 32
P107	12,70	126,65	50,80	638,00	826,60	31,40	57,50	97	101	116	KV - 46	21/23
N. RIF.	TRATTAMENTI TERMICI / HEAT TREATMENTS / TRAITEMENTS THERMIQUES											
SI113	Solubilizzazione/Solution Annealed						At 1120°C for min 1/2 h/inch Quenched water					
Acc. DIN50049 3.1B/EN10204 3.1 Surface and dimensional check according to relevant standard. Steel made by electric furnace. Corrosion test carried out acc. to ASTM G48 method "A" at 50°C exposure time 24 hours. Results: no pitting attack, no weight loss. Material acc. to MDS D54 Rev.3.												
100% Pmi ACCEPTABLE												
FLANGEFITT QA DEPT. 01/16/4589 Item No 039 Date 09/02/12 int. 43 CHECKED & ACCEPTED												
CONFORMS TO NACE MR 01.75 Lat. EC ISO 15156-3												
PROJECT: Ekofisk 2/4-Z CLIENT: AKER EGBERSUND AS CLIENT ART. CODE: LD088935 PRODUCT NO: 178804 Compliance with Client specification: Signed: RB SFF Q.C. - DEPT.												
25162 1824.223(039) FLANGEFITT STAINLESS LTD ISSUED TRUE COPY SFF SIG. [Signature] 100% Pmi ACCEPTABLE TAG NO. LD088935												
COMPONENT MEETS THE REQ. IN PED 97/23 ANNEX I SECT. 4.3												
CHECKED BY: [Signature]												
ESITO DELLE PROVE / TEST ISSUE / RESULT DES ESSAIS: FAVOREVOLE SATISFACTORY SATISFAISANT												
TRADE MARK	P. OFF. A. MELESI & C.		COLLAUDATORE / INSPECTOR (INSPECTEUR)				ENTE COLLAUDATORE / INSPECTION AGENCY AUTORITÉE DE RECETTE					
			[Signature]				[Signature]					



OFFICINE AMBROGIO MELESI & C. S.R.L.

23813 Cortemsa (Lecco) - Italy
Largo De Vecchi 11
P.O. BOX 11

Tel. 0341.98.34.1
Fax 0341.98.34.96 - 98.34.97
E-mail: info@melesi.it
www.melesi.it

Part. UVA. 00231039138
R.E.A. Lecco n. 108835
R.L. Lecco n. 2138
N. Mecc. LC 905895



Messrs.

FLANGEFITT STAINLESS LTD
HAWLEY'S LANE,
WARRINGTON
CHESHIRE WA2 8JB GB

31 January 2012

Your P.O. Nr. F/64589/00
Our ref. 47610
Certificate Nr. M302

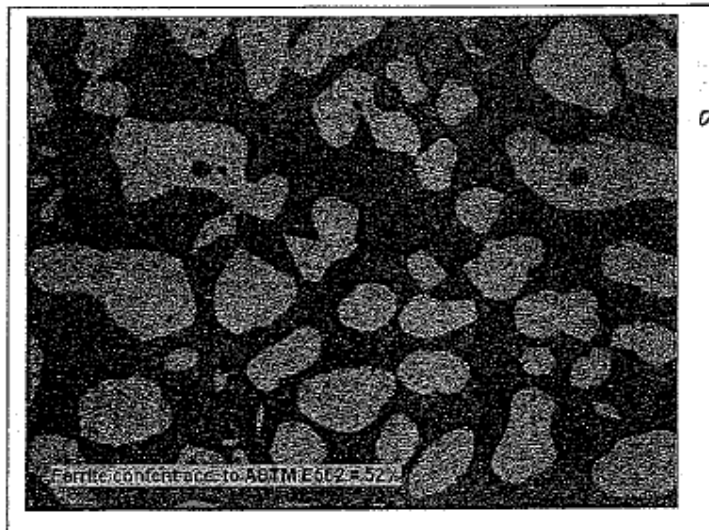
MICROSTRUCTURE

SAMPLE OF ASTM A182 F55 HEAT 529632 P107

THE RESULTS OF METALLOGRAPHIC EXAMINATION SHOW A
REGULAR STRUCTURE FREE FROM GRAIN BOUNDARY CARBIDES,
SIGMA, CHI AND LAVES PHASES AS SHOWN ON BELOW PHOTO.

FERRITE CONTENT ACC. TO ASTM E562

30 FIELDS 16 POINT X FIELD ETCHANT ASTM E407 N°98 NaOH






FLANGEFITT STAINLESS LTD
TRUE COPY
07/01/2012 SIG.....

X 500



Appendix D: MDS SDSS bolts and nuts

 <p>OME METALLURGICA ERBESE CERTIFIED COMPANY</p>		<p align="center">HEAT ANALYSIS CERT. COVER SHEET</p> <p><input checked="" type="checkbox"/> 3.1 ISO 10474 EN 10204</p> <p><input type="checkbox"/> 3.2</p>			ENCLOS.	CMTR N°	SHEET	PAGE
					04	1600307/CS	1/1	1
					DATE:		26/02/2016	
MANUFACTURER'S RAW MATERIAL CERTIFICATES								
LOT	P.O. ITEMS		CERTIFICATE N°.	HEAT NUMBER	DATE	ISSUED BY	MATERIAL	
	FROM	TO						
L001	1		415631	388775	15/12/15	BGH	ASTM A276 UNS S32760 (ASTM A1082 UNS S32760)	
L002	1A		137923/C1	W72502	10/02/15	BÖHLER EDELSTAHL	ASTM A276 UNS S32760 (ASTM A1082 UNS S32760)	
L003	2		264375	307794	29/08/12	BGH	ASTM A276 UNS S32760 (ASTM A1082 UNS S32760)	
<p>- RAW MATERIAL COMING FROM M-650 APPROVED SOURCE STEELMAKER</p> <p>- RAW MATERIAL STARTING BARS ALREADY IN FINAL HEAT TREATMENT CONDITION</p>						<p align="center">PREPARED/APPROVED</p> <div style="display: flex; justify-content: space-around;">   </div> <p align="right">8.2-CMTR-22 19.04.02</p>		

STUD 1/2" Load

GA16000057 del 12/01/2016

 ARN00097747
 Cert. Nr. 415631
 BGH EDELSTAHL FREITAL GMBH
 Nat. UNS S32760
 Coata 388775
 APPROVED by OME S.R.L.

Seite 1 / 2
 Page



BGH Edelstahl Freital GmbH

BGH Edelstahl Freital GmbH, Am Stahlwerk 1, 01705 Freital
 OME Metallurgica Erbeso Srl

Zaunfts-Nr. 415631
 Certificate no.
 No. de certificat

Bescheinigung über Werkstoffprüfung nach DIN EN 10204
 Certificate of material tests according to DIN EN 10204 3.1
 Certificat des essais des matériaux selon DIN EN 10204

Die Lieferung entspricht den vereinbarten Lieferbedingungen.
 Delivery in accordance with the agreed terms of delivery.
 La livraison correspond aux conditions de livraison convenues.

Via Milano 15

22036 Erba (CO)
 Italien

Zeichen des Lieferanten Trade mark Signe du fournisseur
 Stempel des Werkschwerföndigen Inspector's stamp Fonction de l'inspecteur

Kunden-Bestell-Nr. AC151943-1
 Customer order no.
 Cde. no. du client

BGH-Auftrags-Nr. 34874801/197466
 BGH works no.
 BGH référence



Erzeugnisform Product		Blanker Stab, rund, geschält/poliert Round bright bars, peeled/polished											
Werkstoff / Quality		UNS S32760											
Anforderungen Requirements		UNS S32760 ASTM A 276 - 15 UNS S32760 - F55 ASTM A 182 /A 182M - 15 UNS S32760 NORSOK M 630 Edition 6 10/13 UNS S32760 NORSOK MDS - D 57 Rev. 5 10/13 UNS S32760 NACE MR 0175 ISO15156-3 2009+Cir.1:2011 Gefertigt nach QTR_F_E_32760 nach Norsok M-650 Edition 4 Manufactured acc. to QTR_F_E_32760 acc. to Norsok M-650 Edition 4											
Besichtigung und Maßnachprüfung Inspection and dimensional control Inspection et contrôle de dimension ohne Beanstandung without objection				Erschmelzung/Nachbehandlung Melting/secondary refining Mode d'élaboration/traitement ultérieur E- VOD				Verwechslungsprüfung (spezialanalytisch) Identification test (special analysis) examination of identification/analyse spéciale ohne Beanstandung without objection					
Pcs. Item	Anzahl Quantity	Abmessung Dimension								Gewicht Weight	Schmelz-Nr. Heat-No.		
1	2 Bd.	14,300 RD								1692 kg	388775		
Schmelz- Heat %		C	Si	Mn	P	S	Cr	Mo	Ni	Cu	N	W	PRE1
388775		0,023	0,28	0,58	0,023	0,0006	25,55	3,47	7,50	0,56	0,2600	0,540	41,161
		PRE2	PRE1: CR+3.3*MO+16*N2										
42,052		PRE2:	CR+3.3*(MO+(0.5*W))+16*N2										
Wärmebehandlungszustand Condition of heat treat		Lösungsgeglüht solution annealed											
Traitement thermique		1125°C 87s Wasser/water - Abkühlung/cooling < 260°C											
Probe-Nr. Test-No.	Lage loc.	Temp. °C	Rp0,2 N/mm²	Rm N/mm²	A4 %	Z %	Kerbschlagarbeit Impact value J			Probenform Shape of test piece Charpy-V °C		Härte Hardness HBW	
Soll/Req.	L	RT	>=550	>=760	>=25	>=45	>=45			-46			
	L	RT		<=895			>=45			-50		<=290	
008LV1	L	RT	662	877	42	84	360	356	321	-46		278	
008LV1	L						331	381	363	-50			
Prob-Nr Test-No	Temp °C	later. Breitung mm later. expansion			Scherbruchant. % shear fracture								
008LV1	-46	2,4 2,4 2,1			100 100 100 (längs/longitudinal)								
008LV1	-50	2,2 2,2 2,3			100 100 100 (längs/longitudinal)								
Prüfart/test location: mechan. Werte/mechanical test pieces - D/2 / mid thickness Härteprüfung/Hardness test - D/4 mid radius													
Anlagen Encl. Annex Gefügeaufnahme/micrograph				Freital, den Place and date Lieu et date 15.12.2015				Abnahmebeauftragter Inspector representative Inspecteur de réception MÖLLER					
Das Zeugnis wurde maschinell erstellt und ist auch ohne Unterschrift gültig. Ce certificat a été établi sur système informatique et est valable sans signature aussi.													

TRUE COPY

 OME s.r.l.



BGH Edelstahl Freital GmbH

BGH Edelstahl Freital GmbH, Am Stahwerk 1, 01705 Freital
OME Metallurgica Erbeso Srl

Via Milano 15

22036 Erba (CO)
Italien

Kunden-Bestell-Nr.
Customer order no.
Cde. no. du client AC151943-1

BGH-Auftrags-Nr.
BGH works no.
BGH référence 34874801/197466

Zeugnis-Nr.
Certificate no.
No. de certificat 415631

Beschreibung über Werkstoffprüfung nach DIN EN 10204
Certificato di material tests according to DIN EN 10204 3.1
Certificat des essais des matériaux selon DIN EN 10204

Die Lieferung entspricht den vereinbarten Lieferbedingungen.
Delivery in accordance with the agreed terms of delivery.
La livraison correspond aux conditions de livraison convenues.

Zeichen des Lieferanten Trade mark Signe du fournisseur
Stempel des Werkstoffverständigen Inspector's stamp Poinçon de l'inspecteur



Zugprobenform/typ tensile specimen ASTM A 370: Lo = 50 mm ; Do = 12,5 mm		
Charpy-V 10 x 10 V = 2 mm		
Längsproben/longitudinal test specimen		
Proben wurden von der Stabverlängerung entnommen x 6" Länge, gemäß ASTM A 370. Test pieces taken from actual bar prolongation x 6" length according to ASTM A 370.		
Korros.-Test ASTM G48 Meth.A: 50°C/24h: kein Lochfraß/no pitting is observed corrosion test Meth.A: Gewichtsverlust/weight loss: 0,027 g/m ² Proben gebeizt (20% HNO ₃ + 5% HF, 60 °C, 5 Minuten) Samples pickles (20% HNO ₃ + 5% HF, 60 °C, 5 minutes)		
	Rand-near surface	D/2-mid thickness
Deltaferrit/ferrite delta ASTM E 562:	53%	55%
relative Genauigkeit/relative accuracy:	8%	7%
Prüfung/testing: 30 Felder/16 Punkt (30 fields of 16 points)		
Ätzmittel/Etchant: V2A + 30 % NaOH		
US-Prüfung nach/ultrasonic testing acc. to A388/A 388 M (latest Revision) (KSR/FBH max. 1,5 mm): ohne Beanstandung/no objection.		
Fertigung nach QM-System ISO 9001: 2008/ QM system in effect is ISO 9001: 2008		
Kontrolle auf Radioaktivität ohne Befund, der Messwert liegt unter der Nachweisgrenze von 0,1 Bq/g. Radioactivity inspection without objection, the measured value is below the detection limit of 0.1 Bq/g.		
Material wurde nicht reparaturgeschweißt./Material no weld repaired.		
Gefüge frei von intermetallischen und anderen schädlichen Phasen./ Microstructure free from intermetallic or other detrimental phases.		
Das Material ist frei von Quecksilber./Material is free from mercury.		
Stahlhersteller des Ausgangsmaterials: BGH Edelstahl Freital GmbH. Steel manufacturer of starting material: BGH Edelstahl Freital GmbH.		
Anlagen Encl. Annex Gefügebild/micrograph	Freital, den Place and date Lieu et date 15.12.2015	Abnahmebeauftragter Inspector representative Inspecteur de réception Müller
Das Zeugnis wurde maschinell erstellt und ist auch ohne Unterschrift gültig. Ce certificat a été établi au système informatique et est valable sans signature aussi.		

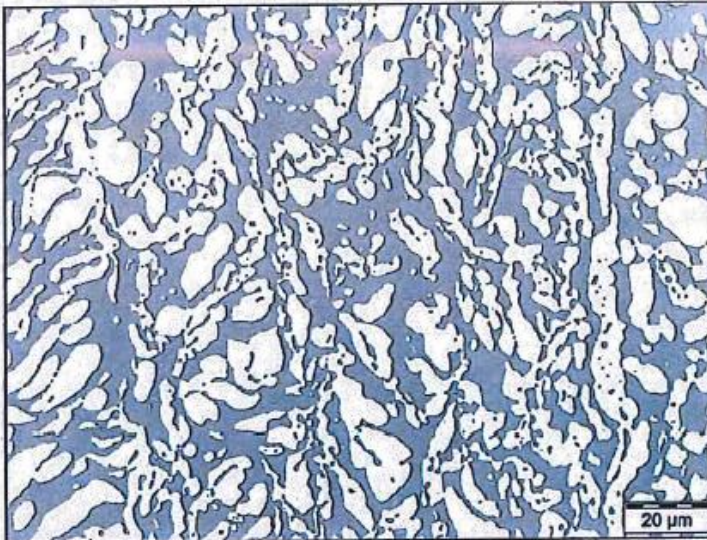
TRUE COPY
OME s.r.l.

Gefügeaufnahmen zum Zertifikat Nr. / Microstructure to certificate No.:

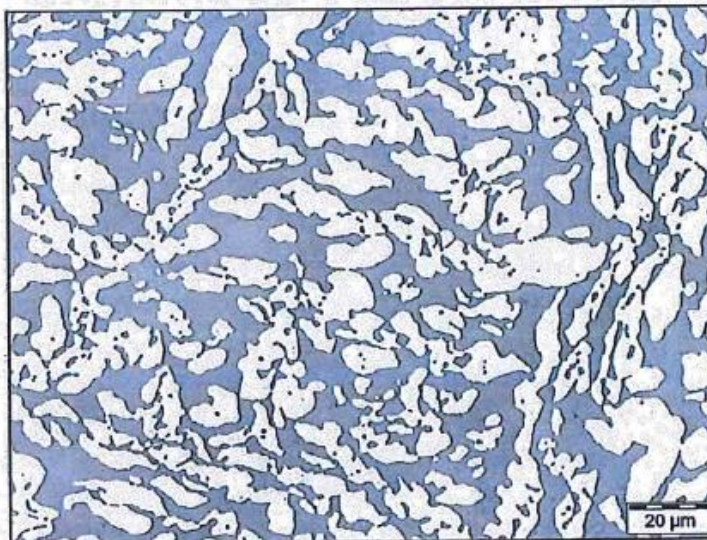
415631

Besteller/Purchaser: OME Metallurgica Erbeso Srl
Bestell-nr./Order-No.: AC151943-1
Werkstoff/Quality: UNS S32760
Chargen-nr./Cast-No.: 388775
Erzeugnisform/Product: Blanker Stab, rund, geschält/poliert / Round bright bars, peeled/polished
Abmessung/Dimension: 14,300 RD
Komm.-nr./Work-No.: 34874801

Proben-nr./Test-No.: 008LV1



500:1 near surface



500:1 mid thickness

TRUE COPY
OME s.r.l. 

NUT 1/2" L002

ABNAHMEPRÜFZEUGNIS
INSPECTION CERTIFICATE
CERTIFICAT DE RECEPTION

ISO 9001:2008 certification
EN ISO 14001:2004 certification




EN 10204-3.1

Cert. No.: 137923 / C1 / 2015.02.10
Blatt/Sheet/Page: 1 / 12

Besteller/Purchaser/Acheteur: CHUN & VOLLERIN SRL VIA VENETO, 11 20090 BUCCINASCO		Empfänger/Consignee/Destinaire: CHUN & VOLLERIN SRL VIA VENETO, 11 20090 BUCCINASCO	
Bestell-Nr./Purchaser order No./No. de commande: 11740 / 0000.00.00		Empfängerref.-Nr./Receiver reference-No./Référence destinataire: -	
Werksauftrags-Nr./Works order-No./No. de la commande de l'usine: 3901437369 / 2015.02.05		Lieferschein-Nr./Delivery note-No./Avis d'expédition du client: 3910183951 / 2015.02.10	
Prüfgegenstand/Object of test/Object d'examen: BÖHLER A911SA W-No. 1.4501 bar, rolled, solution annealed, quenched IBO ECOMAX ISO 286/2 ITk12		Anforderungen/Requirements/Exigence: TSP_K-A911SA_Rev.01_110718 Norsok Standard M-650 Edition 4, September 2011 Norsok Standard M-630 Edition 5, April 2010 Norsok MDS D57 Rev.4 NACE MR0175 / ISO15156-1: 2009 DIN EN10088-3 September 2005 X2CrNiMoCuWN25-7-4 ASTM A182/A182M-11a chemistry only ASTM A276-10 ASTM A479/A479M-11 ASME BPVC 2010 Section II Part A SA-276 ASME BPVC 2010 Section II Part A SA-182/SA-182M chemistry only UNS S32760, F55 Pressure equipment directive PED 97/23/EC	

GA15004144 del 17/07/2015



ARN00081414

Cert. Nr. 137923/C1/2015.02.10
BÖHLER EDELSTAHL GMBH & CO KG
Mat. UNS S32760
Co lata U72502

APPROVED by OME S.R.L.

Pos./Lot	Dimensions	Length	No. of Pieces	Weight kgs	Mat.-ID	Test No.	Heat No.
20/1	16 x 3.950 mm		165	1031,0	7Z86	1267169-3	W72502

GDPIA CONFORME ALL'ORIGINALE
GRUPPO VOLLERIN s.r.l.
Via Veneto 11 - 20090 BUCCINASCO

Reduction ratio = 818,52 : 1


Heat treatment monitoring method in compliance with API 6A PSL3


Quality heat treatment

	Temperature	Soak time	Cooling
Solution annealed	1100°C	0,5 h M	Water

M...holding time at nominal temperature after center of material has reached the tolerance limit.

TRUE COPY

OME s.r.l. 

Chemical Composition (%)										Heat No.
Chemical Composition Steelmaking Process: EAF+AOD										
C	Si	Mn	P	S	Cr	Mo	Ni	W	Cu	
0,019	0,19	0,53	0,025	<0,0003	25,36	3,62	7,03	0,54	0,56	W72502
Al	N	FL014*								
0,012	0,23	41,0								W72502
*FL014 = Cr+3,3*Mo+16*N										
Ferrite content Examination										
The ferrite content was determined in accordance with ASTM E562-11 using the point count method.										
	Surface	1/4 T								
Ferrite	55 %	55 %								
Austenite	45 %	45 %								
Micrographic Examination										
Austenitic-ferritic microstructure										
The microstructure was examined at 100x and 500x magnification.										
The microstructure was examined near surface and center position.										
Etch media: H ₂ O 1000ml, NaOH 400gr										
The material is free from intermetallic and deleterious third phases.										
COPIA CONFORME ALL'ORIGINALE GRUNN & VOLLER s.r.l. Via Veneto 17 - 20090 BRUCINASCIO										
										

Photomicrographs:

The microstructural photographs were examined at 100x and 500x using light microscopy.



Location: Surface
original photo: 100x



Location: Surface
original photo: 500x



Location: center
original photo: 100x



Location: center
original photo: 500x

COPIA CONFORME ALL'ORIGINALE
CHUN & MOLLERIN s.r.l.
Via Veneto 11 20090 BUCCIRASCO

TRUE COPY
OME s.r.l. 

Mechanical Properties
The QTC is a prolongation of the final heat treated bar.

Orientation and location of the tensile test and impact test properties.
LZ = longitudinal, Center, LA = longitudinal, near Surface; L2 = longitudinal, 1/2 Radius (1/4T); Q2 = transverse, 1/2 Radius (1/4T); Q = transverse

Tensile test properties
Orientation and location of the tensile test properties.
LZ = longitudinal, center, LA = longitudinal, near surface
L2 = longitudinal, 1/2 Radius (1/4T); Q2 = transverse, 1/2 Radius (1/4T); Q = transverse

Tensile test in delivery condition

Test no.	Place no.	Testing standard	Location	Temp. grad C	Yield Strength	Ultimate Tensile Strength	Elongation		Reduction of Area
					YS0.2 MPa	UTS MPa	A4 %	A5 %	RoA %
1267169-3	4	EN ISO 6892-1/09	LZ	23	>=550	750 - 930	>=25		>=45
					616	820	41	81	
1267169-3	5	ASTM A370-12a	LZ	23	>=550	750 - 895	>=25		>=45
					598	819	49	85	

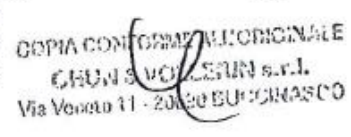
Impact test properties
Orientation and location of the impact test properties.
LZ = longitudinal, center, LA = longitudinal, near surface
L2 = longitudinal, 1/2 Radius (1/4T); Q2 = transverse, 1/2 Radius (1/4T); Q = transverse



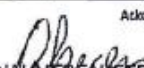
Impact test in delivery condition

Test no.	Place no.	Testing standard	Location	Temp. grad C	Impact energy	Lateral expansion	Shear area
					Charpy-V J	mm	%
1267169-3	95	EN ISO 148/1-10	LZ	23	>=100	Info	Info
					358 333 339	2,27 2,32 2,11	100 100 100
1267169-3	95	ASTM E23-07A E1	LZ	-46	>=45	Info	Info
					319 310 328	2,15 1,83 2,14	100 100 100

Hardness test in delivery condition

Test no.	Place no.	Testing standard	Location	HBW 5/750	HRC
				<=290	<=28
1267169-3	5	ASTM E10-12	Tensile test	269	
1267169-3	4	EN ISO 6506-1	Tensile test	266	
1267169-3	95	ASTM E18-11	Surface		23,2
1267169-3	95	ASTM E18-11	Surface		23,4
1267169-3	95	ASTM E18-11	Surface		23,8
1267169-3	95	ASTM E18-11	1/4 T		24,4
1267169-3	95	ASTM E18-11	1/4 T		24,2
1267169-3	95	ASTM E18-11	1/4 T		24,5


TRUE COPY
 OME s.r.l.

<p>Corrosion Examination</p> <p>Intergranular Corrosion acc.to ISO 3651-2 method C: Satisfactory</p> <p>1/4 T Position pickled specimen: Pitting Corrosion acc.to ASTM G48 method A - 50°C - 24h Corrosion Rate 0,02 g/m², no pitting at 20x magnification</p>		
<p>Nondestructive Examination</p> <p>Material identification test: Positive material identification</p> <p>100% Ultrasonic test A flat bottom hole (FBH) reference technique was used as specified in ASTM A388. The performed US-Test fulfils all requirements of ASTM A 388 acc. to API 6A Para. 7.4.2.4.11 - PSL 3</p> <p>100% Ultrasonic test acc.to EN10228-4 1a The material fulfils quality class 2</p> <p>100% Surface Inspection An Eddy Current test was performed. The bars are without unacceptable surface defects.</p>		
<p>Statements Material produced without ozone depleting substances. The material is free of mercury contamination. No weld repair has been performed on this material. Country of origin and melt: AUSTRIA</p>		
<p>Attachment Ultrasonic Report Z08 - 567 + Z08 - 568 Operators Qualification Furnace chart</p>		
<p>Radioaktivitätskontrolle/Radioactivity Inspection: Co-60<0,1Bq/g; hiermit kleiner als Grenzwert in der anzuwendenden Spezifikation IAEA RS-G-1.7 für unbedenkliche Stoffe. therefore smaller than upper limit required according to specification IAEA RS-G-1.7 for inoffensive material.</p>		
<p>Wir bestätigen hiermit, dass die oben genannten Erzeugnisse den Bestellevorschriften entsprechen. We hereby certify that the above mentioned products are consistent with the order prescriptions. Nous certifions que les produits énumérés ci-dessus sont conformes aux prescriptions de la commande.</p>		
<p>Zeichen des Lieferwerks: Brand of Manufacturer: Marques de l'usine:</p> 	<p>Besichtigung und Nachmessung: Keine Beanstandung Inspection and Checking of Dimensions: Satisfactory Inspection of Control des dimensions: Satisfaisant</p>	<p>Zeichen des Prüfers: Symbol of Inspector: Symbole de l'inspecteur:</p> 
<p>BOHLER Edelstahl GmbH & Co KG Marlazeilerstrasse 25 8805 Kapfenberg, AUSTRIA www.bohler-edelstahl.com</p>	<p>Abteilung / Department Böhler Italia</p> <p>AUSSTELLER / ORIGINATOR / AUTEUR</p>	<p>Akteur</p> <p>DER ABNAHMEBEAUFTRAGTE/ INSPECTOR REPRESENTATIVE/ DU CONTROLEUR</p> 

COPIA CONFORME ALL'ORIGINALE
CHUNG VOLLESEN S.R.L.
Via Venezia 11 - 20099 BUDONISARDI

TRUE COPY
OME s.r.l.

Abteilung/Department EWV/O		Wärmebehandlungsprotokoll Härtelinie / hardening report		BÖHLER EDELSTAHL	
Kunde / customer: Fa./Los Nr.: 1267189 / 01-0 - 6 Gewicht / weight: 1602.0 kg work order: Charge / heat no.: W72602 Marke / material: A8118A WBH Sch.: / code: L01 Abmessung / dimension: Ø00X018 PPI/EK Nr.: _					
Vorgäbelage: continuous heat treating plant: Ofen Nr.: 88 Ofenklasse: 3 (+/-8°C) Ofenqualifizierung lt. AMS2760 letztgültige Rev. furnace no.: furnace class: furnace qualification per AMS2760 latest rev.:					
Solldaten / nominal values ll. EV2 3600/0021/30/letztgültige Rev. / per production prescription					
Gesamt Ofenzeit (+/-10%): total time:		3600 Sek		Ofentemperatur: furnace temperature:	
				1100 °C	
Wasserspannweite: water temperature		min. 5°C, max. 32°C		Metalltemperatur: metal temperature	
				min. 40°C, max. 80°C	
Abkühlmedium: quenching medium:			Luftgebläse (+/-10%): ventilator:		
Wasser (water)			0 Sek.		
			Tauchzeit (+/-25%): immersion time:		
			700 Sek.		
Istdaten / process data					
Auflage Nr.: / lot no.: 5					
Materialantritt / material entrance: 04.02.2013 16:34:21		gesamte Ofenzeit: 3642 Sek		Materialausritt / exit time: 04.02.2013 17:36:04	
Polymertemperatur: polymer temperature		Eintritt/Entrance Ausritt/Exit		Luftgebläse: ventilator	
		°C -		0 Sek.	
Wassertemperatur: water temperature		Eintritt/Entrance Ausritt/Exit		Tauchzeit: immersion time	
		23°C 04.02.2013 17:36:13 19°C 04.02.2013 17:46:55		701 Sek.	
Die Richtigkeit der durchgeführten Wärmebehandlung wird bestätigt: The correctness of the conducted heat treatment is confirmed: Die Prozessdaten werden statistisch ausgewertet process data are statistically evaluated					
				Datum: date: 19.02.13	
				Unterschrift: signature: Krammer Andreas	

4384/12

STU 1/2ⁿ 1003



BGH Edelstahl Lugau GmbH

BGH Edelstahl Lugau GmbH, Gölitzstr. 12, 08385 Lugau

PTM Srl
Prodotti Tecnologica e Materiali

Corso Leone, 85/13

10141 Torino (TO)
Italien



Kunden-Bestell-Nr. 37/11
Customer order no.
Cde. no. du client

BGH-Auftrags-Nr. 26150201/101265
BGH works no.
BGH référence

Zaun-Nr. 264375
Certificate no.
No. de certificat

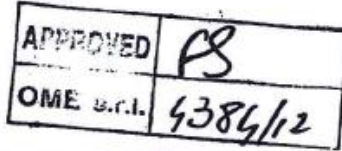
Beschreibung über Werkstoffprüfung nach DIN EN 10204
Certificate of material basis according to DIN EN 10204 3.1
Certificat des essais des matériaux selon DIN EN 10204

Die Lieferung entspricht den vereinbarten Lieferbedingungen.
Delivery in accordance with the agreed terms of delivery.
La livraison correspond aux conditions de livraison convenues.

Zeichen des Lieferanten Trade mark Signe du fournisseur
Stempel des Werkstoffsachverständigen Inspector's stamp Poinçon de l'inspecteur



Erzeugnisform Product		Blanker Stab, rund Round bright bars										
Werkstoff / Quality		UNS S32760 1.4501 X 2 CrNiMoCuWN 25 7 4										
Anforderungen Requirements		ASTM A 276 - 10 NACE MR 0175; NORSOK MDS-D57 Rev. 04-09/10										
Beschreibung und Maßprüfung Inspection and dimensional control Inspection et contrôle de dimension ohne Beanstandung without objection				Erschmelzung/Nachbehandlung Melting/secondary refining Mode d'élaboration/traitement ultérieur E - VOD				Verwechslungsprüfung (spectralanalytisch) Identification test (spectral-analysis) examen d'identification (analyse spectrale) ohne Beanstandung without objection				
Pos. Item	Anzahl Quantity	Abmessung Dimension								Gewicht Weight	Schmelz-Nr. Heat-No.	
	5 bundles	12,700 RD+ 0,000 / - 0,110 DIN EN 10278 /h11								2300	307794	
Schmelze Heat %	C	Si	Mn	P	S	Cr	Mo	Ni	Cu	N	W	PRE
307794	0,024	0,41	0,60	0,025	0,0010	25,60	3,50	7,20	0,58	0,2550	0,540	41,23
Lieferzustand Delivery condition		Lösungsgeglüht, geschält, poliert solution annealed, peeled, polished										
Probe-Nr. Test-No.	Lage	Temp. °C	Rp0,2 N/mm ²		Rm N/mm ²	A4 %	Z %	Kerbschlagarbeit Impact value J	Probenform Shape of test piece Charpy		Härte Hardness HBW /HRC	
Soll/Req.	L	RT	>=550		>=750	>=25	>=45	>=85	-46		<=290/<=32	
	L							>=20	-50			
	L							>=20	-85			
	L								-101			
147FE1	L	RT	588		830	50	80	356 386 399	-46		254 / 24	
147FE1	L							358 364 325	-50			
147FE1	L							346 327 316	-85			
147FE1	L							335 311 320	-101			
154FE1	L	RT	591		831	47	82	344 350 359	-46		250 / 23	
154FE1	L							358 341 316	-50			
154FE1	L							317 303 325	-85			
154FE1	L	RT						302 321 326	-101			
Prob-Nr Test-No	Temp °C	later. Breitung mm later. expansion										
147FE1	-46	2,2	2,3	2,3	(längs/longitudinal)							
147FE1	-50	2,2	2,3	2,2	(längs/longitudinal)							
147FE1	-85	2,4	2,3	2,2	(längs/longitudinal)							
147FE1	-101	2,3	2,2	2,3	(längs/longitudinal)							
154FE1	-46	2,2	2,3	2,3	(längs/longitudinal)							
Anlagen Encl. Annexe	Lugau, den Place and date Lieu et date 29.08.2012					Abnahmebeauftragter Inspector representative Inspecteur de réception Zwroch						
Das Zeugnis wurde maschinell erstellt und ist auch ohne Unterschrift gültig.						This certificate was generated by data system it must not be signed for validity as well. Ce certificat a été établi sur système informatique et est valable sans signature aussi.						





BGH Edelstahl Lugau GmbH

BGH Edelstahl Lugau GmbH, GbHstr. 12, 08383 Lugau

PTM Srl
Prodotti Tecnologia e Materiali

Corso Leone, 85/13

10141 Torino (TO)
Italien

Zeugnis-Nr. 264375
Certificate no.
No. de certificat

Beschreibung über Werkstoffprüfung nach DIN EN 10204
Certificate of material tests according to DIN EN 10204 3.1
Certificat des essais des métaux selon DIN EN 10204

Die Lieferung entspricht den vereinbarten Lieferbedingungen.
Delivery in accordance with the agreed terms of delivery.
La livraison correspond aux conditions de livraison convenues.

Zeichen des Lieferwerkes Stempel des Werkstoffverständigen
Trade mark Inspector's stamp
Signe du fournisseur Poignon de l'inspecteur

Kunden-Bestell-Nr. 37/11
Customer order no.
Cde. no. du client

BGH-Auftrags-Nr. 26150201/101265
BGH works no.
BGH référence



154FE1	-50	2,5	2,3	2,2	(längs/longitudinal)
154FE1	-85	2,2	2,1	2,2	(längs/longitudinal)
154FE1	-101	2,1	2,2	2,2	(längs/longitudinal)

Deltaferrit/ferrite delta ASTM E 562: Rand-near surface:	147FE1	154FE1
	52%	52%
D/2-mid thickness:	51%	49%

US-Prüfung/us test A388/A 388 M (latest Revision) (KSR/FBH max. 1,5mm)
ohne Beanstandung/no objection
2. Versuch: gebeizte Probe (20% HNO + 5% NF, 60 °C/5 Minuten) bei 50 °C, 24h,
Material frei von Sigma- und anderen schädlichen Phasen./
Material free from sigma and other harmful phases.

Korros.-Test ASTM G48 Meth.A: 50°C/24h: kein Lochfraß/no pitting is observed
corrosion test Meth.A: Gewichtsverlust/weight loss:
ungebeizt/unpickled: 0,132 g/m²
gebeizt/pickled: 0,112 g/m²

Korros.-Test ASTM G48 Meth.A: 40°C/48h: kein Lochfraß/no pitting is observed
corrosion test Meth.A: Gewichtsverlust/weight loss:
ungebeizt/unpickled: 0,089 g/m²
gebeizt/pickled: 0,077 g/m²

gebeizte Probe/pickled test pieces (20% HNO + 5% NF, 60 °C/5 Minuten)
Material frei von Sigma- und anderen schädlichen Phasen.
Material free from sigma and other harmful phases.

US-Prüfung/US test A388/A 388 M (latest Revision) (KSR/FBH max.1,5 mm):
ohne Beanstandung/no objection.

TRUE COPY

OME s.r.l.

APPROVED	
OME s.r.l.	9384/12

Anlagen Enc. Annexe	Lugau, den Place and date Lieu et date 29.08.2012	Abnahmebeauftragter Inspector representative Inspecteur de réception Zwoch
---------------------------	--	--

Das Zeugnis wurde maschinell erstellt und ist auch ohne Unterschrift gültig. This certificate was generated by data system it must not be signed for validity as well. Ce certificat a été établi sur système informatique et est valable sans signature auzel.

Wärmebehandlungsbescheinigung
Heat treatment certificate
Attestation de traitement thermique


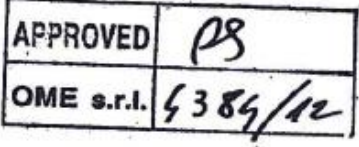



BGH Edelstahl Freital GmbH

Kunden-Bestell-Nr. **F/208/2012**
Customer order no.
Cde. no. du client **Langley/Newcastle**

BGH-Auftrags-Nr. **47750001**
BGH works no.
BGH référence

Zeugnis-Nr. **351199/264375**
Certificate no.
No. de certificat

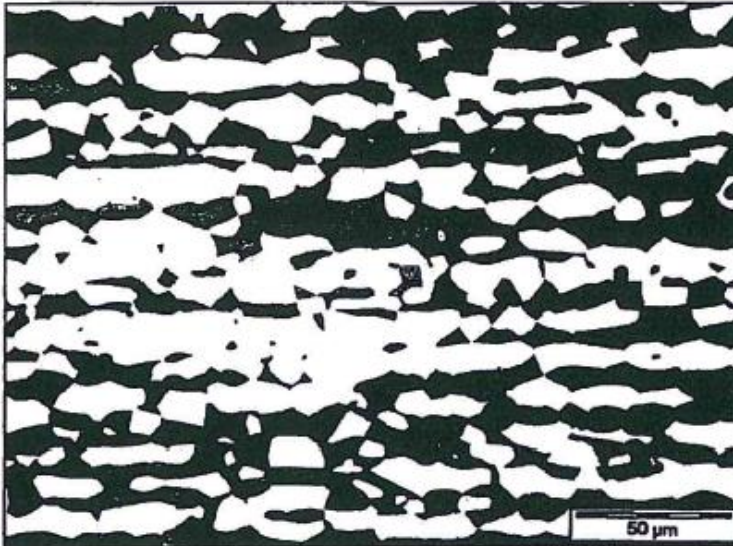
Wärmebehandlungszustand: lösungsgeglüht Condition of heat treatment: solution annealed État de traitement thermique: recuit de mise en solution	
Datum: Date: Date:	15.06.2012
Ofen-Nr.: Furnace no.: No. du four:	474
Aufheizzeit: Heating up time: Temps de montée en température:	4,5 h
Haltezeit: Holding temperature: Température de maintien:	1100 °C
Haltezeit: Holding time: Temps de maintien:	2,5 h
Abkühlmedium: Quenching medium: Moyen de refroidissement:	Wasser / water / eau
 Datum: Date: Date: Ofen-Nr.: Furnace no.: No. du four: Haltezeit: Holding time: Temps de maintien: Abkühlmedium: Quenching medium: Moyen de refroidissement: Wärmebehandlungs-Nr.: 474/3184 Heat treatment lot no.: No. du lot de traitement thermique:	
	
	
Diagramm: Diagram: X Diagramme:	Datum: Date: 10.07.2012 Date:
Abnahmebeauftragter Inspector representative Inspecteur de réception JUNGKUNZ 	
Das Zeugnis wurde maschinell erstellt und ist auch ohne Unterschrift gültig. This certificate was generated by data system it must not be signed for validity as well. Ce certificat a été établi sur système informatique et est valable sans signature aussi.	

Gefügeaufnahmen zum Zertifikat Nr. / Microstructure to certificate No.:

351199 1264375

Besteller/Purchaser: BGH Edelmetall Lugau GmbH
Bestell-nr./Order-No.: F200/2012
Werkstoff/Quality: UNS S32760
Chargen-nr./Cast-No.: 367794
Erzeugnisform/Product: Stab, rund, roh / Round bars,unmachined
Abmessung/Dimension: 15,00 RD
Komm.-nr./Work-No.: 47750001

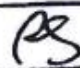
Proben-nr./Test-No.: 147FE1



near surface

500:1

TRUE COPY
OME s.r.l. 

APPROVED	
OME s.r.l.	4384/12



LIQUID PENETRANT EXAMINATION CERTIFICATE

ENCLOS.	CMTR N°	SHEET	PAGE
12	1600307/PT	1/1	1
DATE:			
26/02/2016			

3.1 ISO 10474 EN 10204
 3.2

REF. DOC.	<input checked="" type="checkbox"/> OME PROC. 8.2 - PT REV.0 <input checked="" type="checkbox"/> ASTM A962 - S57	<input checked="" type="checkbox"/> ASTM E1417 <input checked="" type="checkbox"/> MDS VN605 Rev.A	
PRODUCT	<input type="checkbox"/> RAW BARS <input type="checkbox"/> ALCOHOL	<input type="checkbox"/> SEMI-FINISHED PCS. <input type="checkbox"/> ACETONE	<input checked="" type="checkbox"/> FINISHED PCS. <input checked="" type="checkbox"/> SOLVENT
DEGREASING	<input type="checkbox"/> ALCOHOL	<input type="checkbox"/> ACETONE	<input checked="" type="checkbox"/> SOLVENT
PENETRANT	<input checked="" type="checkbox"/> RED PENETRANT *	<input checked="" type="checkbox"/> RED WATER WASHABLE	<input checked="" type="checkbox"/> BATCH N. 079/14
APPLICATION	<input checked="" type="checkbox"/> SPRAY <input checked="" type="checkbox"/> TIME 15' MIN.	<input type="checkbox"/> IMMERSION <input checked="" type="checkbox"/> REMOVAL BY H2O P < 200 KPa / T. < 40° C	<input type="checkbox"/> BRUSH <input type="checkbox"/> REM. BY PAPER
DEVELOPER	<input checked="" type="checkbox"/> BIO. DEVELOPER **	<input checked="" type="checkbox"/> WHITE	<input checked="" type="checkbox"/> BATCH N. 117515
APPLICATION	<input checked="" type="checkbox"/> SPRAY <input checked="" type="checkbox"/> TIME 20' MIN.	<input type="checkbox"/> IMMERSION <input checked="" type="checkbox"/> AIR DRIED	<input type="checkbox"/> BRUSH <input checked="" type="checkbox"/> CLEANED
TEST TEMPER.	<input checked="" type="checkbox"/> 20° C (ROOM)	<input checked="" type="checkbox"/> T. SURFACE 15° C TO 50° C (PIECES)	
OBSERVATION	<input checked="" type="checkbox"/> NATURAL LIGHT Int. > 1000 lx <input type="checkbox"/>	<input checked="" type="checkbox"/> NO INDICATIONS FOUND <input type="checkbox"/>	<input type="checkbox"/> <input type="checkbox"/>



LOT	ITEMS		CONTROLLED QUANTITY					TOTAL QTY	RES.		REMARKS
	FROM	TO	SPOT	5%	10%	100%	PIECES		C	N	
L001	1				X		2	16	X		NO DEFECTS FOUND
L002	1A				X		4	32	X		NO DEFECTS FOUND
L003	2				X		2	16	X		NO DEFECTS FOUND

*RED WW (R2.71) 02011100
 ** ROTRIVEL U (R2.82) 02011200

PREPARED/APPROVED



C = CONFORMING
NC = NON CONFORMING
F 8.2 -CMTR -10/19.04.02

	CERTIFICATE OF COMPLIANCE WITH THE ORDER		ENCLOS.	CMTR N°	SHEET	PAGE
	<input checked="" type="checkbox"/> 2.1 <input type="checkbox"/> 3.2		13	1600307/CC DATE: 26/02/2016	1	
CLIENT: TOOLS AS			ORDER: SAMPLE FOR STAVANGER UNIVERSITY		DATE: 28/01/2016	
PROJECT:			JOB:		DATE:	
<p>ALL MATERIAL SUPPLIED ARE IN FULL ACCORDANCE WITH THE PURCHASE ORDER AND ALL APPLICABLE MATERIAL SPECIFICATIONS</p> <p>ITEM 1 : FOR MICROSTRUCTURE, VERIFICATION OF THE INTERMETALLIC PHASES, FERRITE CONTENT AND CORROSION TEST SEE ATTACHED RAW MATERIAL CERTIFICATE; FOR NUTS 1/2" ITEM 1A SEE ATTACHED BYTEST REPORT NO. RP 0098L16 dd.15.01.2016 FOR STUDS 1/2" ITEM 2 SEE ATTACHED BYTEST REPORT NO. RP 0744L16 dd.26.02.2016</p>						
STATEMENT						
WE HEREBY CERTIFY THAT THE ABOVE DESCRIBED MATERIAL HAS BEEN MANUFACTURED, CONTROLLED THROUGHOUT PROCESSING, EXAMINED AND TESTED SATISFACTORILY IN CONFORMITY WITH MATERIAL SPECIFICATIONS AND ADDITIONAL CUSTOMER REQUIREMENTS.						
					PREPARED / APPROVED	
						
					8.2-CMTR-23 19.04.02	



Bytest

BYTEST S4 - TÜV SÜD Group
bytest@tuv.it - www.tuv.it - (Laboratori-Bytest)
Partita IVA e CF 05102770012 - REA N° 68501769 - Reg. Imprese 3397
Società unipersonale, soggetta al controllo e coordinamento di TÜV SÜD AG

- Sede legale e operativa:
Via Pisa 12 - 10088 - Volpiano (TO)
Tel. 011 037221 - Fax 011.99538.53
- Unità operativa di Benevento:
Zona Industriale ASI-Z5 - SS 90 Ponte Valentino
82100 - Benevento (BN) - Tel. 0824.1755562
- Unità operative Impianti NDT:
C.so Piemonte 8 - 10088 - Volpiano (TO)
Tel. 011 037221
- *Altra sede operativa Bytest

Sistema di Gestione Qualità Certificato
UNI EN ISO 9001
Sistema di Gestione Qualità Aerospaziale Certificato
AS 9100 - EN 9100 - JIS Q 9100
Materials Testing Laboratory NADCAP Test Codes:
F2,F3,G1,G5,A,B,C,N,XN,L1,1,2,1,3,1,4,L5,L6,L7,L8,XL,
M1,M2,M3,C1,Z,XG,XA
Laboratorio Accreditato ACCREDIA N. 9599 secondo UNI
CEI EN ISO/IEC 17025
Prove: Trazione, Resilienza, Durezza, Stress Rupture,
Macrografia, Spettrometria ad emissione ottica, Suscettibilità
alla corrosione intercristallina

RAPPORTO DI PROVA Test Report

Il presente rapporto riguarda esclusivamente i campioni sottoposti a prova.
La riproduzione parziale del presente rapporto è vietata, salvo autorizzazione scritta della Bytest srl.
*This report concerns only the tested specimens.
Partial reproductions of this report without written permission of Bytest srl is forbidden.*
Certificazione di Conformità
Si certifica che tutte le attività oggetto di questo rapporto di prova sono state condotte in conformità ai requisiti della normativa di riferimento indicata, come richiesto dall'ordine d'acquisto.
*Certificate of Conformity
This is to certify that all the activities covered by this test report were conducted in accordance with the requirements of the specified reference standard, as required by purchase order.*

Rapporto N° Report N°	RP	0098L16	
Lotto Bytest N° Bytest Batch N°	0060 - 2016		
OC-Commissa OC-Job n°	18335		
Data emissione Issue date	15.01.2016		
Pagina n° Page n°	2	di of	2

DESCRIZIONE SAGGIO (tipo di prodotto, condizioni): Sample description (product type and condition)	CAMPIONI SPECIMEN
RIFERIMENTI (DISEGNO/PN/LOTTO/COLATA) References (Dwg N./PartN./Batch n./Heat n.)	TIPO MATERIALE - STATO TT - SPECIFICA di Riferimento Material Type - HT condition - Reference Specification
Campione 6.469 - 1/2" (DADI) Colata n. W72502 Pieces Marked: OME-32760-502-18 Specimen 6.469 - 1/2" (NUTS) Heat n. W72502 Pieces Marked: OME-32760-502-18	Acciaio ASTM A1082 Grado UNS S32760 Solubilizzato Check list 2015/1.458 ASTM A1082/A1082M-12 MDS D60 Rev.02 Steel ASTM A1082 Grade UNS S32760 Solution annealed Check list 2015/1.458 ASTM A1082/A1082M-12 MDS D60 Rev.02

NOTA: TUTTE LE INFORMAZIONI SOPRA RIPORTATE SI INTENDONO DERIVANTI ESCLUSIVAMENTE DALLE DICHIARAZIONI DEL CLIENTE CHE RIMANE RESPONSABILE DEI CRITERI DI CAMPIONAMENTO UTILIZZATI. - NOTE: ALL THE ABOVE DATA HAVE BEEN DERIVED EXCLUSIVELY FROM CUSTOMER'S STATEMENTS WHO REMAIN THE WHOLE RESPONSIBLE OF THE APPLIED SAMPLING CRITERIA.

Contenuto del Rapporto di Prova: Test Report Content:

PROVA Test	NORMA DI PROVA Test Standard	CONDIZIONI Conditions	ESITO Result	DETTAGLI ALLEGATO N° Details Annex N°
MICROGRAFIA Micrographic Test	ASTM E3-11 ASTM E562-11	/	CONFORME Satisfactory	1
CORROSIONE Corrosion	ASTM G48-11	Method A 50°C / 24 h	CONFORME Satisfactory	2
				PG-02-05-PLT

Questo rapporto è composto da 2 pagine e da 2 allegati. Documento trasmesso per via elettronica; l'originale vidimato verrà fisicamente consegnato a mezzo posta.
This report is made of 2 pages and 2 annexes. Document transmitted through e-mail; Original signed copy will be mailed.

91 Rapporto redatto da:
Report Issued by:



EMANUELA Marina
PLT

Approvato da:
Approved by:

PIANA Emanuel
PLT

SUPERVISORE (Cliente o Terza Parte)
Witness (Customer or Third Part)

"OME" s.r.l.
METALLURGICA ERBESE
ERBESE (Como)


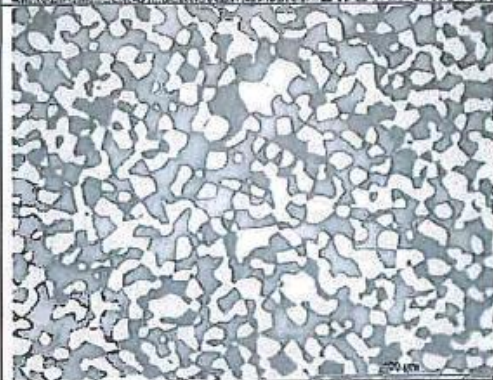
	<p>Campione 6.469 – Superficie esterna Ingrandimento 100x - 500x Attacco: NaOH 20 % elettrolitico Specimen 6.469 – Outer surface 100x - 500x Magnification Etch: 20 % NaOH electrolyte</p>									
	<p>Contenuto massimo di fasi intermetalliche e precipitati <i>Maximum content of intermetallic phases and precipitates</i></p> <table border="1"> <tr> <td>Valori Osservati [%] <i>Observed Values [%]</i></td> <td>< 0.1</td> </tr> <tr> <td>Valori Richiesti [%] <i>Required Values [%]</i></td> <td>≤ 0.1</td> </tr> </table> <p>Contenuto di ferrite secondo ASTM E562-11 <i>Ferrite content according to ASTM E562-11</i></p> <table border="1"> <tr> <td>Valori Osservati <i>Observed Values</i></td> <td>53%</td> </tr> <tr> <td>Valori Richiesti <i>Required Values</i></td> <td>40 ÷ 60</td> </tr> </table>		Valori Osservati [%] <i>Observed Values [%]</i>	< 0.1	Valori Richiesti [%] <i>Required Values [%]</i>	≤ 0.1	Valori Osservati <i>Observed Values</i>	53%	Valori Richiesti <i>Required Values</i>	40 ÷ 60
Valori Osservati [%] <i>Observed Values [%]</i>	< 0.1									
Valori Richiesti [%] <i>Required Values [%]</i>	≤ 0.1									
Valori Osservati <i>Observed Values</i>	53%									
Valori Richiesti <i>Required Values</i>	40 ÷ 60									

Rapporto redatto da:
 Report issued by:
 [Signature] PLT

Approvato da:
 Approved by:
 105 [Signature] PLT
 PINNA Emanuel

SUPERVISORE (Cliente o Terza Parte)
 Witness (Customer or Third Party)

"OME" s.r.l.
 METALLURGICA ERBESE
 ERBA (Como)

	<p>Campione 6.469 – Metà spessore Ingrandimento 100x - 500x Attacco: NaOH 20 % elettrolitico Specimen 6.469 – Mid thickness 100x - 500x Magnification Etch: 20 % NaOH electrolyte</p>													
	<table border="1"> <tr> <td colspan="2" data-bbox="852 786 1356 846"> <p>Contenuto massimo di fasi intermetalliche e precipitati <i>Maximum content of intermetallic phases and precipitates</i></p> </td> </tr> <tr> <td data-bbox="852 846 1114 907"> <p>Valori Osservati [%] <i>Observed Values [%]</i></p> </td> <td data-bbox="1114 846 1356 907"> <p>< 0.1</p> </td> </tr> <tr> <td data-bbox="852 907 1114 967"> <p>Valori Richiesti [%] <i>Required Values [%]</i></p> </td> <td data-bbox="1114 907 1356 967"> <p>≤ 0.1</p> </td> </tr> <tr> <td colspan="2" data-bbox="852 967 1356 1030"> <p>Contenuto di ferrite secondo ASTM E562-11 <i>Ferrite content according to ASTM E562-11</i></p> </td> </tr> <tr> <td data-bbox="852 1030 1114 1090"> <p>Valori Osservati <i>Observed Values</i></p> </td> <td data-bbox="1114 1030 1356 1090"> <p>54%</p> </td> </tr> <tr> <td data-bbox="852 1090 1114 1164"> <p>Valori Richiesti <i>Required Values</i></p> </td> <td data-bbox="1114 1090 1356 1164"> <p>40 + 60</p> </td> </tr> </table>		<p>Contenuto massimo di fasi intermetalliche e precipitati <i>Maximum content of intermetallic phases and precipitates</i></p>		<p>Valori Osservati [%] <i>Observed Values [%]</i></p>	<p>< 0.1</p>	<p>Valori Richiesti [%] <i>Required Values [%]</i></p>	<p>≤ 0.1</p>	<p>Contenuto di ferrite secondo ASTM E562-11 <i>Ferrite content according to ASTM E562-11</i></p>		<p>Valori Osservati <i>Observed Values</i></p>	<p>54%</p>	<p>Valori Richiesti <i>Required Values</i></p>	<p>40 + 60</p>
<p>Contenuto massimo di fasi intermetalliche e precipitati <i>Maximum content of intermetallic phases and precipitates</i></p>														
<p>Valori Osservati [%] <i>Observed Values [%]</i></p>	<p>< 0.1</p>													
<p>Valori Richiesti [%] <i>Required Values [%]</i></p>	<p>≤ 0.1</p>													
<p>Contenuto di ferrite secondo ASTM E562-11 <i>Ferrite content according to ASTM E562-11</i></p>														
<p>Valori Osservati <i>Observed Values</i></p>	<p>54%</p>													
<p>Valori Richiesti <i>Required Values</i></p>	<p>40 + 60</p>													

91 Rapporto redatto da:
 Report Issued by:
 PIATTI Emanuel
 PLT

Approvato da:
 Approved by:
 PIATTI Emanuel
 PLT

SUPERVISORE (Cliente o Terza Parte)
 Witness (Customer or Third Part)

"OME" s.r.l.
 METALLURGICA ERBESE
 ERBA (Como)

Pitting and Crevice Corrosion Resistance of Stainless Steels and Related Alloys by Use of Ferric Chloride Solution ASTM G48-11 – Method A							
Temperatura: Temperature:	50 °C	Tempo di prova: Test time:	24 h	Soluzione di decapaggio: Pickling:	20% HNO ₃ + 5% HF in acqua distillata per 5 min. a 60 °C 20% HNO ₃ + 5% HF in distilled water for 5 min. at 60 °C	Soluzione di prova: Test Solution:	FeCl ₃ – H ₂ O (6% in peso) FeCl ₃ – H ₂ O (6% in weight)
Campione 6.469 Specimen 6.469	Peso del provino prima della prova / Weight before test:					119.5039 [g]	
	Peso del provino al termine della prova / Weight after test:					119.5026 [g]	
	Superficie esposta / Surface exposed:					42.87 [cm ²]	
	Perdita di peso / Loss of weight:					0.0031 [g]	
	Perdita per metro quadro / Loss for square meter					0.303 [g/m ²]	
	Valore richiesto / Required Value					≤ 4.0 [g/m ²]	
Non si rileva la presenza di pitting ad ingrandimento di 20X. Absence of pits at 20X magnification.							

Fine del Rapporto di Prova
End of the Test Report

Rapporto redatto da:
Report issued by: MANO Marinina
PLT

Approvato da:
Approved by: PIANA Emanuel
105
BYTEST PLT

SUPERVISORE (Cliente o Terza Parte)
Witness (Customer or Third Part)

"OMIE" s.r.l.
METALLURGICA ERBESE
ERBA (Como)



Bytest

BYTEST Srl - TÜV SDD Group

bytest@tuv.it - www.tuv.it - (Laboratori-Bytest)

Partita IVA e CF 05102770012 - REA N° 685017/89 - Reg. imprese 3397
Società unipersonale, soggetta al controllo e coordinamento di TÜV SDD AG

- Sede legale e operativa:
Via Pisa 12 - 10089 - Volpiano (TO)
Tel. 011 037221 - Fax 011.99538.53
- Unità operativa di Benevento:
Zona Industriale ASI-Z5 - SS 90 Ponte Valerino
82100 - Benevento (BN) - Tel. 0824.1755662
- Unità operativa impianti NDT:
C.so Piemonte 8 - 10088 - Volpiano (TO)
Tel. 011 037221
- *Altra sede operativa Bytest

Sistema di Gestione Qualità Certificato
UNI EN ISO 9001
Sistema di Gestione Qualità Aerospaziale Certificato
AS 9100 - EN 9100 - JIS Q 9100
Material Testing Laboratory NADCAP Test Codes:
F2,F3,G1,GS,A,B,C,N,KN,L1,1,L2,L3,L4,L5,L6,L7,L8,XL,
M1,M2,M3,Q1,Z,XG,XA
Laboratorio Accreditato ACCREDIA N. 0599 secondo UNI
CEI EN ISO/IEC 17025
Prove: Trazione, Resilienza, Durezza, Stress Rupture,
Macrografia, Spettrometria ad emissione ottica, Suscettibilità
alla corrosione intermetallica

RAPPORTO DI PROVA Test Report

Il presente rapporto riguarda esclusivamente i campioni sottoposti a prova.
La riproduzione parziale del presente rapporto è vietata, salvo autorizzazione scritta della Bytest srl.
This report concerns only the tested specimens.
Partial reproductions of this report without written permission of Bytest srl is forbidden.

Certificazione di Conformità
Certificate of Conformity

Si certifica che tutte le attività oggetto di questo rapporto di prova sono state condotte in conformità ai requisiti della normativa di riferimento indicata, come richiesto dall'ordine d'acquisto.

Certificate of Conformity

This is to certify that all the activities covered by this test report were conducted in accordance with the requirements of the specified reference standard, as required by purchase order.

Rapporto N° Report N°	RP	0744L16	
Lotto Bytest N° Bytest Batch N°	1605 - 2016		
OC-Commessa OC-Job n°	18335		
Data emissione Issue date	26.02.2016		
Pagina n° Page n°	2	di of	2

DESCRIZIONE SAGGIO (tipo di prodotto, condizioni) <i>Sample description (product type and condition)</i>	CAMPIONI <i>SPECIMEN</i>
RIFERIMENTI (DISEGNO/PN/LOTTO/COLATA) <i>References (Dwg N./Part N./Batch n./Heat n.)</i>	TIPO MATERIALE - STATO TT - SPECIFICA di Riferimento <i>Material Type - HT condition - Reference Specification</i>
Campione 856 - Ø 11.35 (BARRE) Colata n. 307794 <i>Specimen 856 - Ø 11.35 (ROUND BARS) Heat n. 307794</i>	Acciaio ASTM A1082 Grado UNS S32760-S Solubilizzato e incrudito Check list 2016/187 ASTM A1082/A1082M-12 Norsok MDS D59 Rev.02 <i>Steel ASTM A1082 Grade UNS S32760-S Solution annealed and Strain Hardened Check list 2016/187 ASTM A1082/A1082M-12 Norsok MDS D59 Rev.02</i>

NOTA: TUTTE LE INFORMAZIONI SOPRA RIPORTATE SI INTENDONO DERIVANTI ESCLUSIVAMENTE DALLE DICHIARAZIONI DEL CLIENTE CHE RIMANE RESPONSABILE DEI CRITERI DI CAMPIONAMENTO UTILIZZATI. - NOTE: ALL THE ABOVE DATA HAVE BEEN DERIVED EXCLUSIVELY FROM CUSTOMER'S STATEMENTS WHO REMAIN THE WHOLE RESPONSIBLE OF THE APPLIED SAMPLING CRITERIA.

Contenuto del Rapporto di Prova: Test Report Content:

PROVA <i>Test</i>	NORMA DI PROVA <i>Test Standard</i>	CONDIZIONI <i>Conditions</i>	ESITO <i>Result</i>	DETTAGLI ALLEGATO N° <i>Details Annex N°</i>
MICROGRAFIA <i>Micrographic Test</i>	ASTM E3-11 ASTM E562-11	/	CONFORME <i>Satisfactory</i>	1
CORROSIONE <i>Corrosion</i>	ASTM G48-11		Method A 50°C / 24 h	CONFORME <i>Satisfactory</i>

PG-02-05-PLT

Questo rapporto è composto da 2 pagine e da 2 allegati. Documento trasmesso per via elettronica; l'originale vidimato verrà fisicamente consegnato a mezzo posta.

This report is made of 2 pages and 2 annexes. Document transmitted through e-mail; Original signed copy will be mailed.

Rapporto redatto da:
Report Issued by:

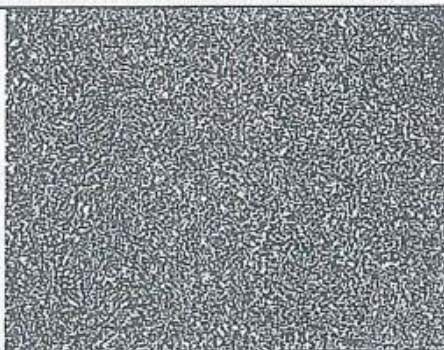
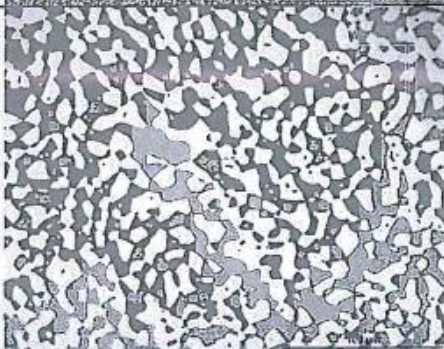


35
BYTEST
MIGLIORINI Stefano

Approvato da:
Approved by:

59
BYTEST
CARUSO Pietro

SUPERVISORE (Cliente o Terza Parte)
Witness (Customer or Third Part)

"OME" s.r.l.
METALLURGICA ERBESE
ERBA (Como)

	<p>Campione 856 – Superficie esterna Ingrandimento 100x - 500x Attacco: NaOH 20 % elettrolitico Specimen 856 – Outer surface 100x - 500x Magnification Etch: 20 % NaOH electrolyte</p>	
	<p>Contenuto massimo di fasi intermetalliche e precipitati <i>Maximum content of intermetallic phases and precipitates</i></p>	
	<p>Valori Osservati [%] <i>Observed Values [%]</i></p>	<p>< 0.1</p>
	<p>Valori Richiesti [%] <i>Required Values [%]</i></p>	<p>≤ 0.1</p>
	<p>Contenuto di ferrite secondo ASTM E562-11 <i>Ferrite content according to ASTM E562-11</i></p>	
	<p>Valori Osservati <i>Observed Values</i></p>	<p>50%</p>
<p>Valori Richiesti <i>Required Values</i></p>	<p>40 + 55</p>	
	<p>Campione 856 – Metà spessore Ingrandimento 100x - 500x Attacco: NaOH 20 % elettrolitico Specimen 856 – Mid thickness 100x - 500x Magnification Etch: 20 % NaOH electrolyte</p>	
	<p>Contenuto massimo di fasi intermetalliche e precipitati <i>Maximum content of intermetallic phases and precipitates</i></p>	
	<p>Valori Osservati [%] <i>Observed Values [%]</i></p>	<p>< 0.1</p>
	<p>Valori Richiesti [%] <i>Required Values [%]</i></p>	<p>≤ 0.1</p>
	<p>Contenuto di ferrite secondo ASTM E562-11 <i>Ferrite content according to ASTM E562-11</i></p>	
	<p>Valori Osservati <i>Observed Values</i></p>	<p>51%</p>
<p>Valori Richiesti <i>Required Values</i></p>	<p>40 + 55</p>	

Rapporto redatto da:
 Report Issued by:

Approvato da:
 Approved by:

SUPERVISORE (Cliente o Terza Parte)
 Witness (Customer or Third Part)

35

 MICELONICO Francesco

59

 CARUSO Pietro

"OME" s.r.l.
 METALLURGICA ERBESE
 ERBA (Como)

<i>Pitting and Crevice Corrosion Resistance of Stainless Steels and Related Alloys by Use of Ferric Chloride Solution ASTM G48-11 – Method A</i>							
Temperatura: Temperature:	50 °C	Tempo di prova: Test time:	24 h	Soluzione di decapaggio: Pickling:	20% HNO ₃ + 5% HF in acqua distillata per 5 min. a 60 °C 20% HNO ₃ + 5% HF in distilled water for 5 min. at 60 °C	Soluzione di prova: Test Solution:	FeCl ₃ – H ₂ O (6% in peso) FeCl ₃ – H ₂ O (6% in weight)
Campione 856 Specimen 856	Peso del provino prima della prova / Weight before test:					53.2516 [g]	
	Peso del provino al termine della prova / Weight after test:					53.2505 [g]	
	Superficie esposta / Surface exposed:					28.08 [cm ²]	
	Perdita di peso / Loss of weight:					0.0011 [g]	
Perdita per metro quadro / Loss for square meter					0.392 [g/m ²]		
Valore richiesto / Required Value					≤ 4.0 [g/m ²]		
Non si rileva la presenza di pitting ad ingrandimento di 20X. <i>Absence of pits at 20X magnification.</i>							

Fine del Rapporto di Prova
End of the Test Report

Rapporto redatto da:
Report Issued by:

30
BYTEST
MIGLIORE
C. Venturano

Approvato da:
Approved by:

59
BYTEST
CARUSO Pietro

SUPERVISORE (Cliente o Terza Parte)
Witness (Customer or Third Part)

"OME" s.r.l.
METALLURGICA ERBESE
ERBA (Como)



HEAT TREATMENT CERTIFICATE

ENCLOS.	CMTR N°	SHEET	PAGE
08	1600041/HT	1/1	1
DATE:			
19/02/2016			

3.1
 3.2

ISO 10474 EN 10204

REF. DOC. OME PROC. 7.5 - HT ASTM A1082

NO-HLD-10-T522-110002

PRODUCT RAW BARS SEMI-FINISHED PIECES FINISHED PCS.

FACILITIES ELECTRIC FURNACE CONTROLLED ATMOSPHER.

CAPACITY 1000 kg/h CAPACITY 2000 kg/h

LOT	P.O. ITEMS / MATERIAL	NOTE	ANN E A L I N G	Q U E N C H I N G	T E M P E R I N G	PARAMETERS		COOLING				H.T. DATE	CHART ENCL.	
						t ° C	MIN HOLD TIME (minutes)	O I L	W A T E R	A I R	O I L + H 2 O		Y E S	N O
L002	1A UNS S32760	NUT 1/2"	X			1120	20'	X						X
L003	2 UNS S32760	STUD 1/2"	X*			1120	20'	X						X



FOR MATERIAL ASTM UNS S32760 – STUDS 1/2" – ITEM 1 : STARTING BARS ALREADY IN FINAL HEAT TREATMENT CONDITION




* PLUS STRAIN HARDENING




PREPARED / APPROVED






F 8.2 -CMTR -04 19.04.02


INSPECTION CERTIFICATE				CERT. TYPE	CMTR Nr.	SHEET				
LIST OF SUPPLIED PRODUCTS				ISO 10474	1600307/1	1/8				
				EN 10204	DATE	26/02/2016				
CUSTOMER : TOOLS AS				ORDER No.: SAMPLE FOR STAVANGER UNIVERSITY Date: 28/01/2016						
DESTINATION :				PROJECT No.:						
TOOLS AS P.B. 696 1411 KOLBOTN				JOB No.:						
LOT	OME ITEM	P.O. ITEM	Q.TY	Dimension	Drawing No.	Spec / Grade	Heat No.	Marking	Cond.	Coat.
L001	10	1	16 No.	1/2" 13 UNC x 70	ANSI B16.5	ASTM A1082 / A1082M UNS S32760	388775	OME.IT-32760-75	SO	
L002	20	1A	32 No.	1/2" 13 UNC	ANSI B16.2.2-Tab.10	ASTM A1082 / A1082M UNS S32760	W72502	OME-32760-502-18	SO	038
L003	30	2	16 No.	1/2" 13 UNC x 70	ANSI B16.5	ASTM A1082 / A1082M UNS S32760	307794	OME.IT-32760-94	ST	
VISUAL / DIMENSIONAL EXAMINATION : Conforming				MELT PROCESS : Electric Furnace						
OME Metallurgica Erbese S.r.l. Via Milano, 15 22036 ERBA (CO) Italy Phone +39 031 641606 r.a. - Fax +39 031 645618 E-Mail: info.ome@ome.it - http://www.ome.it				Statement THIS IS TO CERTIFY THAT THE CONTENTS OF THE CERTIFICATE ARE CORRECT AND ACCURATE AND THAT ALL OPERATIONS PERFORMED ARE IN COMPLIANCE WITH THE APPLICABLE SPECIFICATIONS AND PURCHASE ORDER REQUIREMENTS. MATERIAL FREE FROM MERCURY OR RADIO-ACTIVITY CONTAMINATION						
				F 8.2 - CMTR - 20						

INSPECTION CERTIFICATE																	
HEAT ANALYSIS											CERT. TYPE ISO 10474 EN 10204 3.1		CMTR Nr. 1600307/1 DATE 26/02/2016		SHEET 2/6		
CUSTOMER : TOOLS AS											ORDER No.: SAMPLE FOR STAVANGER UNIVERSITY Date: 28/01/2016						
DESTINATION : TOOLS AS P.B. 686 1411 KOLBOTN											PROJECT No.:						
											JOB No.:						
LOT	Heat No.	C	Mn	Si	P	S	Cr	Ni	Mo	V	Ti	Cu	W	Al	B	Nb	Co
		Zn	Pb	Sn	Be	O	N	H	Fe	Nb+Ta	Cb	Al+Ti	Cb+Ta				
L001	388775	0,023	0,580	0,280	0,023	0,0006	25,550	7,500	3,470			0,560	0,540				
L002	W72502	0,019	0,530	0,190	0,025	0,0003	25,360	7,030	3,520			0,560	0,540				
L003	307794	0,024	0,600	0,410	0,025	0,001	25,600	7,200	3,500			0,580	0,540				
<p>OME Metallurgica Erbesse S.r.l. Via Milano, 15 22036 ERBA (CO) Italy Phone +39 031 641606 r.a. - Fax +39 031 645618 E-Mail: info.ome@ome.it - http://www.ome.it</p>																	
Statement											<p>THIS IS TO CERTIFY THAT THE CONTENTS OF THE CERTIFICATE ARE CORRECT AND ACCURATE AND THAT ALL OPERATIONS PERFORMED ARE IN COMPLIANCE WITH THE APPLICABLE SPECIFICATIONS AND PURCHASE ORDER REQUIREMENTS.</p> <p>MATERIAL FREE FROM MERCURY OR RADIOACTIVITY CONTAMINATION</p>						
																	
F 8.2 - CMTR - 29																	



INSPECTION CERTIFICATE							CERT. TYPE			CMTR Nr.		SHEET							
TENSILE TEST							ISO 10474 EN 10204			1600307/1 DATE 28/02/2016		3/6							
CUSTOMER : TOOLS AS							ORDER No.: SAMPLE FOR STAVANGER UNIVERSITY Date: 28/01/2016												
DESTINATION : TOOLS AS P.B. 686 1411 KOLBOTHN							PROJECT No.:												
							JOB No.:												
LOT	SPECIMEN					REQUIRED VALUES						OBTAINED VALUES							
	NO.	DIA. mm	AREA mm ²	L mm	T °C	Measure Unit	MIN Rp 0.2	R		MIN E %	MIN R.A. %	Rp 0.2	R	E %	R.A. %				
L001		12,5	122,66	50,00	Room	MPa	550	760		16	33	662	877	42,0	84,0				
L002		12,5	122,66	50,00	Room	MPa	550	760		16	33	581	814	45,1	87,5				
L003		12,5	122,66	50,00	Room	MPa	725	860		16	33	1004	1075	23,4	77,1				
OME Metallurgica Erbese S.r.l. Via Milano, 15 22036 ERBA (CO) Italy Phone +39 031 641606 r.a. - Fax +39 031 645618 E-Mail: Info.ome@ome.it - http://www.ome.it							Statement THIS IS TO CERTIFY THAT THE CONTENTS OF THE CERTIFICATE ARE CORRECT AND ACCURATE AND THAT ALL OPERATIONS PERFORMED ARE IN COMPLIANCE WITH THE APPLICABLE SPECIFICATIONS AND PURCHASE ORDER REQUIREMENTS. MATERIAL FREE FROM MERCURY OR RADIO-ACTIVITY CONTAMINATION												
F.8.2 - CMTR - 05																			

INSPECTION CERTIFICATE										CERT. TYPE		CMTR Nr.		SHEET								
IMPACT TEST										ISO 10474		1600307/1		4/8								
										EN 10204		DATE		28/02/2016								
CUSTOMER : TOOLS AS										ORDER No.: SAMPLE FOR STAVANGER UNIVERSITY Date: 28/01/2016												
DESTINATION : TOOLS AS P.B. 686 1411 KOLBOTTN										PROJECT No.:		JOB No.:										
LOT	SPECIMEN					MINIMUM REQUIRED VALUES				OBTAINED VALUES												
	NO.	IZOD	KV	ISOV	KCU	T °C	M.Unit	MIN.	AVE.	L.E.	ABSORBED ENERGY			LATERAL EXP.			SHEAR %					
											1	2	3	AVE.	1	2	3	60	70	80	90	
L001		X				-50	J	35	45		360	356	321	346								
L002		X				-50	J	35	45		316	322	334	324								
L003		X				-46	J	35	45		53	47	49	50								




OME Metallurgica Erbesse S.r.l. Via Milano, 15 22036 ERBA (CO) Italy Phone +39 031 641606 r.a. - Fax +39 031 645618 E-Mail: info.ome@ome.it - http://www.ome.it		Statement THIS IS TO CERTIFY THAT THE CONTENTS OF THE CERTIFICATE ARE CORRECT AND ACCURATE AND THAT ALL OPERATIONS PERFORMED ARE IN COMPLIANCE WITH THE APPLICABLE SPECIFICATIONS AND PURCHASE ORDER REQUIREMENTS. MATERIAL FREE FROM MERCURY OR RADIOACTIVITY CONTAMINATION			
				F 8.2 - CMTR - 06	



INSPECTION CERTIFICATE										CERT. TYPE		CMTR Nr.		SHEET						
HARDNESS TEST										3.1		1600307/1		5/8						
CUSTOMER: TOOLS AS										ORDER No.: SAMPLE FOR STAVANGER UNIVERSITY Date: 28/01/2016										
DESTINATION: TOOLS AS P.B. 686 1411 KOLBOTN										PROJECT No.:					JOB No.:					
LOT	NO. OF TEST	REQUIRED VALUES								OBTAINED VALUES										
		AFTER HEAT TREAT. x 24h				ROOM TEMPERATURE				AFTER HEAT TREAT. x 24h				ROOM TEMPERATURE						
		HB	HRB	T °C	HARD. MIN	HB	HRB	HRC	HV	HARDNESS		CONTR.	HARDNESS		CONTR.	HARDNESS		PL	CPL	
								MIN	MAX	QTY	MIN	MAX	QTY	MIN	MAX	C	NC	C	NC	
L001						X								1						
L001						X								10%	272	281				
L002						X								1	250	257	X			
L002						X								10%	249	259				
L003						X								1	316	325				
L003						X								10%	316	326				

PL = Proof Load CPL = Cone Proof Load C = Conforming NC = Not Conforming


<p>OME Metallurgica Erbesi S.r.l.</p> <p>Via Milano, 15 22036 ERBA (CO) Italy</p> <p>Phone +39 031 641606 r.a. - Fax +39 031 645618 E-Mail: info.ome@ome.it - http://www.ome.it</p>	<p>Statement</p> <p>THIS IS TO CERTIFY THAT THE CONTENTS OF THE CERTIFICATE ARE CORRECT AND ACCURATE AND THAT ALL OPERATIONS PERFORMED ARE IN COMPLIANCE WITH THE APPLICABLE SPECIFICATIONS AND PURCHASE ORDER REQUIREMENTS.</p> <p>MATERIAL FREE FROM MERCURY OR RADIO-ACTIVITY CONTAMINATION</p>	<p>Prepared</p>  <p>G. ROSSINI</p>	<p>Approved</p>  <p>D. FRIGENIO</p>
---	--	---	--

F 8.2 - CMTR - 07

INSPECTION CERTIFICATE		CERT. TYPE ISO 10474 EN 10204 3.1	CMTR Nr. 1800307/1 DATE 28/02/2016	SHEET 6/6	
Declarations		ORDER No. SAMPLE FOR STAVANGER UNIVERSITY Date: 28/01/2016:			
CUSTOMER :TOOLS AS		PROJECT : No.:			
DESTINATION : TOOLS AS P.B. 686 1411 KOLBOTN		JOB No.:			
Conforming ASTM A1082 / A1082M - 12 Ed. PROOF LOAD TEST ACCORDING TO ASTM A194 (LOAD ACCORDING TO ASTM A194 TABLE 3 - Gr.7M) PREN ≥ 40.0% HEAT 388775 - PREN = 41,161% HEAT W72502 - PREN = 41% HEAT 307794 - PREN = 41,23% * IMPACT TEST PERFORMED BY SUBSIZE SPECIMEN (10 x 5 mm)		Material Specification QTR NO. 1401 Rev.5 MDS D59 Rev.2 QTR NO. 1402 Rev.2 QTR NO. 1301 Rev.3 MDS D80 Rev.2			
Coating 038 = PICKLING & PASSIVATION		Condition SO = SOLUTION TREATED ST = SOLUTION TREATED / STRAIN HARDENED			
Generic Specification					
OME Metallurgica Erbesa S.r.l. Via Milano, 15 22036 ERBA (CO) Italy Phone +39 031 641606 r.a. - Fax +39 031 645618 E-Mail: info.ome@ome.it - http://www.ome.it		Statement THIS IS TO CERTIFY THAT THE CONTENTS OF THE CERTIFICATE ARE CORRECT AND ACCURATE AND THAT ALL OPERATIONS PERFORMED ARE IN COMPLIANCE WITH THE APPLICABLE SPECIFICATIONS AND PURCHASE ORDER REQUIREMENTS. MATERIAL FREE FROM MERCURY OR RADIOACTIVITY CONTAMINATION			
				F 6.2 - CMTR - 30	


	P.M.I. CERTIFICATE				ENCLOS.	CMTR N°	SHEET	PAGE			
	<input checked="" type="checkbox"/> 3.1 <input type="checkbox"/> 3.2				18	1600307/PMI	1/1	1			
					ISO 10474 EN 10204				DATE: 26/02/2016		
REF. DOC.	<input checked="" type="checkbox"/> OME PROC. 8.2-PMI			<input checked="" type="checkbox"/> Material ASTM A1082 UNS S32760							
PRODUCT	<input type="checkbox"/> RAW BARS			<input type="checkbox"/> SEMI-FINISHED PIECES			<input checked="" type="checkbox"/> FINISHED P.				
EQUIPMENT	<input checked="" type="checkbox"/> NITON XLt 800			<input type="checkbox"/> FOERSTER MAGNATEST I 3.610							
METHOD	<input checked="" type="checkbox"/> PHOTOGEN PIPE			<input type="checkbox"/> ELECTROMAGNETIC							
LOT	ITEM (HEAT)	CONTROLLED QUANTITY			VERIFIED ELEMENTS						
		10%	CHECK PCS.	TOTAL QTY.	Cr Req. 24.0-26.0 %	Ni Req. 6.0-8.0 %	Mo Req. 3.0-4.0 %	Cu Req. 0.50-1.00 %	W Req. 0.50-1.00 %	N C	C
L001	1 (388775)	X	2	16	Min Max	25.51 25.58	7.46 7.53	3.45 3.52	0.55 0.61	0.52 0.59	X X
L002	1A (W72502)	X	4	32	Min Max	25.30 25.39	6.98 7.07	3.59 3.68	0.53 0.60	0.51 0.57	X X
L003	2 (307794)	X	2	16	Min Max	25.55 25.63	7.16 7.22	3.47 3.56	0.52 0.59	0.53 0.62	X X
<input checked="" type="checkbox"/> EXAMINED PIECES HAVE BEEN "PMI" MARKED <input checked="" type="checkbox"/> THE OPERATORS PERFORMING THE PMI TEST HAVE BEEN TRAINED AND QUALIFIED FOR ITS EXECUTION <input checked="" type="checkbox"/> CONTROL EXECUTED ACC.TO SPEC. TR 1427 Ver.2 <input type="checkbox"/>						PREPARED/APPROVED 					
C = CONFORMING						NC = NON CONFORMING					
						F 8.2 -CMTR -15 19.04.02					

Appendix E: MDS 316L bolts and nuts

 I.M.L. - INDUSTRIA MECCANICA LIGURE S.P.A. Via Giancarlo Farina, 25 - 16030 Casarza Ligure - GE - ITALY Tel. +39 0185 467661 - Fax +39 0185 466510 - E-mail quality.iml@farinagroup.com MATERIAL TEST DEPARTMENT		COMPANY WITH QUALITY SYSTEM ISO 9001: 2008 CERTIFIED BY RINA CERT. N° 23/91/S																																											
INSPECTION CERTIFICATE EN 10204:2004 / 3.1		Nr ^{PO} 2015-C_IML-26723	Data / Dated 19.05.2015																																										
WURTH INDUSTRI NORGE AS Rasteinvegen 7 2870 DOKKA - NORWAY		Ordine / PO 83116075 Item 001 DDT / Delivery note 2015-2E301-0000777 Packing List 2015-2E301-0000777 Fattura / Invoice 2015-2E401-0000763 Ns. rif. / Our ref. 2015-2E201-0000516-0001																																											
Dest. WURTH INDUSTRI NORGE AS Bodriffsveien 5 4353 KLEPP STASJON - NORWAY																																													
Cod. colata Heat Code 6D	Nr. colata Heat Nr 369009	Quantità Quantity 173,00	Descrizione Description STUDBOLT B8M CL 2 1/2" L75mm(3") / MARKED IML-B8M UNDERLINE-6D Mat. No. 494731375 090 1																																										
Mat. in acc. a / Mat. in acc. to ASME SA ASTM A320/A320M-14 Gr. B8M cl 2 NACE MR 0175 - ISO 15156 Ed. 2009 / NACE MR 0103 Ed. 2012 P.E.D. 97/23/EC ANNEX 1 PAR. 4.3																																													
<table border="1"> <thead> <tr> <th>Elementi / Elements</th> <th>C</th> <th>Si</th> <th>Mn</th> <th>S</th> <th>P</th> <th>Cr</th> <th>Ni</th> <th>Mo</th> <th>Ti</th> <th>Cu</th> <th>V</th> <th>Nb</th> <th>N</th> </tr> </thead> <tbody> <tr> <td>LADLE ANALYSIS</td> <td>0,027</td> <td>0,330</td> <td>1,720</td> <td>0,029</td> <td>0,035</td> <td>16,600</td> <td>10,000</td> <td>2,000</td> <td>0,000</td> <td>0,000</td> <td>0,000</td> <td>0,000</td> <td>0,034</td> </tr> <tr> <td>LADLE ANALYSIS</td> <td>0,000</td> <td></td> <td></td> <td></td> <td></td> <td></td> <td></td> <td></td> <td></td> <td></td> <td></td> <td></td> <td></td> </tr> </tbody> </table>				Elementi / Elements	C	Si	Mn	S	P	Cr	Ni	Mo	Ti	Cu	V	Nb	N	LADLE ANALYSIS	0,027	0,330	1,720	0,029	0,035	16,600	10,000	2,000	0,000	0,000	0,000	0,000	0,034	LADLE ANALYSIS	0,000												
Elementi / Elements	C	Si	Mn	S	P	Cr	Ni	Mo	Ti	Cu	V	Nb	N																																
LADLE ANALYSIS	0,027	0,330	1,720	0,029	0,035	16,600	10,000	2,000	0,000	0,000	0,000	0,000	0,034																																
LADLE ANALYSIS	0,000																																												
<table border="1"> <thead> <tr> <th>Provetta</th> <th>Forma</th> <th>Snervamento</th> <th>Snervamento</th> <th>Rottura</th> <th>Allungamento</th> <th>Contrazione</th> </tr> <tr> <th>Test specimen</th> <th>Shape</th> <th>Yield Strength</th> <th>Yield Strength</th> <th>Tensile</th> <th>Elongation</th> <th>Reduction of area</th> </tr> <tr> <th>Sez/Secl mm2 L mm</th> <th>1=0 - 2=□</th> <th>MPa</th> <th>MPa</th> <th>MPa</th> <th>%</th> <th>%</th> </tr> </thead> <tbody> <tr> <td>122,85 50,00</td> <td>1</td> <td>20</td> <td>655,0</td> <td>775,0</td> <td>32,5</td> <td>68,4</td> </tr> </tbody> </table>				Provetta	Forma	Snervamento	Snervamento	Rottura	Allungamento	Contrazione	Test specimen	Shape	Yield Strength	Yield Strength	Tensile	Elongation	Reduction of area	Sez/Secl mm2 L mm	1=0 - 2=□	MPa	MPa	MPa	%	%	122,85 50,00	1	20	655,0	775,0	32,5	68,4														
Provetta	Forma	Snervamento	Snervamento	Rottura	Allungamento	Contrazione																																							
Test specimen	Shape	Yield Strength	Yield Strength	Tensile	Elongation	Reduction of area																																							
Sez/Secl mm2 L mm	1=0 - 2=□	MPa	MPa	MPa	%	%																																							
122,85 50,00	1	20	655,0	775,0	32,5	68,4																																							
<table border="1"> <thead> <tr> <th>DUREZZA / HARDNESS</th> <th colspan="6">RESILIENZA / IMPACT TEST</th> </tr> <tr> <th>HBW</th> <th>Tipo/Type</th> <th>Provetta / Test Specimen</th> <th>°C</th> <th>1-Joule</th> <th>2-Joule</th> <th>3-Joule</th> <th>Media/Average</th> </tr> </thead> <tbody> <tr> <td>277,0 - 281,0</td> <td>KV</td> <td>10x10mm</td> <td>-10</td> <td>200</td> <td>209</td> <td>203</td> <td>204,0</td> </tr> </tbody> </table>				DUREZZA / HARDNESS	RESILIENZA / IMPACT TEST						HBW	Tipo/Type	Provetta / Test Specimen	°C	1-Joule	2-Joule	3-Joule	Media/Average	277,0 - 281,0	KV	10x10mm	-10	200	209	203	204,0																			
DUREZZA / HARDNESS	RESILIENZA / IMPACT TEST																																												
HBW	Tipo/Type	Provetta / Test Specimen	°C	1-Joule	2-Joule	3-Joule	Media/Average																																						
277,0 - 281,0	KV	10x10mm	-10	200	209	203	204,0																																						
Tratt. Term. / Heat treatment Carbide Solution Treated and Strain Hardened ELECTRIC FURNACE																																													
Dim in acc. a / Dim. acc. to ASME B1.1 Ed.2003																																													
Marcatura in acc. Marking in acc. to	MSS SP25 Ed. 2013	Vis. & Dim.	SATISFACTORY																																										
		Origine Origin of Steel	SPAIN																																										

Note / Notes 100% MANUFACTURED IN ITALY
 SUPPLIED MATERIAL MEETS SPECIFICATIONS AND P.O. REQUIREMENTS

UFFICIO CONTROLLO QUALITA' QUALITY CONTROL DEPARTMENT Boris Fizzotti - Q.C. Manager 	ENTE UFFICIALE DI COLLAUDO INSPECTION AUTHORITY	MARCHIO PRODUZIONE MANUFACTURER'S SYMBOL IML or 
---	---	--

	I.M.L. - INDUSTRIA MECCANICA LIGURE S.P.A. Via Giancarlo Farina, 25 - 16030 Casarza Ligure - GE - ITALY Tel. +39 0185 467661 - Fax +39 0185 466510 - E-mail quality.iml@farinagroup.com MATERIAL TEST DEPARTMENT	COMPANY WITH QUALITY SYSTEM ISO 9001: 2008 CERTIFIED BY RINA CERT. N° 23/91/S
	INSPECTION CERTIFICATE EN 10204:2004 / 3.1	

WURTH INDUSTRI NORGE AS Rostveien 7 2870 DOKKA - NORWAY	Ordine / PO Item 83116075 001 DDT / Delivery note 2015-2E301-0000777 Packing List 2015-2E401-0000763 Fattura / Invoice 2015-2E401-0000763 Ns. rif. / Our ref. 2015-2E201-0000616-0001
--	--

Dest. WURTH INDUSTRI NORGE AS Bedriftsveien 5 4353 KLEPP STASJON - NORWAY	NO
--	----

Cod. colata Heat Code	Nr. colata Heat Nr	Quantità Quantity	Descrizione Description
S	345843	346,00	HEX.NUT 1/2" Gr.8 M / MARKED IML-8M-1/2-S Mail. No. 494731375 090 1

Mat. in acc. a / Mat. in acc. to ASME SA ASTM A194/A194M-14a Gr.8M
 NACE MR 0175 - ISO 15156 Ed. 2009 / NACE MR 0103 Ed. 2012
 P.E.D. 97/23/EC ANNEX 1 PAR. 4.3

Elementi / Elements	C	Si	Mn	S	P	Cr	Ni	Mo	Ti	Cu	V	Nb	N
LADLE ANALYSIS	0,023	0,460	1,610	0,026	0,032	16,850	10,100	2,020	0,090	0,000	0,000	0,000	0,034
LADLE ANALYSIS	0,000												

DUREZZA / HARDNESS	HBW	Tipo/Type	Provetta / Test Specimen	°C	1-Joule	2-Joule	3-Joule	Media/Average
	281,0 - 285,0	KV	10x10mm	-10	198	205	201	201,3

Proof load test	11350 lbf SATISFACTORY
-----------------	------------------------

Tratt. Term. / Heat treatment	Carbide Solution Treated	ELECTRIC FURNACE
-------------------------------	--------------------------	------------------

Dim in acc. a / Dim. acc. to	ASME B1.1 Ed.2003
------------------------------	-------------------

Marcatura in acc. / Marking in acc. to	MSS SP25 Ed. 2013	Vis. & Dim.	SATISFACTORY	Origine / Origin of Steel	SPAIN
--	-------------------	-------------	--------------	---------------------------	-------

Note / Notes 100% MANUFACTURED IN ITALY
 SUPPLIED MATERIAL MEETS SPECIFICATIONS AND P.O. REQUIREMENTS

UFFICIO CONTROLLO QUALITA' QUALITY CONTROL DEPARTMENT Giosè Fizzoli - Q.C. Manager 	ENTE UFFICIALE DI COLLAUDO INSPECTION AUTHORITY	MARCHIO PRODUZIONE MANUFACTURER'S SYMBOL IML 
---	--	--

Appendix F: Calculations on nut and holder

Bolts

Shear area from table

$$A_s := 0.92 \text{ cm}^2$$

UTS strength SA bolt

$$R_{mSA} := 877 \text{ MPa}$$

UTS strength CS bolt

$$R_{mCS} := 1075 \text{ MPa}$$

Force at fracture for SA bolt

$$F_{SA} := R_{mSA} \cdot A_s = 80.684 \text{ kN}$$

Force at fracture for CS bolt

$$F_{CS} := R_{mCS} \cdot A_s = 98.9 \text{ kN}$$

Nut and holder

UTS nut

$$R_{mNut} := 814 \text{ MPa}$$

UTS holder

$$R_{mHolder} := 975 \text{ MPa}$$

Threads per inch

$$n := 13 \cdot \frac{1}{\text{in}}$$

Length of thread engagement
(conservative)

$$L_e := 0.34 \text{ in}$$

Min major diameter of external threads

$$D_{smin} := 0.4985 \text{ in}$$

Max pitch diameter of internal threads

$$E_{nmax} := 0.4565 \text{ in}$$

Shear strength of the nut

$$S_{uNut} := R_{mNut} \cdot 0.6 = 488.4 \text{ MPa}$$

Shear strength of the holder

$$S_{uHolder} := R_{mHolder} \cdot 0.6 = 585 \text{ MPa}$$

Area when shear occurs at the roots of the threads

$$A_{ts} := \pi \cdot n \cdot L_e \cdot D_{smin} \cdot \left(\left(\frac{1}{2n} \right) + 0.57735 \cdot (D_{smin} - E_{nmax}) \right) = 2.801 \text{ cm}^2$$

Capacity of duplex nuts (all SA)

$$F_{capNut} := S_{uNut} \cdot A_{ts} = 136.779 \text{ kN}$$

Capacity of S165m holder

$$F_{capHolder} := S_{uHolder} \cdot A_{ts} = 163.832 \text{ kN}$$

Utilization of nuts when using CS bolts

$$UR_1 := \frac{F_{CS}}{F_{capNut}} = 0.723$$

Utilization of holder when using CS bolts

$$UR_2 := \frac{F_{CS}}{F_{capHolder}} = 0.604$$

Appendix G: MDS S165M holders

1x63

CO #	Item #	Del #	Heat	Lot	Code #	Cust.art.	Qty	Description
45590			257985				0	Ruestfritt rundt slppt

RUUKKI

This document is electronically reproduced and is identical to the original.

**Acciaierie
Valbruna S.p.A.**



QUALITY MANAGEMENT SYSTEM
CERTIFIED BY LLOYD'S REGISTER

**CERTIFICATO DI COLLAUDO
ABNAHMEPRÜFZEUGNIS
INSPECTION CERTIFICATE
CERTIFICAT DE RECEPTION
EN 10204 (2004) , 3.1**

36100 VICENZA (Italia) - Viale della scienza, 25 z.l.
Stab.: 39100 BOLZANO (Italia) - Via A. Volta, 4
Officio / Bureau / Procesi / Office
VALBRUNA NORDIC AB
LOVARTSGATAN 7
65221-KARLSTAD - SWEDEN-SE

Avviso di Spedizione: D-BZ12006769
Lieferungs/Packing list L

Certificato nr: MEST274789/2012/
Prüfung/Test/Exp. id

Produttore: **STABILIMENTO DI BOLZANO**
Hersteller/Produktionsprodukt

Ordine nr: R21146
Bestell/Your order/Commande

Conferma ordine nr: E112003022
Werk/Dat Order/Ref. nr.

Marchio di Fabbrica:
Züchten des Lieferanten
Trade mark
Signe de l'usine producteur



Stato di fornitura: - Hardened and Tempered Bright Ground
Lieferzustand/Delivery state/État de livraison

Tipo di Elaborazione: E+AOD
Erzeugnisart/Manufacturing process/Mode de fabrication

Punzone del Collaudatore:
Stempel des Werkst. zur verbindlichen
Inspektion à stamp/Punçon de l'auditeur



Specifiche:
Anforderungen / Requirements / Exigences
MS-RB-4418.4.8. 1.4418 QT900

EN 10088-3 2005 1.4418 QT900

EN 10272 2007 1.4418 QT900

Qualità: 1.4418
Werkstoff/Grade/Reference

Marca: PKA7914
Markenbezeichnung
Designation

Tolleranza: DIN 871 - h9
Toleranz/Allowance/Tolerance

Punzonatura: 1.4418
Kennzeichnung/Marking/Marking

Pos. nr. Part. nr. Nr. de partie	Oggetto Designation Produit designation Descr. du produit	Dimensioni - mm Abmessungen Dimensions Dimension	Lunghezza - mm Länge Length Langueur	Colata Schmelze Heat Coulée	Pezzi Stückzahl Pieces Pièces	Peso - KG Gewicht Weight Poids	Lotto nr. Losn. Lot n. Lot n.
0020	Round	50,000	5030 / 5740	257985		3825,0	209301491

TEST ALLO STATO DI FORNITURA										
Test on delivery condition / Prüfung auf Lieferzustand / essai à l'état de fourniture / Proba sobre el material así como entregado										
TEST	Proveita/Prüfung Essai/Prüfung Lunghezza/Length Durezza/Hardness Larghezza/Width Larg. de larg. mm	°C	Snervamento Streckgrenze Yield Stress Rp 0,2% N/mm ²	Snervamento Streckgrenze Yield Stress Rp 1% N/mm ²	Resistenza Zugfestigkeit Tensile strength Rm N/mm ²	Allungamento Zugdehnung Elongation A5 %	Stirazione Zugverschiebung Elongation Z %	Resistenza Kerbschlag Impact KV J	Durezza Härte Rockwell HB	
Valori richiesti 1 Anforderungen/Required values Valeurs demandées		min max	750	800	900 1050	16	40	80	280 340	
A	10,00	20	814	838	975	20	62	154	151	150
C	10,00	20	819	848	985	18	60	148	149	154

TEST										
TEST	Proveita/Prüfung Essai/Prüfung Larg. de larg. mm	°C	Resistenza Zugfestigkeit Tensile strength KV J	Espansione laterale Lateral Expansion			Shear			
Valori richiesti 1 Anforderungen/Required values Valeurs demandées		min max	32	32	32					
B	10X10	-40	140	135	136					
D	10X10	-40	138	131	135					

1) Lunghezza/Length, 2) Durezza/Hardness, 3) Temperatura/Temperature

Analisi chimica

Chemische Zusammensetzung/Chemical Analysis/Analyse chimique

Colata Heat Schmelze/Heat	min max	0,00 0,050	0,00 0,70	16,00 17,00	0,80 1,25	0,60	4,50 5,50	0,0050	0,040	0,005	0,015	0,020	0,030	-	-	-	-
257985	C %	Si %	Mn %	Cr %	Mo %	Cu %	Ni %	Ti %	P %	S %	N %						
	0,024	0,43	0,82	15,67	0,93	0,33	5,31	0,0005	0,027	0,013	0,035						

Colata Heat Schmelze/Heat	min max	0,000	-	-	-	-	-	-	-	-	-	-	-	-	-	-	-
257985	Cb(Nb)%	0,005															
	0,005																

UT-TESTING ACCORDING TO MS-RB-4418.1: OK
Material hardened 1040° C for 1h/air.
Tempered 560° C for 12h/air.

Sono state soddisfatte tutte le condizioni richieste Controllo antimiscelanza: OK Controllo visivo e dimensionale: soddisf. le esigenze

Bolzano, 27/11/12 BILDER (Int. MCR)	# collaudatore di stabilimento / der Werkstättverständiger / Works Inspector / L'agent d'usine <i>M. Rizzotto</i>	Pagina - 1 di 2
---	--	-----------------

Acciaierie Valbruna S.p.A.



QUALITY MANAGEMENT SYSTEM
CERTIFIED BY LLOYD'S REGISTER

CERTIFICATO DI COLLAUDO ABNAHMEPRUEFZEUGNIS INSPECTION CERTIFICATE CERTIFICAT DE RECEPTION EN 10204 (2004) , 3.1

36100 VICENZA (Italia) - Viale della scienza, 25 z.I.
Stab.: 39100 BOLZANO (Italia) - Via A. Volta, 4

Clienti / Besteller/Purchaser/Client
VALBRUNA NORDIC AB
LOVARTSGATAN 7
85221-KARLSTAD - SWEDEN-SE

Produttore: **STABILIMENTO DI BOLZANO**
Hersteller/Usine producer

Stato di fornitura: - Hardened and Tempered Bright Ground
Lieferzustand/état de livraison

Avviso di Spedizione: D-BZ12006789
Lieferanzeige/Facking list/RL

Ordine nr: R21146
Bestell./Your order/Commande

Tipo di Elaborazione: E+AOD
Erzeugung/Producing process/Mode of elaboration

Certificato nr: MEST274788/2012/
Prüfung/Test/Exam

Conferma ordine nr: E112003022
Werk/D or Order/Part nr.

Marchio di Fabbrica:
Zeichen des Lieferanten
Trade mark
Sigle de l'usine producteur

Funzione del Collaudatore:
Stempel des Werkstoffschwerfändigen
Inspector's stamp/Prüfung de l' usager



Die gestellten Anforderungen sind in Anlage erfüllt
The material has been furnished in accordance with the requirements
Le matériel a été fourni conforme aux exigences

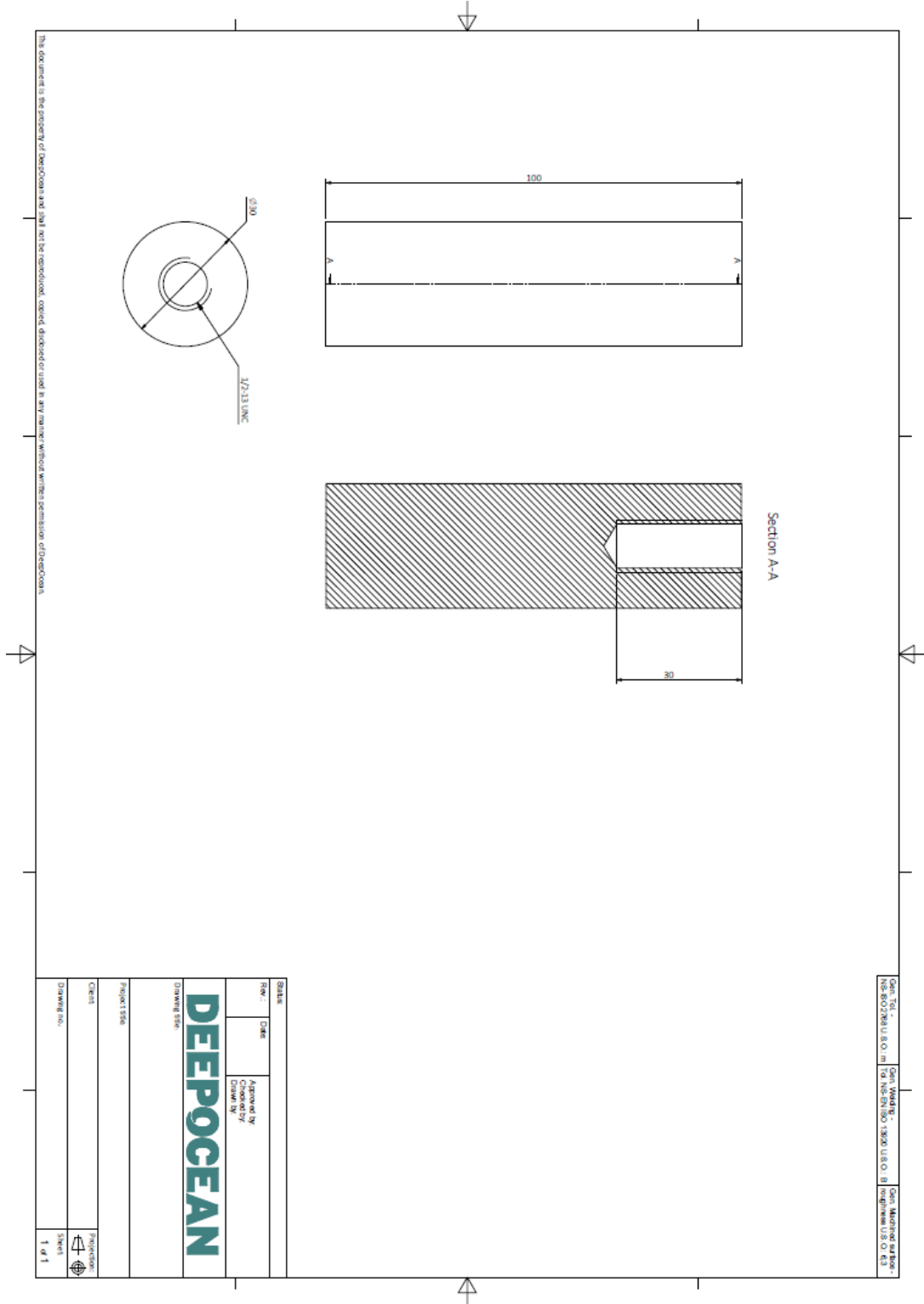
Verwechslungsprüfung: spektralanalytisch durchgeführt
Analysing testing performed: OK
Contrôle anti-mélange fait: n.s.s.

Besichtigung und Abmessung: ohne Beanstandung
Visual inspection and dimensional check: satisfactory
Contrôle visuel et dimensionnel: satisfaisant

Melted and manufactured in Italy No welding or weld repair Material free from Mercury contamination
We declare that the finished product is checked for radioactive contamination through Portal System when it leaves the production plant.
The Quality Management System is Certified acc. Pressure Equipment Directive [97/23/EC] Annex 1,s.,4.3 by TÜEV and LLOYD'S
Any act of tampering, modification, alteration, counterfeiting and/or falsification and/or any other action which modifies the contents of this test certificate shall constitute a violation of applicable civil and criminal laws. Acciaierie Valbruna shall protect its rights and interests before any competent court, authority and jurisdiction.
The supplied product conforms to requirements expressly requested by the purchaser and conforms to requirements specified by certified norms and standards. Should the product be used for more severe, critical and/or in any case different applications than those the material is generally intended for, any different and/or supplementary requirements shall be specifically demanded, at least, upon order of the Product by the Purchaser. Acciaierie Valbruna SpA shall not be responsible for any improper use of the Products.

<p>Bolzano,27/11/12 BEL/006 (Mod. NC22)</p>	<p>Il collaudatore di stabilimento / der Werkstoffschwerfändige / Works inspector / L' agent d' usine <i>M. Rizzotto</i></p>	<p>Pagina - 2 di 2</p>
---	--	------------------------

Appendix H: Holder manufacturing drawing



Appendix I: Calculations on theoretical strain

B8M cl 2	SDSS SA	SDSS CS
$R_{p0.2b8m} := 655 \text{ MPa}$	$R_{p0.2SA} := 662 \text{ MPa}$	$R_{p0.2CS} := 1004 \text{ MPa}$
$R_{mb8m} := 775 \text{ MPa}$	$R_{mSA} := 877 \text{ MPa}$	$R_{mCS} := 1075 \text{ MPa}$
$E_1 := 193 \text{ GPa}$	$E_2 := 199 \text{ GPa}$	$E_3 := 199 \text{ GPa}$
$\varepsilon_{b8m} := \frac{R_{p0.2b8m}}{E_1} = 0.00339$	$\varepsilon_{SA} := \frac{R_{p0.2SA}}{E_2} = 0.00333$	$\varepsilon_{CS} := \frac{R_{p0.2CS}}{E_3} = 0.00505$
Original length $L_0 := 36 \text{ mm}$	Tensile area $A_0 := 0.92 \text{ cm}^2$	

Theoretical strain at yield

B8M cl 2

Strain at yield 0.2% $\varepsilon_{yield} := 0.002 + \varepsilon_{b8m} = 0.0054$

Force at yield 0.2 % $F_{yield} := R_{p0.2b8m} \cdot A_0 = 60.26 \text{ kN}$

Force at fracture $F_{fract} := R_{mb8m} \cdot A_0 = 71.3 \text{ kN}$

$$F := \frac{F_{fract}}{g} = 7.271 \text{ tonne}$$

Elongation at yield $\Delta L := L_0 \cdot \varepsilon_{yield} = 0.194 \text{ mm}$

SDSS SA

Strain at yield 0.2% $\varepsilon_{yield} := 0.002 + \varepsilon_{SA} = 0.0053$

Force at yield 0.2 % $F_{yield} := R_{p0.2SA} \cdot A_0 = 60.904 \text{ kN}$

Force at fracture $F_{fract} := R_{mSA} \cdot A_0 = 80.684 \text{ kN}$

$$F := \frac{F_{fract}}{g} = 8.227 \text{ tonne}$$

Elongation at yield $\Delta L := L_0 \cdot \varepsilon_{yield} = 0.192 \text{ mm}$

SDSS CS

Strain at yield 0.2% $\varepsilon_{yield} := 0.002 + \varepsilon_{CS} = 0.00705$

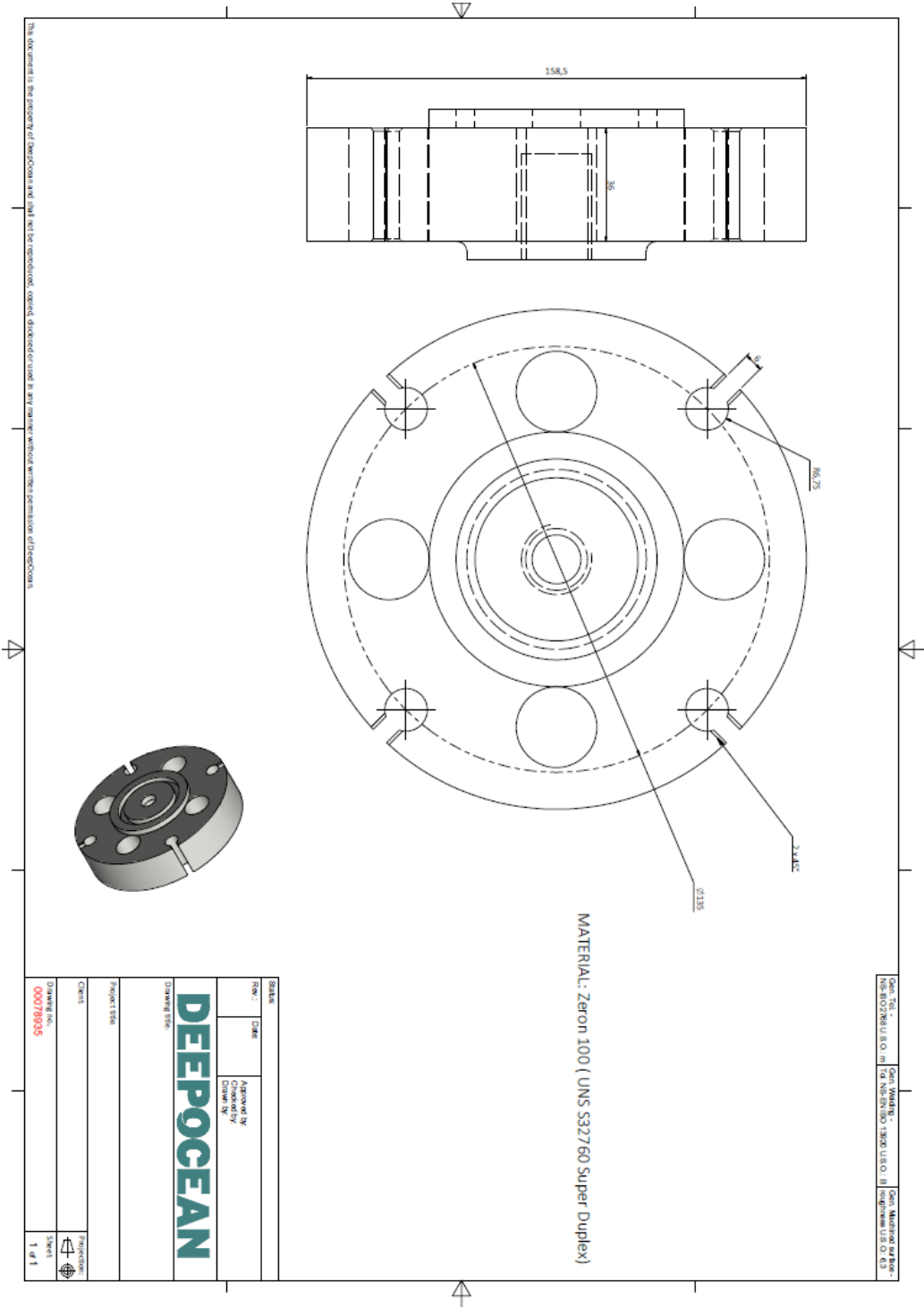
Force at yield 0.2 % $F_{yield} := R_{p0.2CS} \cdot A_0 = 92.368 \text{ kN}$

Force at fracture $F_{fract} := R_{mCS} \cdot A_0 = 98.9 \text{ kN}$

$$F := \frac{F_{fract}}{g} = 10.085 \text{ tonne}$$

Elongation at yield $\Delta L := L_0 \cdot \varepsilon_{yield} = 0.254 \text{ mm}$

Appendix J: Flange manufacturing drawing



Appendix K: MSDS Magnesium chloride



SIKKERHETS DATABLAD

I henhold til forordning (EF) nr. 1907/2006
Versjon 2.0
Revisjonsdato 21.03.2013

1. IDENTIFIKASJON AV STOFF/STOFFBLANDING OG FORETAK

1.1. Produktidentifikasjon

Handelsnavn	MG KOMBI®
Kjemikalienavn	Magnesiumklorid hexahydrat
Molekylformel	$MgCl_2 \cdot 6 H_2O$
CAS-nr.	7791-18-6
EC-nr.	232-094-6

1.2. Identifiserte anvendelsesområder og anvendelser som frarådes

Anvendelsesområde	Støvbinding (grus og asfalt) og snø- og istinemiddel
-------------------	--

1.3. Leverandørinformasjon

Foretak	GC Rieber Salt AS Skur 86 Sjursøya 0193 Oslo
Telefon	23 03 50 90
Fax	22 19 77 07
Epost	salt.oslo@gcrieber.no
Web	www.gcrieber-salt.no

1.4. Nødnummer

Nødtelefon	Giftinformasjonssentralen 22 59 13 00
------------	---------------------------------------

2. FAREIDENTIFIKASJON

2.1. Klassifisering av stoff/stoffblanding

Stoffet er ikke klassifisert som farlig i henhold til bestemmelse (EF) nr. 1272/2008

Stoffet er ikke klassifisert som farlig i henhold til direktiv 67/548/EØF

2.2. Etikettelementer

Stoffet er ikke merkepliktig i overenstemmelse med EF-direktiver eller respektive nasjonale lover.

2.3. Andre farer

Ingen data tilgjengelig

Sikkerhetsdatablad MG KOMBI®

3. SAMMENSETNING/OPPLYSNINGER OM BESTANDDELER

3.1. Stoffer

% w/w	CAS-nr.	Kjemikalienavn
ca. 100%	7791-18-6	Magnesiumklorid hexahydrat

9. FYSISKE OG KJEMISKE EGENSKAPER

9.1. Grunnleggende fysiske og kjemiske egenskaper

Utseende/form	Fast
Farge	Hvit
Lukt	Luktfri
pH	6-7,5 (20 °C)
Smelte-/frysepunkt	714 °C
Kokepunkt	1412 °C
Flammepunkt	Ingen data tilgjengelig
Damptrykk	Ingen data tilgjengelig
Relativ tetthet	1,570 g/mL
Vannløselighet	157 g/100 mL
Viskositet	Ingen data tilgjengelig
Ekspløsjonsegenskaper	Ingen data tilgjengelig
Oksidasjonsegenskaper	Ingen data tilgjengelig

9.2. Andre opplysninger

Ingen data tilgjengelig

Appendix L: Magnesium chloride solutions

$$Mg := 24.31 \frac{gm}{mol} \quad O := 16 \frac{gm}{mol} \quad Cl := 35.45 \frac{gm}{mol} \quad H := 1 \frac{gm}{mol}$$

$$MgCl_2 := Mg + 2 \cdot Cl = 95.21 \frac{gm}{mol}$$

$$H_2O := 2 \cdot H + O = 18 \frac{gm}{mol}$$

$$\% Cl \quad P := \frac{2 \cdot Cl}{MgCl_2} = 0.745$$

Solubility in water	
	anhydrous 52.9 g/100 mL (0 °C)
	54.3 g/100 mL (20 °C)
	72.6 g/100 mL (100 °C)
	hexahydrate
	167 g/100 mL (20 °C)

Max Concentration of MgCl₂ at 20 deg

Weight of magnesiumchloridehydrate $W_{MgCl_2 \cdot 6H_2O} := MgCl_2 + 6 \cdot H_2O = 203.21 \frac{gm}{mol}$

$$X_{MgCl_2} := \frac{MgCl_2}{W_{MgCl_2 \cdot 6H_2O}} = 0.469$$

Added MgCl hydrat

$$I_{mgcl} := 116 \text{ gm} = 116 \text{ gm}$$

Water from MgCl₂ hydrat

$$Y_{H_2O} := I_{mgcl} \cdot (1 - X_{MgCl_2}) = 61.651 \text{ gm}$$

MgCl₂ from MgCl₂ hydrat

$$Z_{MgCl_2} := I_{mgcl} \cdot X_{MgCl_2} = 54.349 \text{ gm}$$

Added water

$$W_{H_2O} := 38.35 \text{ gm} = 38.35 \text{ gm}$$

$$W_{total} := Y_{H_2O} + W_{H_2O} = 100.001 \text{ gm}$$

Calculated total volume gives an increase of 19,8 % in total volum according to standard G36

$$z := 1.198$$

Total solution

$$W_{sol} := W_{total} \cdot z = 119.801 \text{ gm}$$

Concentration of MgCl₂

$$C_1 := \frac{Z_{MgCl_2}}{I_{mgcl} + W_{H_2O}} = 0.35$$

Concentration of Cl-

$$C_2 := \frac{P \cdot Z_{MgCl_2}}{I_{mgcl} + W_{H_2O}} = 0.26$$

Max Concentration of MgCl₂ at 100 deg

Weight of magnesiumchloridehydrate $W_{MgClH_2O} := MgCl_2 + 6 \cdot H_2O = 203.21 \frac{gm}{mol}$

$$X_{MgCl_2} := \frac{MgCl_2}{W_{MgClH_2O}} = 0.469$$

Added MgCl hydrat $I_{mgcl} := 155 \text{ gm} = 155 \text{ gm}$

Water from MgCl₂ hydrat $Y_{H_2O} := I_{mgcl} \cdot (1 - X_{MgCl_2}) = 82.378 \text{ gm}$

MgCl₂ from MgCl₂ hydrat $Z_{MgCl_2} := I_{mgcl} \cdot X_{MgCl_2} = 72.622 \text{ gm}$

Added water $W_{H_2O} := 18 \text{ gm} = 18 \text{ gm}$

Calculated total volume gives an increase of 19,8 % in total volum according to standard $W_{total} := Y_{H_2O} + W_{H_2O} = 100.378 \text{ gm}$

$$z := 1.198$$

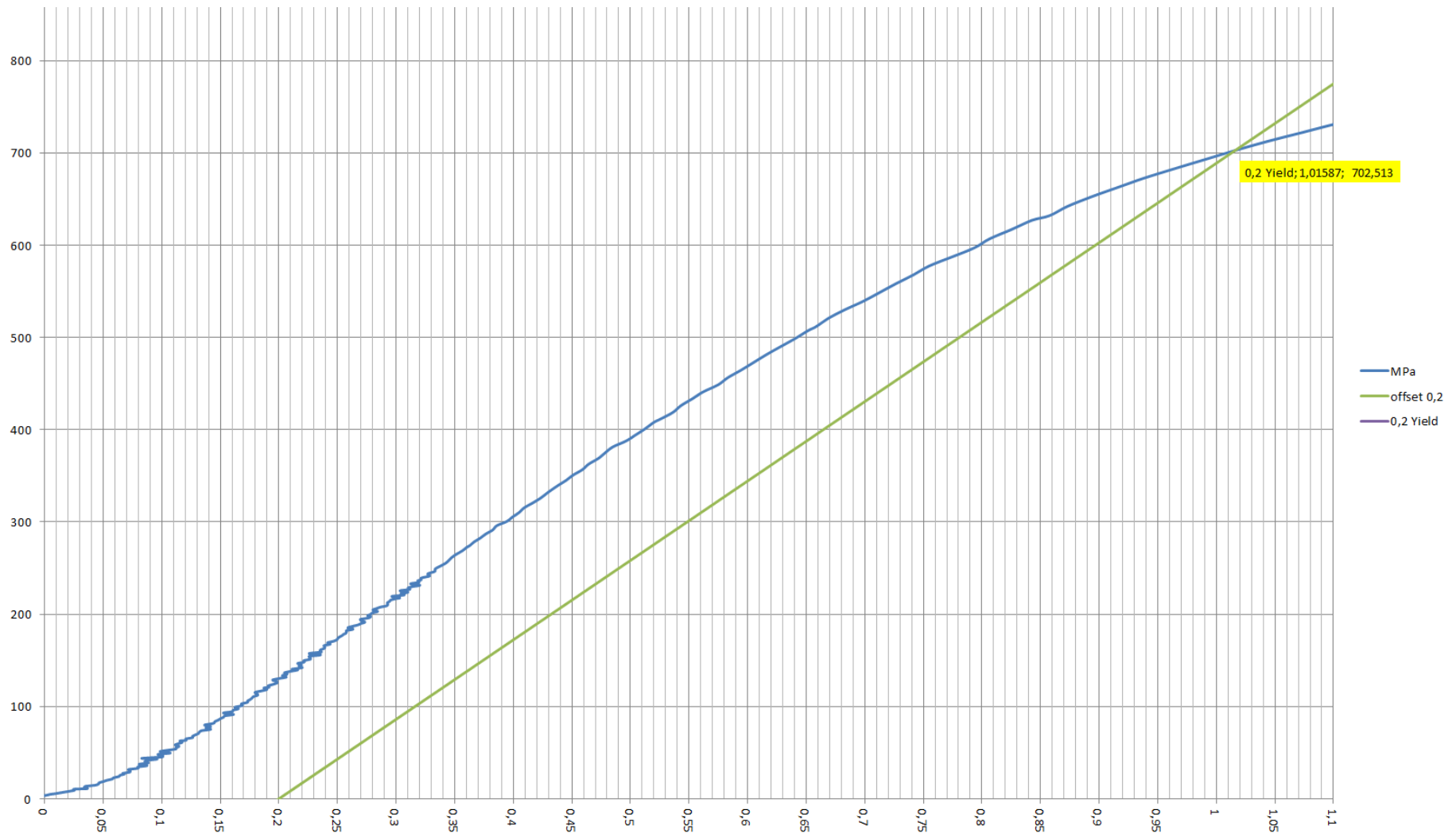
Total solution $W_{sol} := W_{total} \cdot z = 120.253 \text{ gm}$

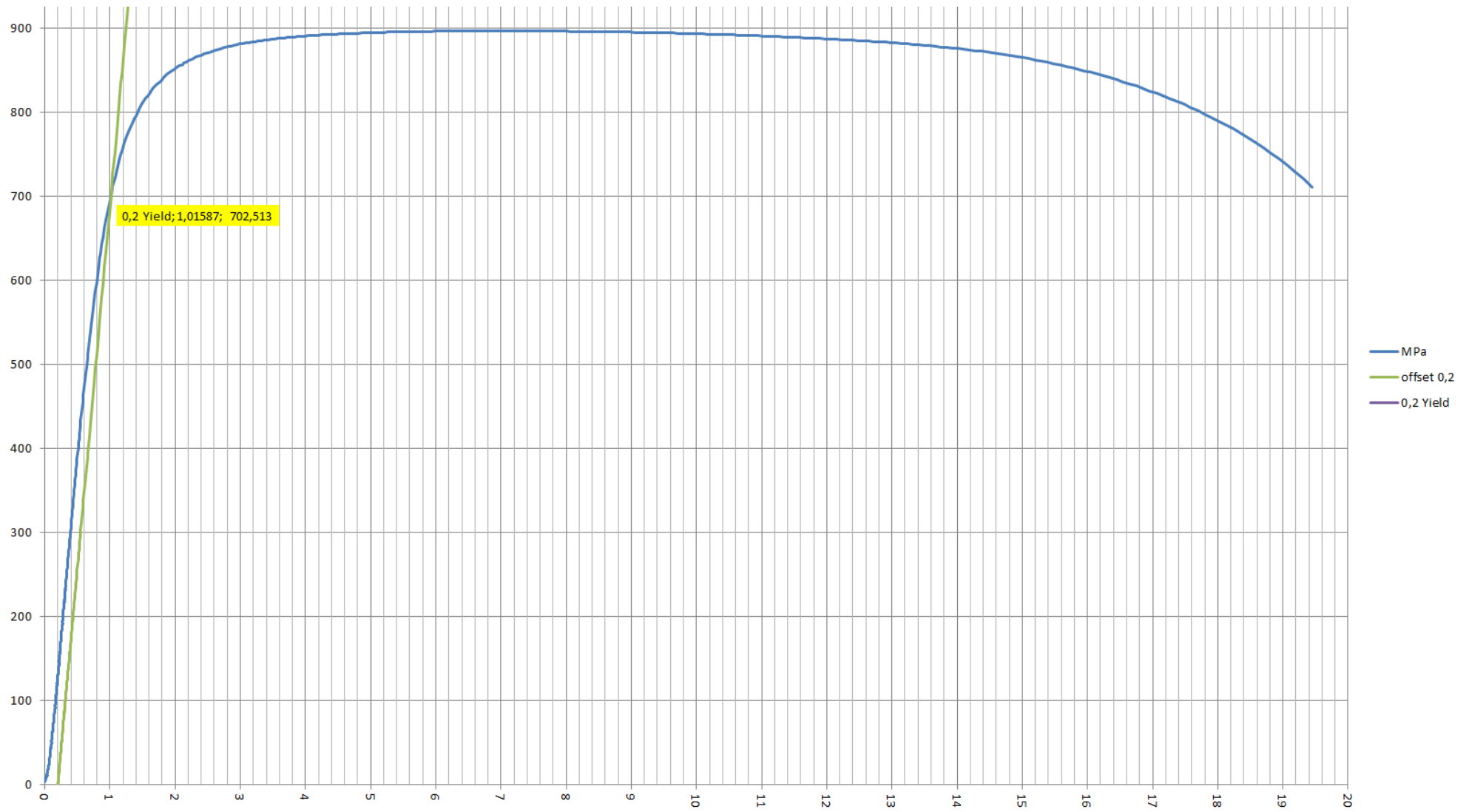
Concentration of MgCl₂ $C_1 := \frac{Z_{MgCl_2}}{I_{mgcl} + W_{H_2O}} = 0.42$

Concentration of Cl- $C_2 := \frac{P \cdot Z_{MgCl_2}}{I_{mgcl} + W_{H_2O}} = 0.31$

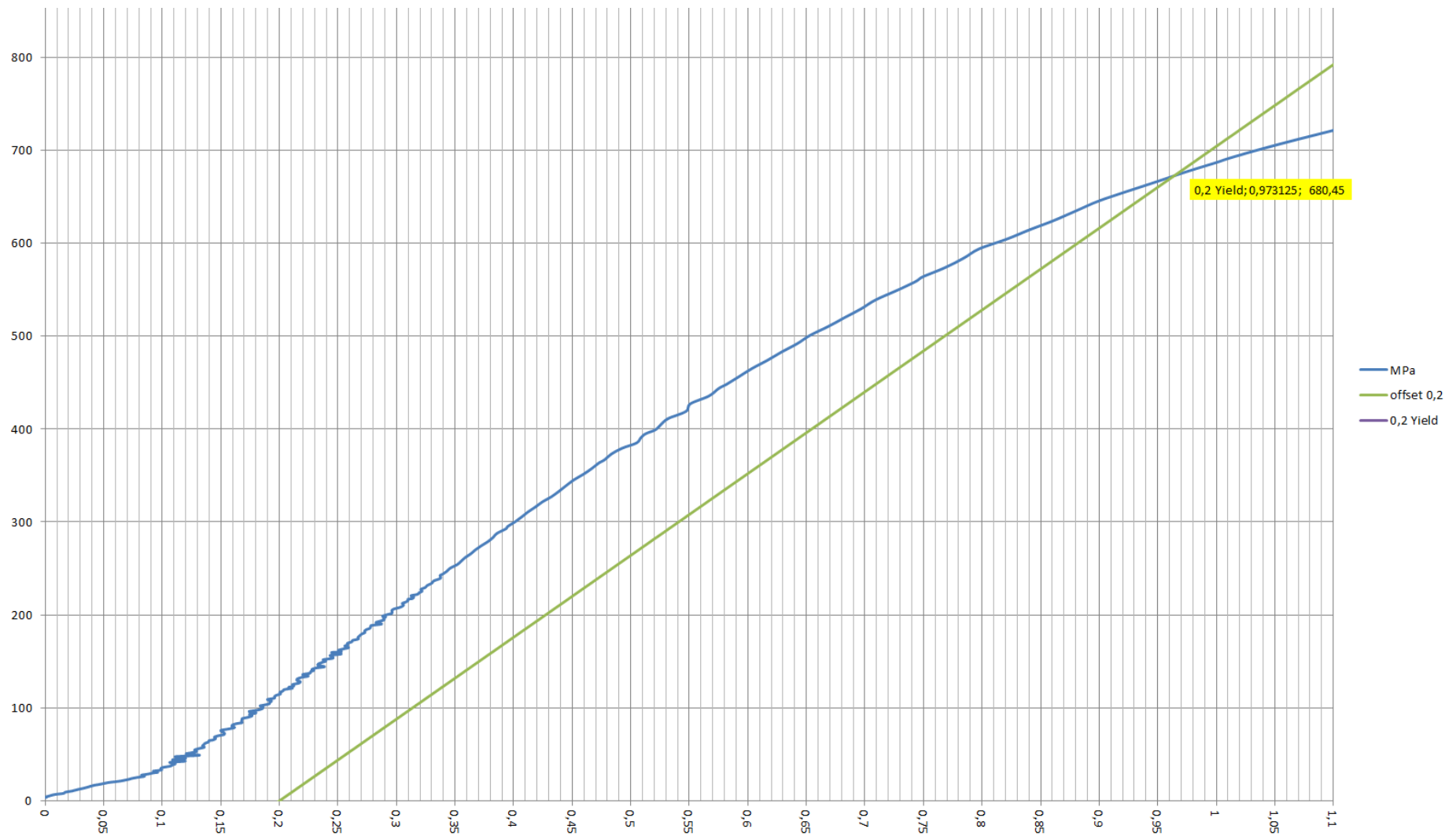
Appendix N: Stress-strain curves from tensile testing

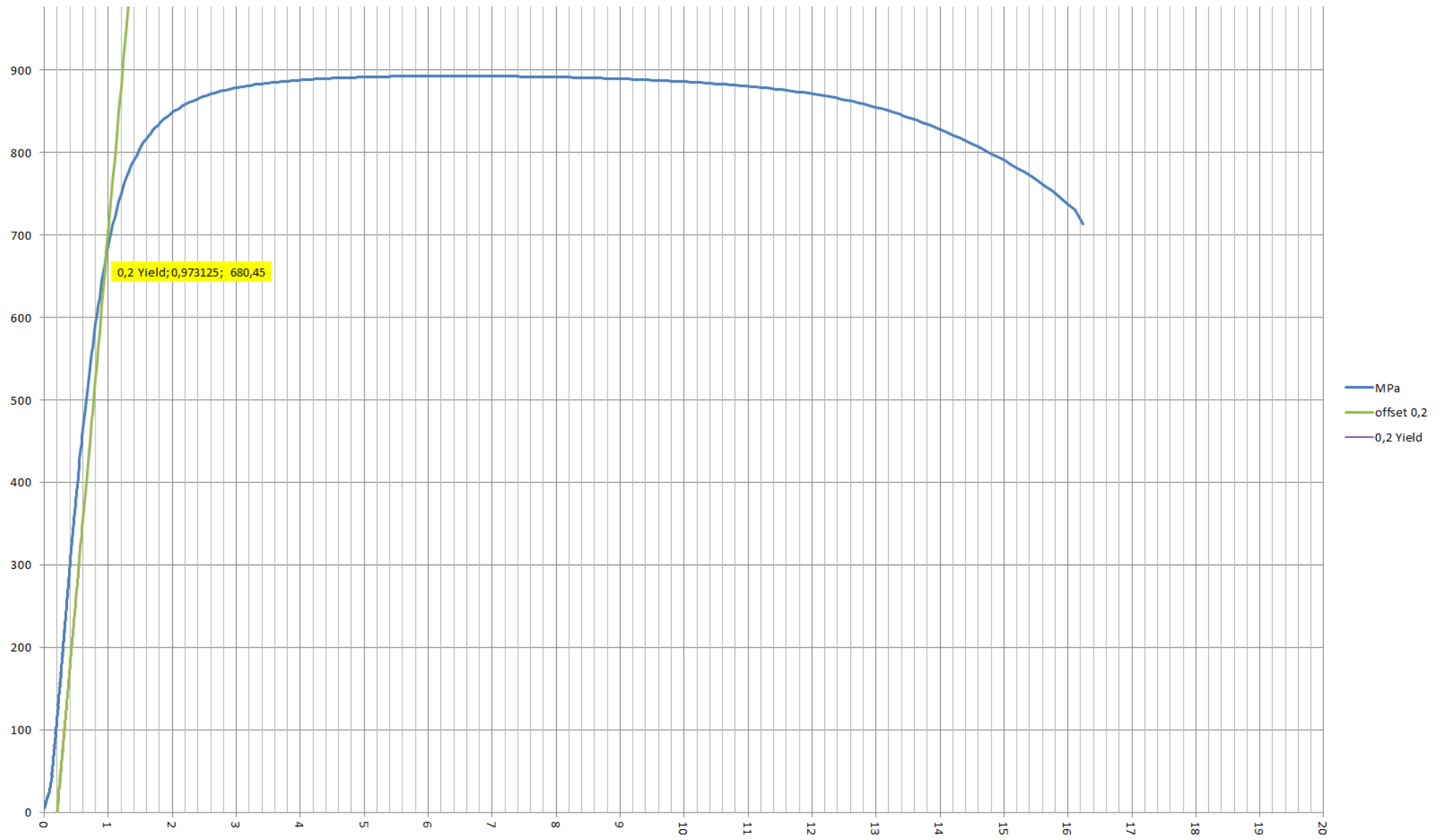
Test 1 316L



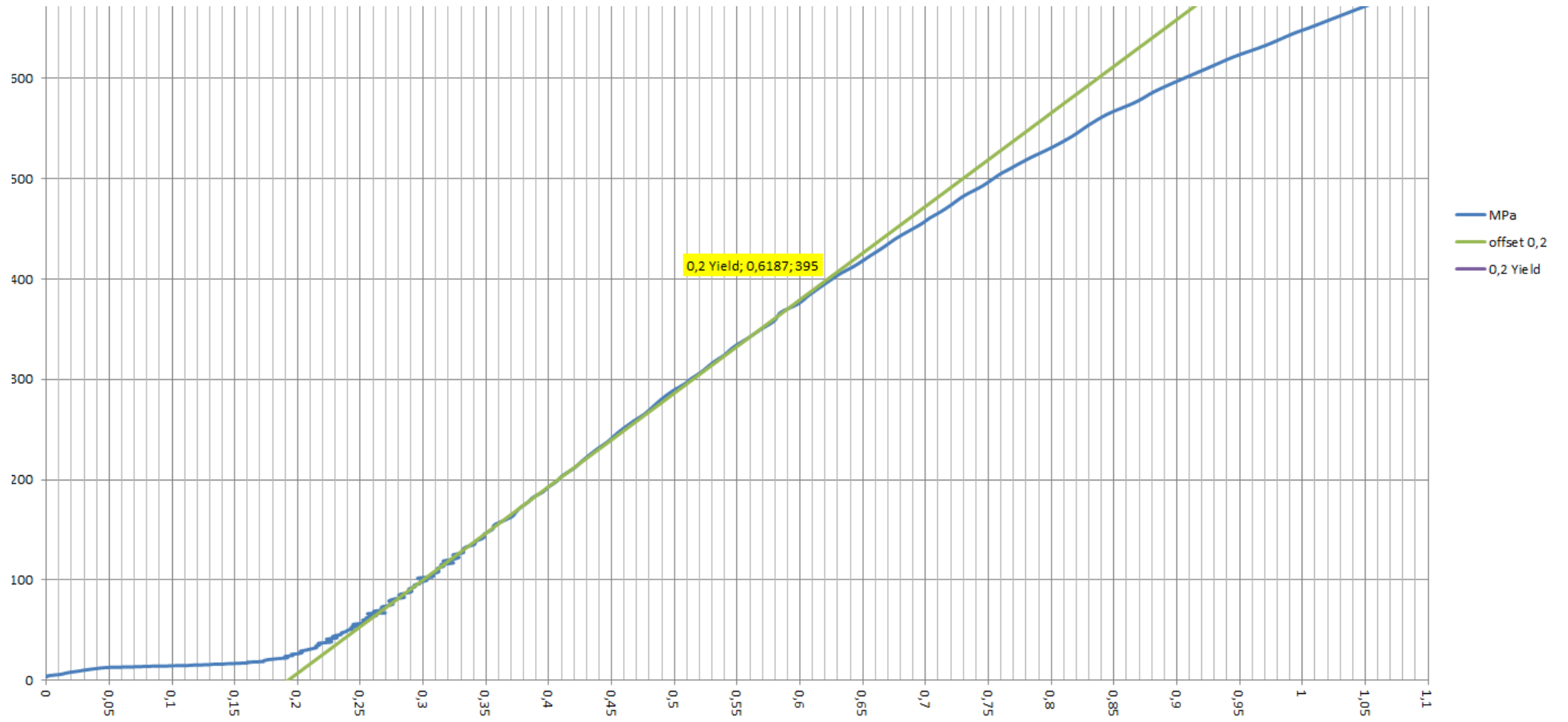


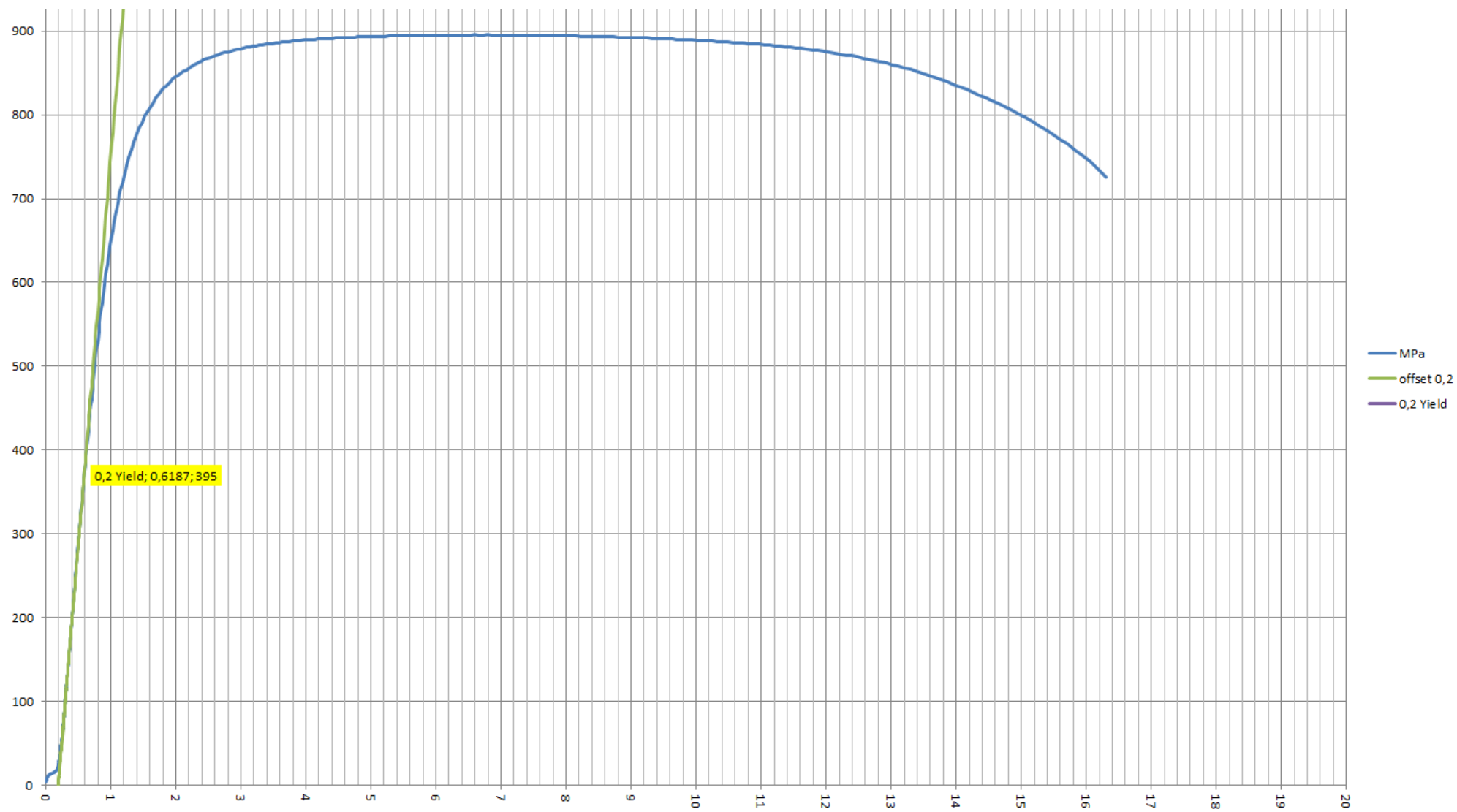
Test 2 316 L



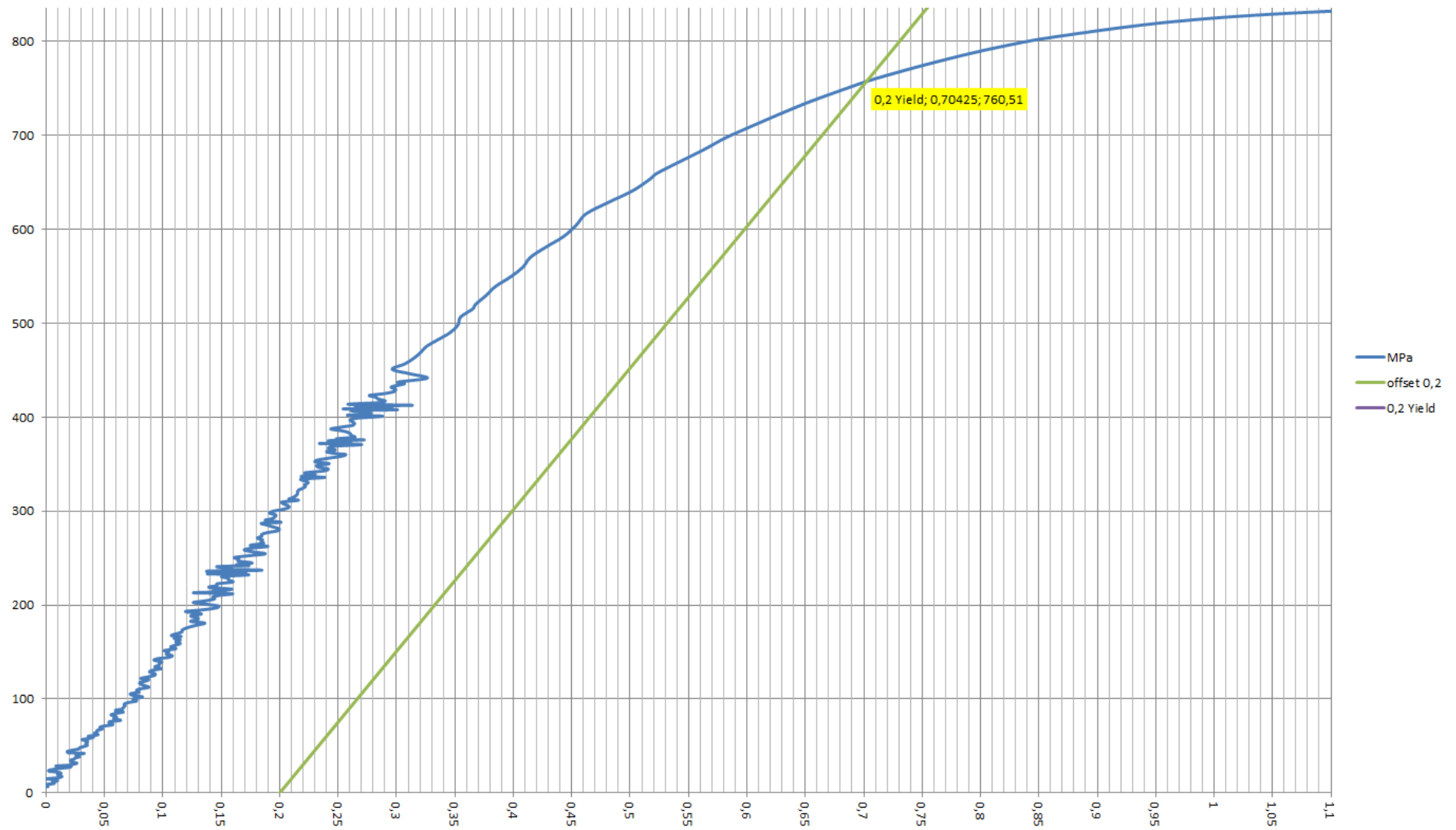


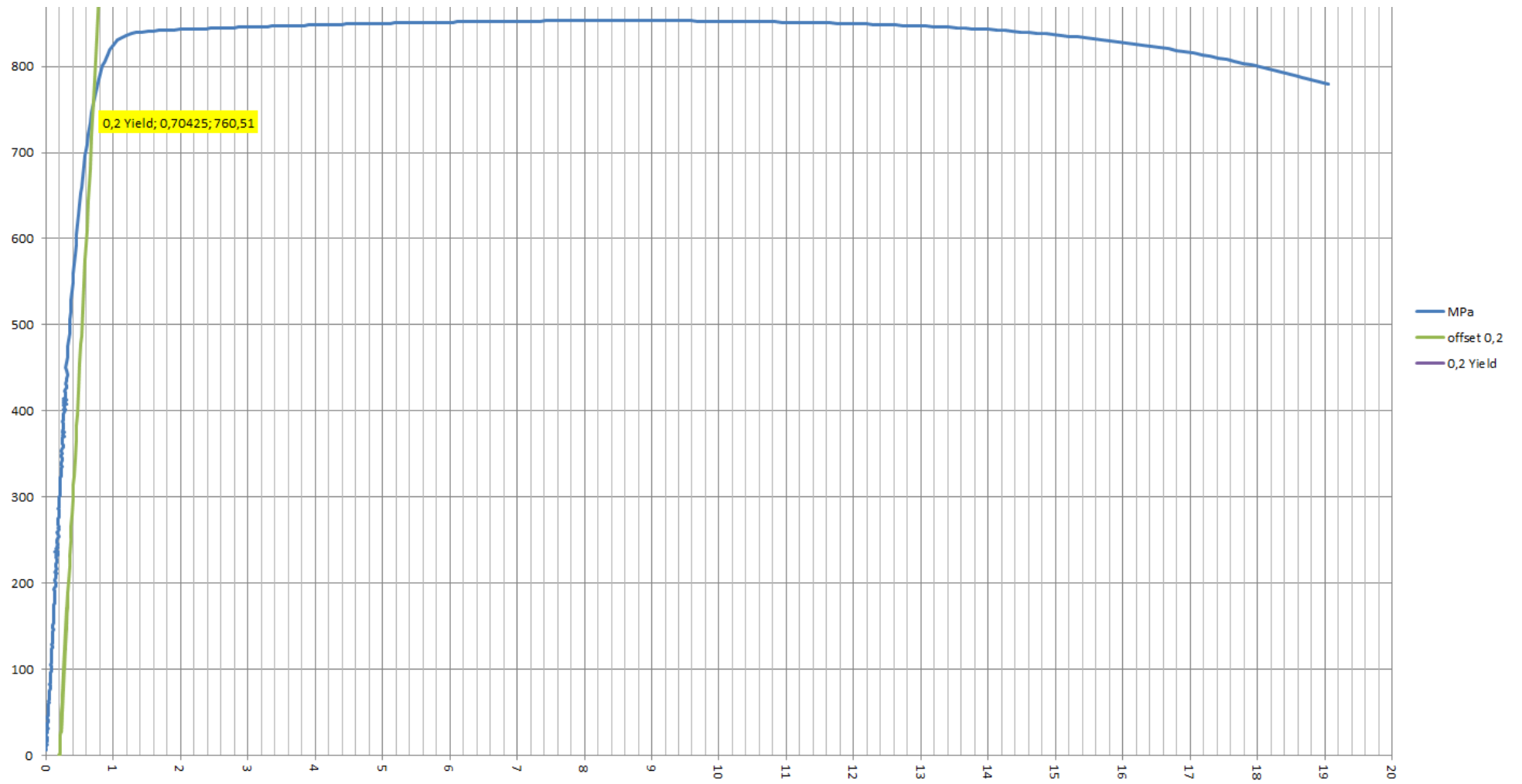
Test 3 316L



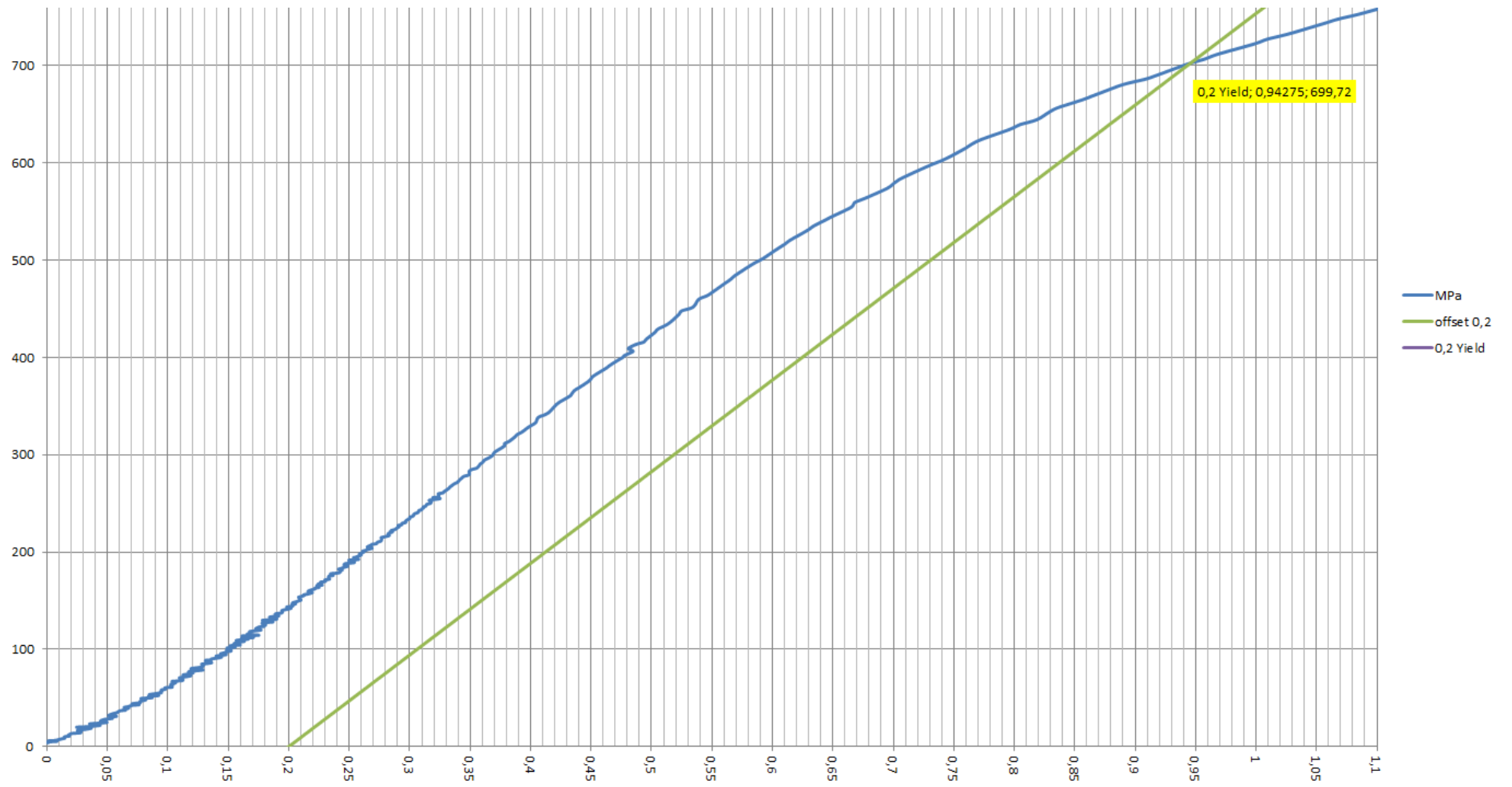


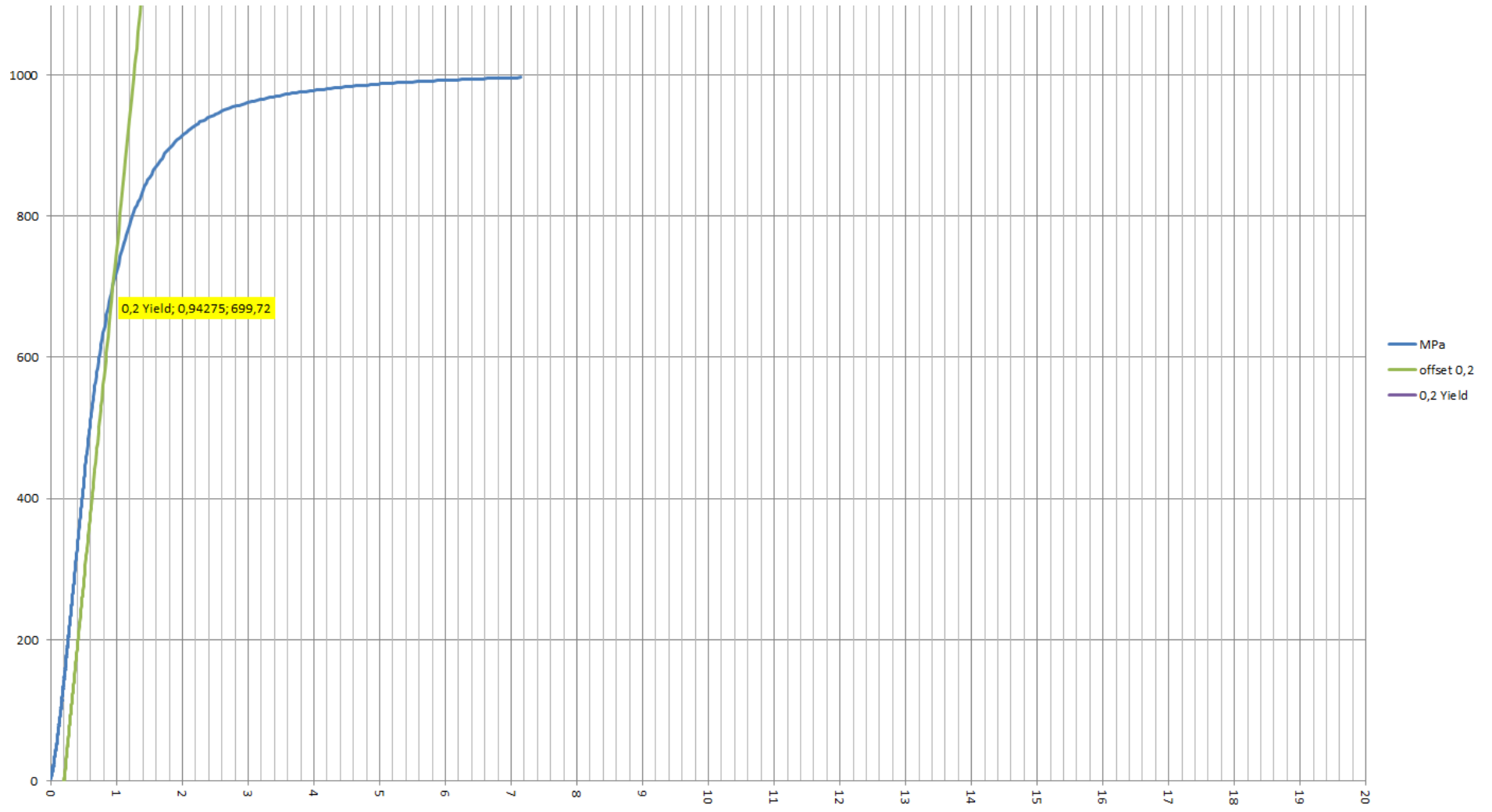
Test 4 316 L



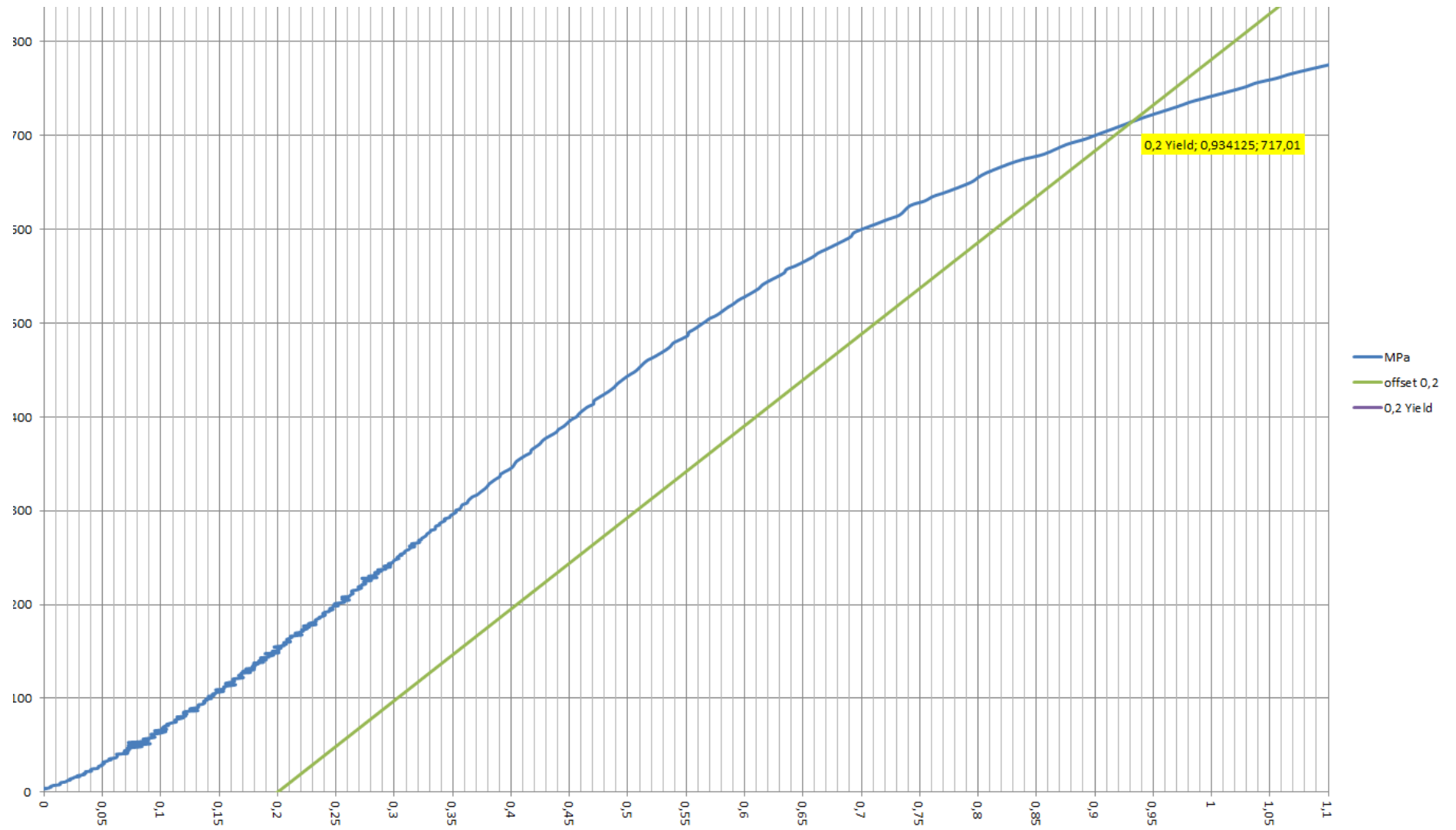


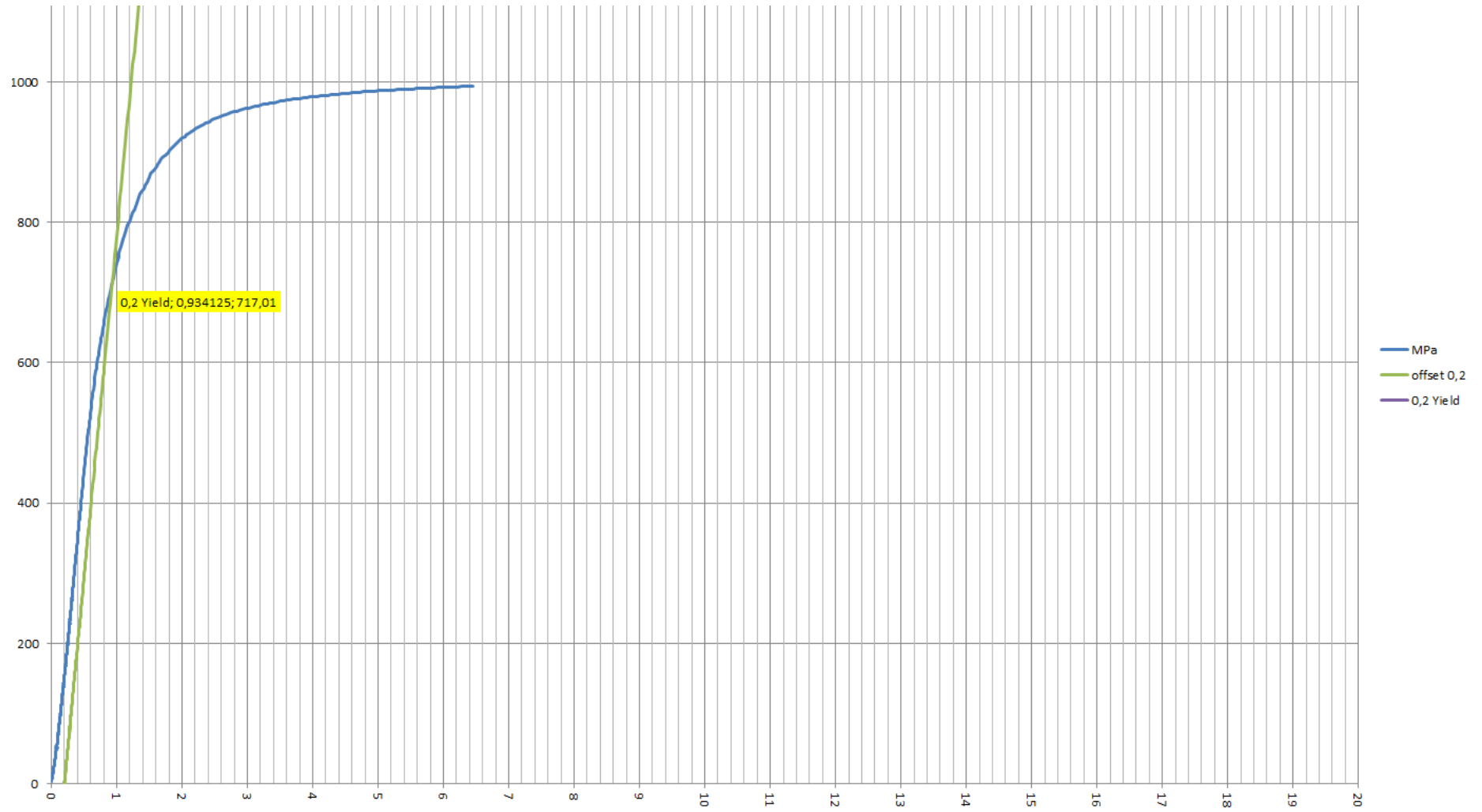
Test 5 SDSS SA



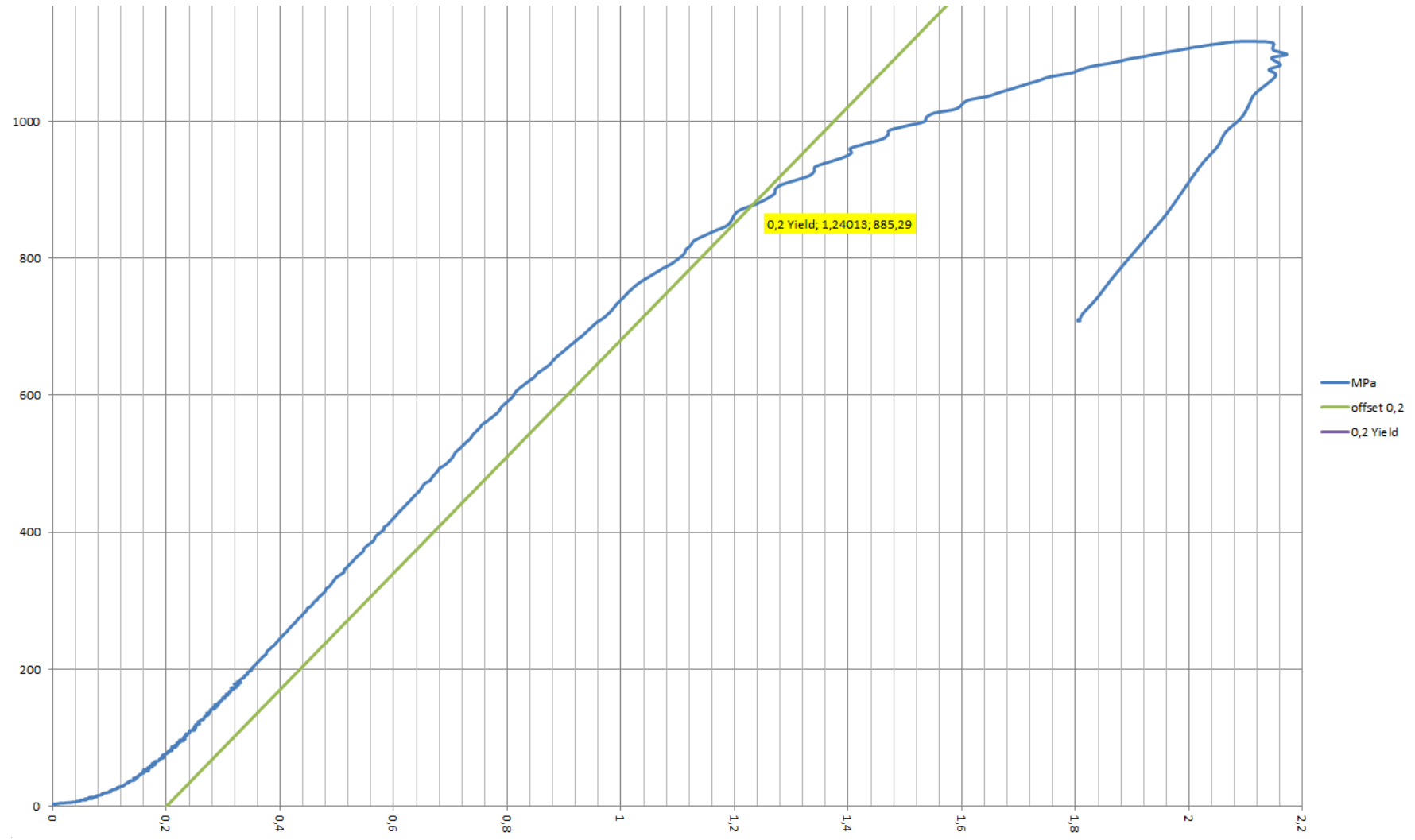


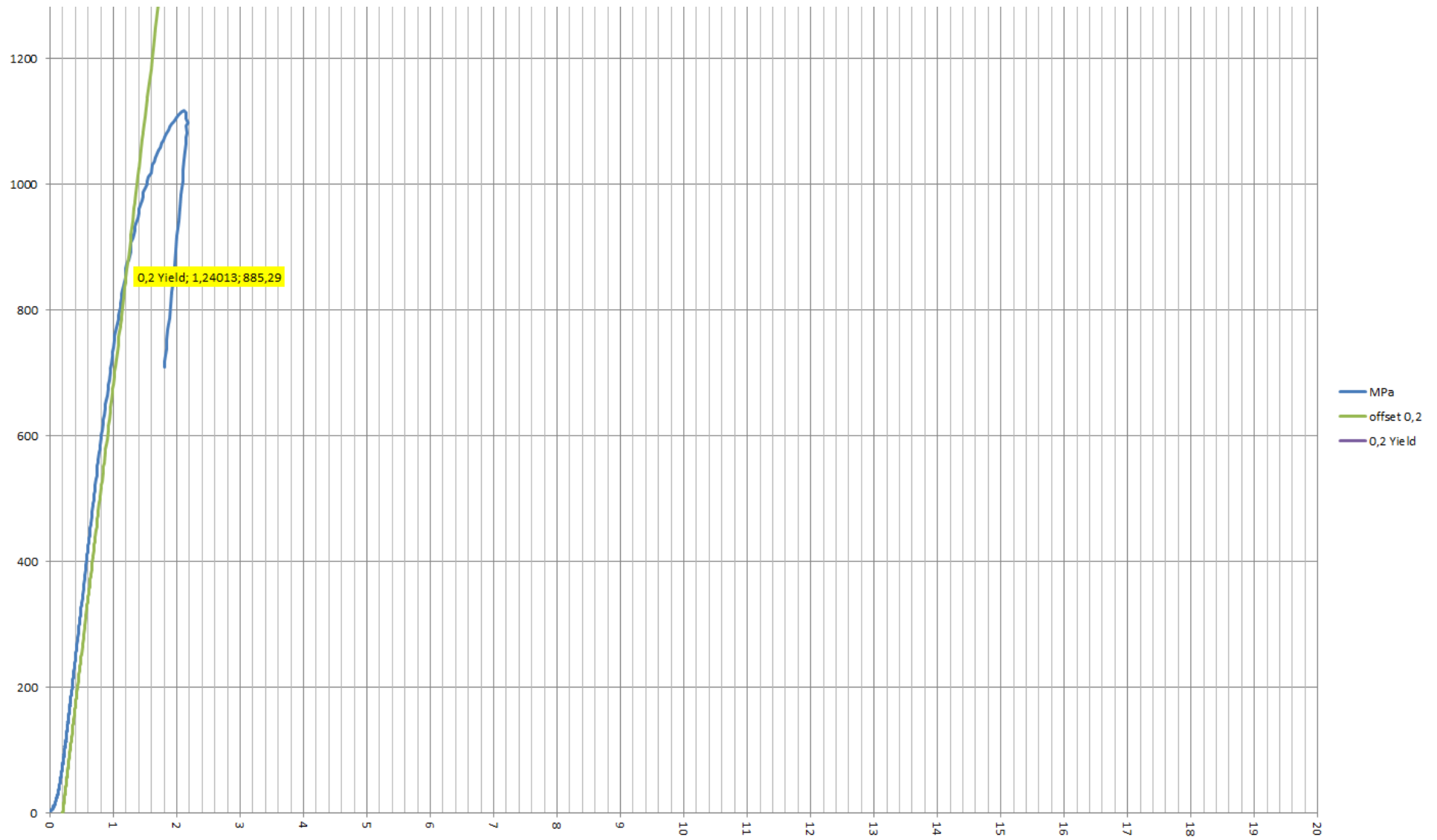
Test 6 SDSS SA





Test 7 SDSS CS





Test 8 SDSS CS

